universität wien

DISSERTATION / DOCTORAL THESIS

Titel der Dissertation / Title of the Doctoral Thesis

„Characterization of a novel virulence factor important for colonization of *Zea mays* by the smut *Ustilago maydis*“

verfasst von / submitted by

Alexandra Stirnberg, BSc MSc

angestrebter akademischer Grad / in partial fulfilment of the requirements for the degree of

Doctor of Philosophy (PhD)

Wien, 2016 / Vienna 2016

Studienkennzahl lt. Studienblatt / degree programme code as it appears on the student record sheet:	A 794 685 490
Dissertationsgebiet lt. Studienblatt / field of study as it appears on the student record sheet:	Molekulare Biologie
Betreut von / Supervisor:	Dr. Armin Djamei

Acknowledgements

First and foremost, I would like to thank my supervisor Dr. Armin Djamei. Without you none of this would have been possible. Thank you for taking me along to join your group in Vienna, for your constant support, your time and your trust in me and my capabilities.

I would also like to thank all current and former members of the lab (not only but especially: Jason Bosch, Janos Bindics, Angelika Czedik-Eysenberg, Klaus Ehrlinger, Michelle Gallei, Tilo Guse, Gesa Hoffmann, Fernando Navarrete, Franziska Rabe, Julia Riefler, Sonja Schmidt, Denise Seitner, Robert Sperrer and Simon Uhse) for creating a great work environment and your constant willingness to help out.

Additionally, I would like to acknowledge all people from my former laboratory in Marburg, especially Prof. Dr. Regine Kahmann. Thank you for allowing me to be part of your group and making this one year in Marburg very memorable. I also thank Daniel Lanver for sharing expression data of selected effectors.

I am thankful to the two PhD schools I was lucky to be a part of: the VBC PhD program in Vienna (and its coordinators Ines Crisostomo and Christopher Robinson) and the IMPRS-Mic in Marburg.

A very special thanks goes to all members of the GMI and the support facilities not only at GMI, but the whole campus. Without your constant effort to generate a superb working atmosphere on a professional and personal level this would not have been possible. Especially, I would like to thank Iulia for keeping me sane on rough days.

I was also very lucky to have excellent scientist as part of my thesis committee, my reviewers and my examiners for this thesis. Thank you: Gerhard Adam, Michael Bölker, Saskia Hogenhout, Regine Kahmann, Jürgen Kleine-Vehn, Ortrun Mittelsten Scheid, Alexander Stark and Alga Zuccaro. Thank you for your support and advice for my research.

Last but not least, I would like to thank my favourite people in the world: my family (Mama, Papa, Consi und Karl), my friends (especially Lena, Hendrik, Moni and Gudi), and Nick. You mean the world to me and without I would not be where I am today.

Parts of this thesis were published in the following article:

Stirnberg A, Djamei A. 2016. Characterization of ApB73, a virulence factor important for colonization of *Zea mays* by the smut *Ustilago maydis*, Mol Plant Path, Accepted manuscript online: 9 JUN 2016, DOI: 10.1111/mpp.12442

Summary

The biotrophic fungus *Ustilago maydis* is the causal agent of corn smut disease. To suppress plant defences and to modulate the host metabolism, the pathogen makes use of hundreds of small secreted effector proteins.

This thesis describes the identification of ApB73 (Apathogenic in B73), a so far uncharacterized protein, that is essential for the successful colonization of *Zea mays* by *U. maydis*.

The gene *apB73* is transcriptionally induced during the biotrophic stages of the fungus. The deletion of the *apB73* gene in *U. maydis* results in cultivar-specific loss of gall formation. Additionally, deletion of ApB73 leads to a defect resulting in an impaired process of spore formation, making ApB73 ultimately essential for *U. maydis* to complete the biotrophic phase of its dimorphic life cycle. The ApB73 protein is highly conserved among closely related smut fungi. Despite that, among three tested orthologs, only the ortholog of the maize-infecting head smut *Sporisorium reilianum* can complement the mutant phenotype of *U. maydis*.

ApB73 is secreted into the biotrophic interface. However, the secreted protein seems to associate to fungal cell wall components or the fungal plasma membrane rather than freely diffusing within the biotrophic interface.

ApB73 is a novel, conserved and important virulence factor of *U. maydis* that localizes to the interface between the pathogen and its host *Zea mays*.

Zusammenfassung

Der biotrophe Pilz *Ustilago maydis* ist der Erreger des Maisbeulenbrands. Zur Unterdrückung der Pflanzenabwehr und Reorganisation des Wirtsmetabolismus verwendet das Pflanzenpathogen *U. maydis* hunderte kleine sekretierte Proteine, sogenannte Effektoren.

Innerhalb dieser Arbeit soll der Effektorkandidat ApB73 (Apathogen in B73) näher beschrieben werden. ApB73 ist ein bislang nicht charakterisiertes Protein, welches von essentieller Bedeutung für die erfolgreiche Koloniesierung von *Z. mays* durch *U. maydis* ist.

apB73 ist während der biotrophen Lebensphase des Pilzes transkriptionell hochreguliert und führt im Falle einer Deletion des Genes zum Kulturvarietät spezifischen Verlust der Tumorbildung. Zusätzlich führt das Fehlen von ApB73 zu einem Defekt, der es den Mutanten nicht mehr erlaubt Sporen zu bilden. Folglich, ist es *U. maydis* ohne ApB73 schlussendlich nicht möglich die biotrophe Phase seines Lebenszyklus zu vollenden.

ApB73 ist auf Proteinebene unter eng verwandten Brandpilzen hoch konserviert. Dennoch ist von drei getesteten Orthologen nur das Ortholog des Maiskopfbrand Erregers *Sporisorium reilianum* in der Lage den Virulenzdefekt von *U. maydis apB73* Mutanten zu komplementieren.

Das ApB73 Protein wird vom Pilz in die biotrophe Interaktionszone sekretiert. Hier jedoch diffundiert es nicht frei, sondern bleibt an die Komponenten der pilzlichen Zellwand oder Plasmamembran gebunden.

ApB73 ist ein neuer, konservierter und wichtiger Virulenzfaktor von *U. Maydis,* der in der Interaktionszone zwischen dem Pflanzenpathogen und seinem Wirt *Z. mays* agiert.

Table of Contents

1 Introduction

Around 90% of the world's food supply is covered by only 15 plant species, with the most important three (maize, rice and wheat) taking up two thirds (http://www.fao.org/docrep/u8480e/u8480e07.htm).

This illustrates the tremendous value of plants in human nutrition. However, the yield of monocotyledonous cereals like maize, barley, wheat or rice is constantly threatened by various factors, including water and nutrient deficiency, as well as pathogens. With incurring losses of over 200 billion US $ in the US alone, fungi cause more economic damage than any other microorganism. Despite this, more than 600 billion US $ are spent annually for fungicides in the US (Birren *et al.*, 2003). Additionally, the main practice of agriculture nowadays involves the growth of monocultures on vast areas of land, making it easy for pathogens to spread and promoting the evolution of resistant strains (Stukenbrock & McDonald, 2008).

Accordingly, the understanding of pathogenic interactions between plants and fungi is of high importance. This interaction is shaped not only by the capabilities of the host plant to defend itself, but also by the tools used by the fungus, to overcome these limits set by the host. The main participants in this interplay will be described in the following sub-chapters, first describing the immune system of the plant, and later focussing on the toolbox that fungi developed to overcome the plant defence system, especially the role of effectors.

1.1. The defence system of the plant

Plants are exposed to a variety of biotic and abiotic stresses; however, as they are sessile organisms they cannot move to escape these stresses and rather had to evolve elaborate and precise mechanisms to defend themselves (Sharma *et al.*, 2013). Here, I will mainly focus on biotic stresses and, to be more precise, on pathogens. Over millions of years of coevolution between plants and their pathogens, the plants innate immune system evolved sophisticated strategies to deal with the invaders on very different levels.

Physical barriers like the waxy cuticle and the cell wall are part of a structural protection mechanism that plants employ to defend themselves against biotic stresses (Koeck *et al.*, 2011). On top of that, plants evolved a two layered innate immune system.

The membranes of plant cells are equipped with pattern recognition receptors (PRRs) that allow them to detect slow evolving conserved molecules (pathogen/microbe-associated molecular patterns, PAMP/MAMPs) specific and essential to pathogens (like

flagellin or chitin). Those receptors will activate downstream signalling, resulting for example in the closure of stomata - an easy entry point for filamentous pathogens - or in the accumulation of reactive oxygen species (ROS). At this point, the plants' defence system also involves the secretion of antimicrobial compounds and hydrolytic enzymes which are both harmful for the pathogen, as well as the secretion of inhibitors to inactivate plant damaging enzymes secreted by the pathogen.

This first layer of the plants' immune system is PAMP triggered immunity (PTI). PTI successfully prohibits the colonialization of plants by non-pathogens, i.e. organisms that did not evolve to avoid recognition or to overcome this first layer of defence (compare Nurnberger *et al.*, 2004; Jones & Dangl, 2006; Asai & Shirasu, 2015). Successful pathogens, however, evolved tools termed effectors to directly or indirectly suppress PTI, allowing them to manipulate the system by primarily interfering with this first layer of defence.

Plants on the contrary had to find a way to deal with effector triggered susceptibility (ETS), and subsequently evolved resistance (R) proteins that react to this by directly or indirectly monitoring the presence or action of specific effectors, then called avirulence (Avr) proteins. This response by the plant using R genes is known as effector triggered immunity (ETI). Examples for these R proteins are the NB-LRR proteins named after their domains: a characteristic nucleotide binding (NB) domain and a leucine rich repeat (LRR) domain (Jones & Dangl, 2006).

This 'battle' continues, as over time individuals on both sides will by chance acquire mutations that will allow them to circumvent the (counter) attack. Those individuals, with the locally most beneficial adaptation, will proliferate better, resulting in the persistence of such favourable mutations (Figure 1.1).

However, the broad conservation of PAMPs as well as PRRs and the efficiency of NB-LRR receptors indicates that the evasion of plant recognition seems to be challenging for pathogens (McHale *et al.*, 2006; Zipfel, 2014). This is especially true for biotrophic pathogens, as it is vital to them to keep their host plants alive, requiring them to find invasion strategies that cause minimal damage.

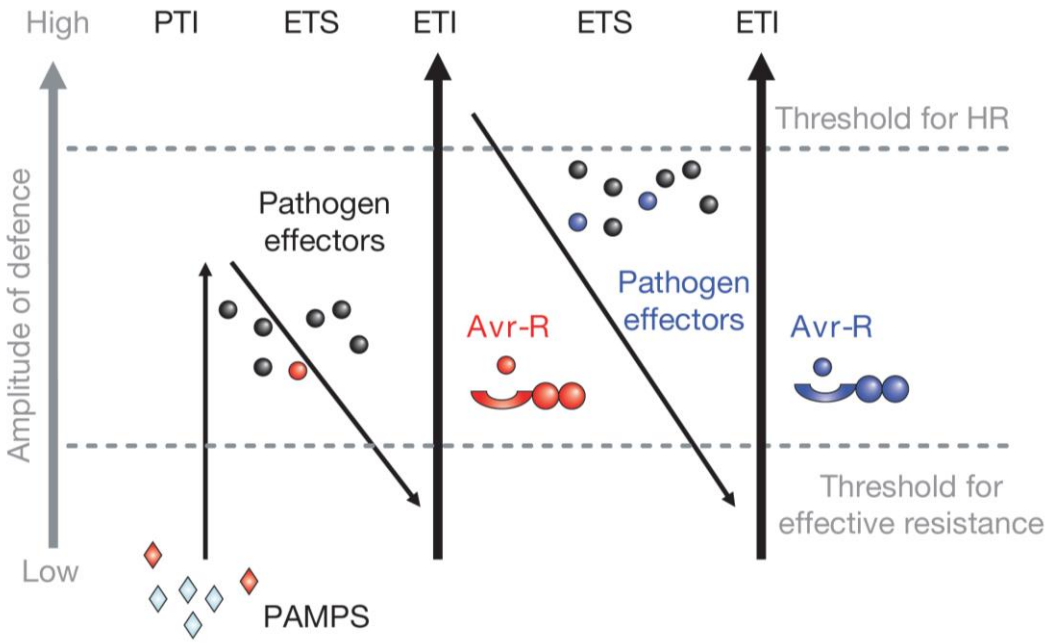

Figure 1.1 The output of the plant immune system visualized in a zig-zag model.
In the first phase, pathogen/microbe associated molecular pattern (PAMPS/MAMPs; red squares) are successfully detected by the plant and PAMP triggered immunity (PTI) is established. In a second phase though, effectors are secreted by the pathogen capable of overcoming PTI, thereby leading to effector triggered susceptibility (ETS). Over time evolution on the plant side will result in the emergence of Resistance proteins (R) that can interact with effectors (Avr protein, red), resulting in effector triggered immunity (ETI). ETI is characterized by a much stronger reaction than PTI, and as a consequence, it passes the threshold for the hypersensitive response (HR) leading to cell death. In phase 4 new pathogen effectors may have evolved (and the red one was lost) that can therefore overcome the red R protein resulting again in ETS. Plants that have R proteins detecting these new effectors can again reach a level of ETI (Jones & Dangl, 2006).

1.2. Evasion of plant recognition and the role of effectors

As mentioned before, biotrophic pathogens evolved sophisticated strategies to evade recognition by the host plant as well as suppressing immune responses. The main focus in this chapter lies on the action of secreted molecules, termed effectors, used by pathogens to manipulate plant immunity and establish a successful infection.

Effectors act on all levels. On the one side, they interfere with the two layers of plant innate immunity by acting not only on pathways activated upon PAMP recognition, but also by fighting back against the consequences of R proteins (Bent & Mackey, 2007). On the other side, many pathogens have evolved different classes of effectors that cover all ‘physical’ places, i.e. the apoplastic space and the plants’ cytoplasm, to ensure the establishment of pathogenicity.

The role of apoplastic effectors can be variable; however, as all pathogens deal with similar challenges, certain core targets - as it became evident over the last years – are addressed by various pathogens. Filamentous fungal pathogens, for example, are all challenged by the recognition of chitin by the plant. As a consequence, fungal pathogens evolved effectors capable of sequestering chitin (e.g. Avr4, van den Burg *et al.*, 2006;

Ecp6, de Jonge *et al.*, 2010; Slp1, Mentlak *et al.*, 2012; and Mg3LysM, Marshall *et al.*, 2011). Another common mechanism used by plants to defend themselves is the secretion of proteases into the apoplast, making it a frequent target of the action of effectors. Examples of organisms secreting effectors that inhibit host proteases are *Cladosporium fulvum (*AVR2, Shabab et al., 2008), *Phytophtora infestans* (AVRblb2, Bozkurt *et al.*, 2011 and EPIC2b, Tian *et al.*, 2007 among others) and *Ustilago maydis* (Pit2, Mueller *et al.*, 2013).

Whereas pathogens that only grow within the plants' apoplast are likely sufficiently prepared to conquer defence responses of the plant by only employing apoplastic effectors (according to current knowledge, e.g. *C. fulvum*, Stergiopoulos & de Wit, 2009), many pathogens that grow intracellularly make additional use of effectors that act in the cytoplast. Cytoplasmic effectors, ergo those that are translocated into the plant cell, can redirect the plant nutrient flow or re-channel metabolic pathways. Similarly to apoplastic effectors, cytoplasmic effectors from multiple pathogens interfere with similar pathways, for example hormone signalling or the host ubiquitination system (Bos *et al.*, 2010; Djamei *et al.*, 2011; Park *et al.*, 2012; Asai *et al.*, 2014).

In spite of the apparently vital role of effector proteins for the success of an infection, deletions of specific effector genes often do not result in a measurable phenotype (Kämper *et al.*, 2006; Lindeberg *et al.*, 2012; Schilling *et al.*, 2014). An extreme example was published in a study from 2012 which looked at 78 genes from *Magnaporthe oryzae*, the causal agent of rice blast disease. Despite the fact that all genes were shown to be upregulated during the colonization of the host rice, only one gene was identified that, under the tested conditions, had an effect on virulence when deleted (Saitoh *et al.*, 2012). This could be due to a number of reasons, but is most likely due to the functional redundancy of effector proteins. Additionally, it should be considered that narrow experimental test conditions cannot display all selective parameters a pathogen is exposed to in nature.

Although many effectors seem to target conserved hubs in the plants' defence system (Mukhtar *et al.*, 2011), their similarity to known proteins on the sequence level is usually limited. Some effector candidates can be clustered to effector families based on sequence homologies (Kämper *et al.*, 2006), but they rarely resemble known proteins from databases. The more common picture is that effectors lack any kind of conserved domain making it difficult to predict them or their function. Even among species of the same genus, sequences can vary quite broadly and amino acid conservation across families is rarely described (Sperschneider *et al.*, 2015a). The reasoning here is that effector proteins are exposed to high selection pressure due to the co-evolving defence

system of the plant (Jia *et al.*, 2000; Jones & Dangl, 2006; Le Roux *et al.*, 2015). This high variability on the sequence level hampers the prediction of effectors by bioinformatic means. As a result, currently most effectors are identified using an approach that is based on specific characteristics rather than sequence conservation (Sperschneider *et al.*, 2015b). For example, due to an effectors' place of action, these proteins have to be secreted by the pathogen. Secretion mostly occurs over the ER-Golgi route, meaning that most effectors must contain an N-terminal secretion signal/signal peptide (SP). However, it should be mentioned that secretion of effectors using unconventional secretion has been rarely described as well (Liu *et al.*, 2014). Also characteristic for effector gene candidates is their specific expression pattern that usually correlates with the infection process *on planta*. Widely used prediction parameters are also the small size (Kamoun, 2006) and cysteine richness (Ellis *et al.*, 2009) of effector proteins, although these very strict categories ignore the fact that large as well as cysteine-less effectors have been characterized (Catanzariti *et al.*, 2006; Djamei *et al.*, 2011; Feng *et al.*, 2012).

1.3. The pathosystem *Ustilago maydis – Zea mays*

Over the last decades, the fungus *Ustilago maydis* became the most studied subject within the field of plant pathogenic basidiomycetes (Djamei & Kahmann, 2012). *U. maydis* causes smut disease on all aerial parts of one of the most important crop plants corn and on its progenitor teosinte (both *Zea mays* L.; Christensen, 1963; Brefort *et al.*, 2009; Figure 1.2).

Figure 1.2 Symptoms caused by *Ustilago maydis* on *Zea mays*.
U. maydis causes symptoms on all aerial parts of maize. Shown here are tumor developments on the corn cob (left) and the maize leaf (right).

One key element that allowed the establishment of this fungus as a model organism was its ability to grow axenically and saprophytically under laboratory conditions, making it accessible for genetic manipulation. The yeast like form of *U. maydis*, called sporidium, represents the saprophytic stage of its dimorphic life cycle

(Figure 1.3). To enter the dikaryotic pathogenic stage, two compatible sporidia need to mate, forming a filamentous dikaryon, the infectious life form of *U. maydis*. To proceed its development as a dikaryon, the fungus needs cues from the plant including hydrophobicity and cutin monomers which allow the fungus to initiate the formation of infection structures, termed appressoria (Snetselaar & Mims, 1992; Mendoza-Mendoza *et al.*, 2009). At this stage, before the first penetration attempt, the active suppression of the plant defence by the fungus is initiated (Doehlemann *et al.*, 2008; Bielska *et al.*, 2014). Accordingly, the massive transcriptional induction of hundreds of effector genes starts as early as 24 hours post infection (Mueller *et al.*, 2008). This is essential, especially when considering that *U. maydis* as a biotrophic pathogen is completely dependent on living plant tissue, ergo the survival of the host.

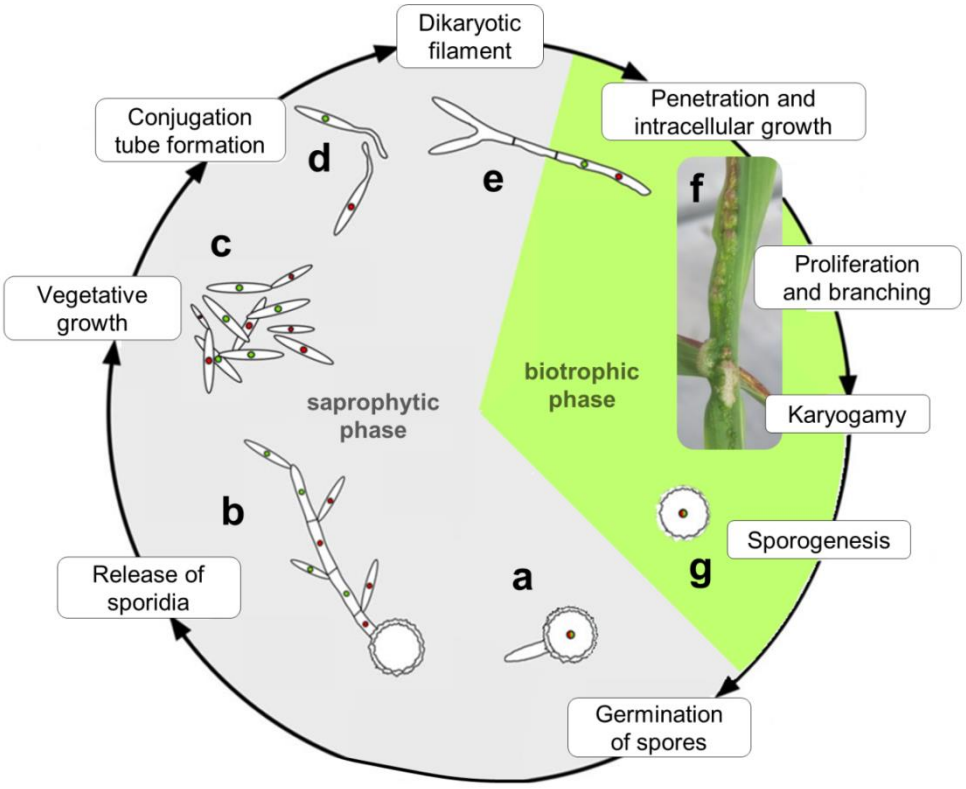

Figure 1.3 Dimorphic lifecycle of *Ustilago maydis*.
The lifecycle of *U. maydis* can be separated into a saprophytic (a-e) and a biotrophic phase (f-g). The saprophytic phase is initiated with the germination of diploid spores (a). The formed basidium (b) releases haploid sporidia (c) that display the vegetative growth form of *U. maydis*. After initiation of conjugation tube formation (d), sporidia of different mating types merge and form a dikaryotic filament, initiating the pathogenic life cycle of *U. maydis*. After penetration of the plants' epidermis via appressoria, the fungal hyphae grow inter- and intracellularly and induce tumor formation (f). Finally, the fungal hyphae aggregate and start to fragment, resulting in karyogamy followed by the formation of new diploid spores (g). Modified from Farfsing, 2004 and Kämper *et al.*, 2006.

The formed appressoria allow for the successful penetration of the plant cell. As a result, the plants' plasma membrane (PM) invaginates, forming the biotrophic interaction zone. Despite the penetration of the cell wall and its intracellular growth, the fungus is never in direct contact with the plants' cytoplasm (Snetselaar & Mims, 1993;

Doehlemann *et al.*, 2009). Within the next few days the fungus starts to massively proliferate inter- and intracellularly, resulting in the formation of tumorous tissue. Inside these structures karyogamy occurs, the fungal hyphae start to fragment and differentiate into melanised diploid teliospores (Banuett & Herskowitz, 1996). Teliospores display the resting stage within the fungal life cycle and can survive long periods of time even under harsh conditions. Under favourable circumstances they germinate and go through meiosis to form haploid sporidia.

Concluding this life cycle would be impossible without the establishment of biotrophy. This goal, as mentioned before, is achieved by the action of numerous effector proteins encoded in the *U. maydis* genome (Kämper *et al.*, 2006). On the genome level, many of them are arranged in clusters. Despite their vital role, only four of the twelve described effector clusters result in a reduction of virulence when deleted (Kämper *et al.*, 2006).

The fact that *Ustilago maydis* is the only smut fungus known today that can induce prominent symptoms on all aerial parts of its host rather than being restricted to the floral organs implicates certain features allowing for this expansion. When considering that the fungus' ability to cause tumors is achieved by fungal signals manipulating the normal program employed for cell proliferation, it makes sense, that within recent years, experimental data has emerged suggesting that alterations within the effector repertoire of *U. maydis* have led to this change (Callow, 1975; Skibbe *et al.*, 2010). Studies investigating transcriptional changes during pathogenic development of *U. maydis* on maize show that the plant organs subjected to tumor formation (here: seedlings, adult leaves and tassels) show very different responses in respect to upregulated genes. Looking at 261 *in silico* predicted secreted fungal proteins that are differentially expressed, only 21% are expressed in all three organs three days post infection, in contrast to 45% with an organ-specific expression pattern. Interestingly, the expression of host genes also shows organ-specific responses, with only 7% differentially expressed transcripts in tassel infections in contrast to more than 30% in infected seedlings (Skibbe *et al.*, 2010). By now, several effectors were identified that show an organ-specific phenotype, meaning that they are dispensable when infecting one organ, but of importance when infecting another (Schilling *et al.*, 2014; Redkar *et al.*, 2015a). Out of these organ-specific effectors, only one was functionally characterized (Redkar *et al.*, 2015a). This fits with the observation that until today, only very limited studies are available explaining the precise role of effector proteins in general. However, the few ones already characterized cover very different key nodes in the plants' defence system addressed by this filamentous pathogen.

As already mentioned, the first obstacles *U. maydis* encounters are at the plants' surface, meaning, for example, enzymes secreted by the plant with the purpose of attacking the fungus. Among the already characterized effectors from *U. maydis*, two counteract the attack of proteolytic enzymes: Pep1 and Pit2 (Protein essential for penetration 1 and Protein involved in tumors 2, Doehlemann *et al.*, 2009; Doehlemann *et al.*, 2011). Both effectors act in the biotrophic interface. Pep1 inhibits plant peroxidases ergo it interferes with the oxidative burst by scavenging reactive oxygen species generated by the plant (Hemetsberger *et al.*, 2012). Pit2 on the other hand inhibits cysteine proteases to suppress the immunity of the host plant maize (Mueller *et al.*, 2013).

As important as the successful handling of key molecules in the biotrophic interface, like e.g. the mentioned plant enzymes, is the directed manipulation of plant metabolism. To achieve this, the effector protein has to translocate into the plant cell. Until today, the molecular mechanism by which effectors are translocated in the *U. maydis/ Z. mays* pathosystem has not been determined (Tanaka *et al.*, 2015). To experimentally show the process of translocation or the presence of a translocated protein is one of the more difficult challenges within the field of *U. maydis* research, as common techniques, successful in other pathosystems, give inconclusive results. The only reliable approach so far indicating the translocation of an effector protein, requires the researcher to employ immunoelectron microscopy (Tanaka *et al.*, 2015). However, even the use of immunoelectron microscopy is not without challenges, as the method is not only technically demanding, but also requires strong expression of the analysed protein. Additionally, the protein needs to be tagged, which in some cases may lead to a non-functional fusion protein. Despite those difficulties, three cytoplasmic effectors have been functionally characterized until today. These translocated proteins tackle different metabolic branching points important for the defence system of the plant. Cmu1 (chorismate mutase 1), a secreted chorismate mutase re-channels chorismate into the phenylpropanoid pathway to outcompete its usage for the biosynthesis pathway of the plant defence hormone salicylic acid (Djamei *et al.*, 2011). Another characterized translocated effector is Tin2 (Tumor inducing 2,Tanaka *et al.*, 2014). Tin2 is proposed to interfere with a secondary metabolite pathway, the biosynthesis of lignin. It promotes the biosynthesis of anthocyanin, a vacuolar pigment accumulating in infected tissues, by stabilizing the maize protein kinase ZmTTK1. By doing so, it limits the availability of precursor molecules needed for lignin biosynthesis (Tanaka *et al.*, 2014). Just recently the effector See1 (Seedling efficient effector 1, Redkar *et al.*, 2015a) was characterized. See1 is an organ-specific effector of *U. maydis*, important for the infection of maize

seedlings, but dispensable for the infection of tassel tissue. See1 interacts with the maize homolog of SGT1 (Suppressor of G2 allele of skp1) involved in cell cycle control in yeast (Redkar *et al.*, 2015a).

Little research has been conducted investigating the role of specific maize proteins required for the interaction of *Z. mays* and *U. maydis*. One emerging picture though is that there seem to be no gene-for-gene interactions among the players of this pathosystem known until today. It rather seems to be the case that the interplay of different genes results in the observed differences in disease severity and frequency when looking at different maize varieties (Baumgarten *et al.*, 2007). The most commonly used maize cultivar (cv.) in the *Ustilago maydis* field is Early Golden Bantam (EGB). EGB, as a sweet corn variety, is reported to be more susceptible to *U. maydis* infection than field corn (Agrios, 1988; White, 1999). Another relevant maize accession is the inbred line B73, an important commercial cultivar, which is widely used in a variety of research areas and has recently been fully sequenced (Schnable *et al.*, 2009). However, despite the fact that a lot of data is available regarding B73s susceptibility to a range of pathogens(Wisser *et al.*, 2006), there are no studies so far using B73 as a host for *U. maydis*.

1.4. Smut fungi related to *Ustilago maydis*

Genetically, the model fungus *U. maydis* is closely related to a variety of other plant pathogenic smuts. Of main interest among those which have been established as model systems, are *Ustilago hordei*, a fungus causing head galls on *Hordeum vulgare*, *Sporisorium reilianum*, a head smut that infects maize, and *Sporisorium scitamineum*, which causes disease on all species of sugar cane. Interesting for different reasons are two other species, namely *Melanopsichium pennsylvanicum* and *Ustilago bromivora.* In contrast to the other mentioned smuts that only infect specific monocot hosts, *M. pennsylvanicum* infects a dicotyledonous host plant, namely species of the genus Persicaria (Sharma *et al.*, 2014). *Ustilago bromivora* on the other hand, a so far rather poorly characterized head smut, infects the model grass *Brachypodium distachyon* which would allow much faster studies on the plant side of smut host interactions (Barbieri et al., 2011). Despite their differences, all mentioned smut fungi use effectors to establish biotrophy (Doehlemann *et al.*, 2009; Schirawski *et al.*, 2010; Sharma *et al.*, 2014).

1.5. Goal of this thesis

The goal of this thesis is to elucidate the role of UMAG_02011 (ApB73, apathogenic in B73) within the *U. maydis* - *Z. mays* interaction.

From published microarray data it is known that *apB73* is upregulated during biotrophy, making it an interesting candidate for a role in virulence.

To investigate the role of *apB73,* the involvement of ApB73 in virulence or in other fungal processes had to be addressed. In case of results pointing towards a possible role in virulence, strains carrying deletions of *apB73* will be subjected to virulence assays using different maize accessions. Next, it will be examined if ApB73 qualifies as an effector or virulence factor, by analysing if ApB73 is secreted into the biotrophic interface.

Additionally, the thesis aims to conduct experiments shedding light towards a possible function of this protein, by identifying its place of action and possible interaction partners.

Finally, it will be looked at orthologous proteins of ApB73 from related smut fungi to determine similarities and differences among them. To this end, different orthologs will be subjected to assays revealing a possible functional redundancy.

2 Results

2.1. Discovery of ApB73

One of the characteristic features of an effector is its specific expression during pathogenic development. Accordingly, I had a look at published microarray data to search for potential effector candidates, ergo genes specifically upregulated during biotrophic growth stages (Skibbe *et al.*, 2010). Within the data, I found UMAG_02011 (ApB73, apathogenic in B73), a 709 amino acid (aa) large protein with a putative N-terminal secretion signal (Petersen *et al.*, 2011). To confirm the microarray results, quantitative real time PCR analysis of *apB73* was performed on maize tissue infected with the *U. maydis* wildtype strains FB1/FB2 and harvested at various time points. The values were normalized to the constitutively expressed gene peptidyl-prolyl isomerase (*ppi*) and the reference was set to the values obtained for axenic culture by arbitrarily setting it to 1. The data show that *apB73* is upregulated more than a 100 fold during the biotrophic growth stages of *U. maydis* (Figure 2.1).

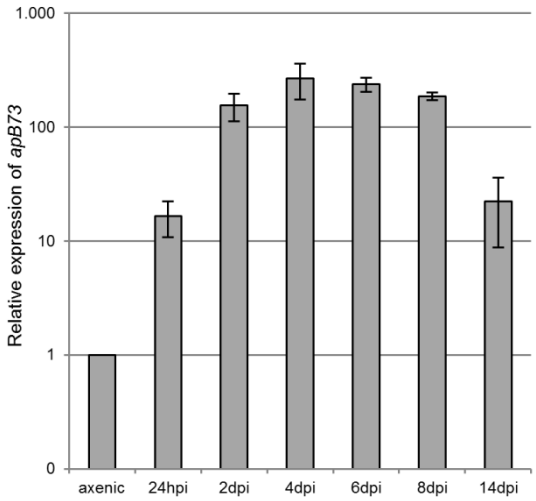

Figure 2.1 *apB73* is upregulated during biotrophic growth stages.
Transcript levels of *apB73* measured at different growth stages of FB1/FB2 by quantitative real time PCR. Samples were taken from axenic culture and during different stages of maize infection, ranging from 24 hours post infection (hpi) to 14 days post infection (dpi). For normalization, the constitutive gene peptidyl-prolyl isomerase (*ppi*) was used and values for axenic culture were arbitrarily set to 1. Three biological replicates were analysed, error bars indicate standard deviation.

2.2. Bioinformatical analysis of ApB73

After confirming that *apB73* is transcriptionally upregulated during biotrophic stages, bioinformatic tools were used to see if any further information can be obtained analysing its amino acid composition. *apB73* (UMAG_2011) is located on chromosome three of the *Ustilago maydis* genome. It does not contain any introns and, considering the flanking genes, is not predicted to be part of a gene cluster as it has been described for many other *U. maydis* effector genes (Kämper *et al.*, 2006). The upstream flanking coding sequence (CDS) is UMAG_02010 (*aro-8*), which is predicted to be related to the family

of II 2-keto-3-deoxy-D-arabino-heptulosonate 7-phosphate synthases involved in amino acid metabolism. The next CDS downstream of *apB73* is UMAG_02012, a hypothetical protein that may be involved in sugar, glucoside, polyol and carboxylate metabolism. The flanking genes are not predicted to be secreted. ApB73, however, has an 19 amino acid long N-terminal secretion signal according to the prediction program SignalP indicating its secretion (Petersen *et al.*, 2011).

With 709 aa, ApB73 is a fairly big protein, especially when considering it as a candidate for an effector protein. Despite that size, available prediction programs and similarity searches fail to determine known protein domains in ApB73, apart from the mentioned N-terminal SP.

Orthologous proteins to ApB73 can be found in several related smut fungi, including *S. reilianum*, *S. scitamineum, U. hordei, U. bromivora* and *M. pennsylvanicum*. None of the mentioned orthologous proteins has been characterized so far. Interestingly, ApB73 orthologs can also be found in several Pseudozyma species, e.g. *P. aphidis*, a non-pathogenic yeast-like fungus (Buxdorf *et al.*, 2013). However, as this is also true for many other already characterized effector proteins from *U. maydis* (e.g. Cmu1, Tin2 and Pep1), a possible role in a non-pathogenic fungus does not exclude a possible function in the pathogenicity of *U. maydis*.

2.3. ApB73 is not needed for non-infection related stress responses

During the infection process, the pathogen is exposed to a variety of stresses, either as a result of its own elevated metabolism or due to the defence machinery of the host. Therefore, it was tested if upregulation of *apB73* is a response to stress in general, or if it is specifically required for the establishment of biotrophy. To this end, growth assays of *apB73* deletion and overexpression strains on different stress providing media were performed.

To elucidate the specific role of ApB73*,* deletion strains in the background of the solopathogenic progenitor strain SG200 were generated by homologous recombination (Kämper *et al.*, 2006). Additionally, an overexpressor strain was produced by ectopically introducing ApB73 into SG200 under the strong constitutive *oma* promoter (Flor-Parra, 2006). The resulting strains were spotted onto different stress inducing media, including cell wall stress (Calcofluor, Congo red), oxidative stress (H_2O_2), salt stress (NaCl) and nutrient limitation (ammonium minimal and nitrate minimal medium). Growth rates were observed two days later (Figure 2.2).

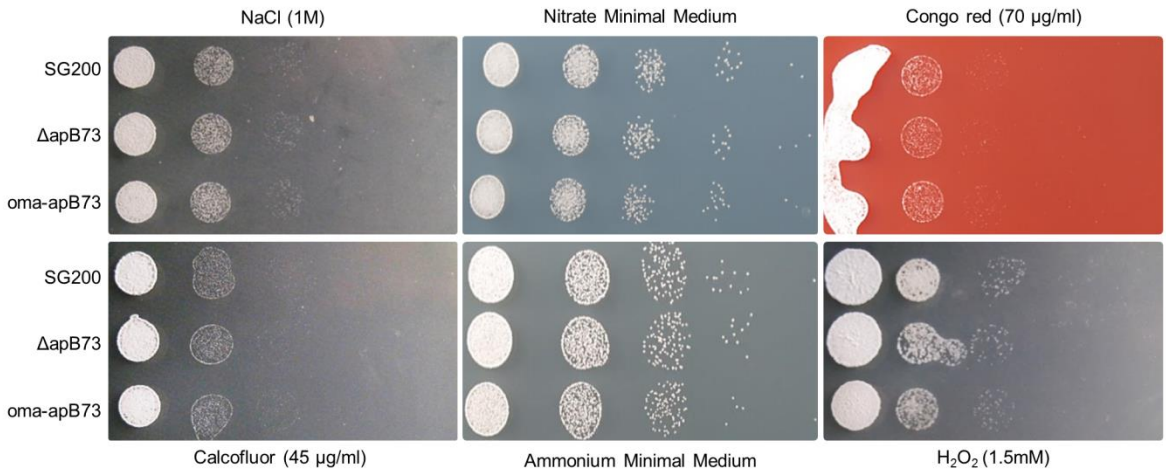

Figure 2.2 ApB73 does not affect fungal growth under stress conditions.
Growth of *U. maydis* strains SG200, SG200ΔapB73 and SG200ΔapB73-P_{oma}-apB73 on media inducing different stresses. First, *U. maydis* pre-cultures were grown to an OD_{600} of 1.0. Cells were washed in water, and 10 fold serial dilutions were prepared. Seven microliters from each of these solutions were dropped on the different media. Pictures were taken 48 hours later. Media used from top left to bottom right: CM agar containing 1M NaCl; Nitrate Minimal medium; CM agar supplied with Congo red (70 µg/mL); CM agar supplied with Calcofluor (45 µg/mL); Ammonium Minimal Medium; CM agar supplied with 1.5 mM H_2O_2.

No differences in the growth behaviour of the deletion mutant or the overexpressor strain in comparison to the progenitor strain SG200 were observed. This indicates that, under the tested conditions, ApB73 is not required for non-infection related stress responses.

2.4. ApB73 has a severe impact on virulence

Next, it was tested if ApB73 is important for virulence of *U. maydis*. To do so, disease assays were performed. Seven day old maize seedlings of cv. B73 were infected with the solopathogenic progenitor strain SG200, the deletion strain SG200ΔapB73 and a complementation strain SG200ΔapB73-P_{apB73}-ApB73-HA. The complementation strain was generated by ectopic integration of ApB73-HA under its native promoter into the *ip* locus (Keon *et al.*, 1991; Loubradou *et al.*, 2001) of SG200ΔapB73 and was used to ask for gene-specific causality of a possible effect. One prerequisite for pathogenicity is *b*-dependent filamentous growth (Kahmann & Kämper, 2004), which can be tested on charcoal plates. Unimpaired mixed strains of compatible mating types form mating hyphae resulting in a fluffy colony morphology (to illustrate this behaviour see Figure 2.3).

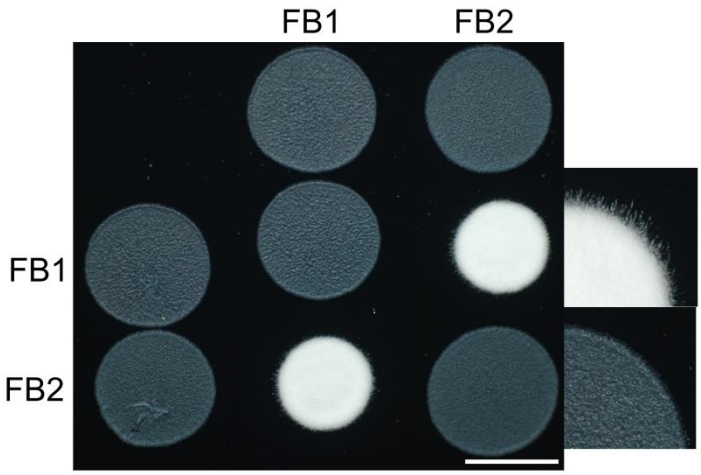

Figure 2.3 Filament induction on charcoal plates after mating wildtype strains FB1 and FB2.
U. maydis pre-cultures of the two wildtype strains FB1 and FB2 were grown to an OD_{600} of 1.0 and individually or as a mixture dropped on charcoal plates. The two strains, FB1 and FB2, have different mating types that allow them to mate (recognizable by the fuzzy/more white colony morphology), whereas strains with the same mating type cannot mate when mixed together resulting in no filament formation. The right panel shows a close up of the charcoal induced filaments. Picture was taken 24 hours after dropping. Bar = 0.5 cm.

The induction of *b*-dependent filamentous growth was tested for the *apB73* mutant strain and the complementation strain, and neither of them was impaired (Figure2.4a). The results of the virulence assay are shown in Figure 2.4b.

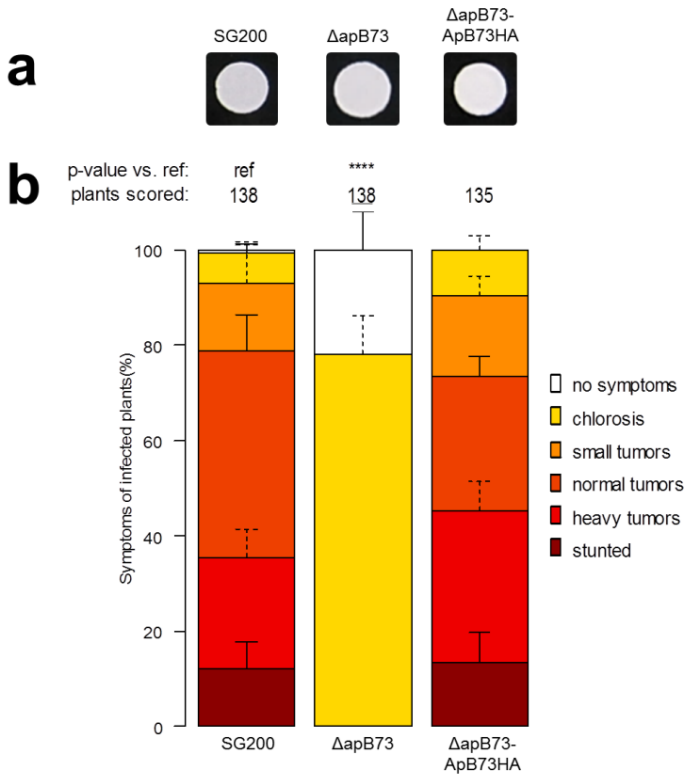

Figure 2.4 ApB73 is essential for virulence of *U. maydis* in maize accession B73.
(a) Filament formation on charcoal plates. Shown are the progenitor strain SG200, the deletion strain ΔapB73 and the complementation strain ΔapB73-apB73HA. Pictures were taken 24h after spotting. **(b)** Disease rating of maize seedlings of cv. B73 infected with the progenitor strain SG200, the SG200ΔapB73 deletion strain or the complementation strain SG200ΔapB73-apB73HA. Disease scores are shown on the right. Mean values of three independent infections are depicted and the total number of infected plants is indicated above the respective columns. Mean and standard deviation of relative counts from replicates are displayed. For clarity, only positive error bars are shown. P-values were calculated by Fisher's exact test. ****, P <0.0001. Tumor formation is abolished in SG200ΔapB73 and can be complemented by introducing *apB73HA*.

The virulence assay shows that the deletion of *apB73* results in a complete loss of tumor formation on maize cv. B73. The strongest symptom observed here is chlorosis. The complementation strain SG200ΔapB73-P_{apB73}-apB73HA causes symptoms similar to SG200, illustrating that reintroduction of ApB73 fully restores the virulence defect of the mutant strain.

2.5. Microscopic analysis of the virulence defect

The dramatic virulence phenotype caused by the deletion of *apB73* indicates that the protein could be part of one or several infection strategies developed by the fungus to overcome the various constraints imposed by the plant. One possibility, as it has been shown for the effector Pep1 (Doehlemann *et al.*, 2009), would be that ApB73 is required for the fungus' ability to penetrate the epidermis. If this was the case, this should be visible when microscopically observing infected plant tissue. Accordingly, microscopy of different fungal infection stages, namely two and seven days post infection, was performed, using SG200, SG200ΔapB73 and the complementation strain SG200ΔapB73-P_{apB73}-apB73HA. For visualization, two different stains were applied. To observe the fungus, chitin, a characteristic component of fungal cell walls, was stained in green using wheat germ agglutinin (WGA) coupled to Alexa Fluor 488 (AF488). As a counterstain propidium iodide was applied to stain the plant cell wall and dead cells red (Figure 2.5).

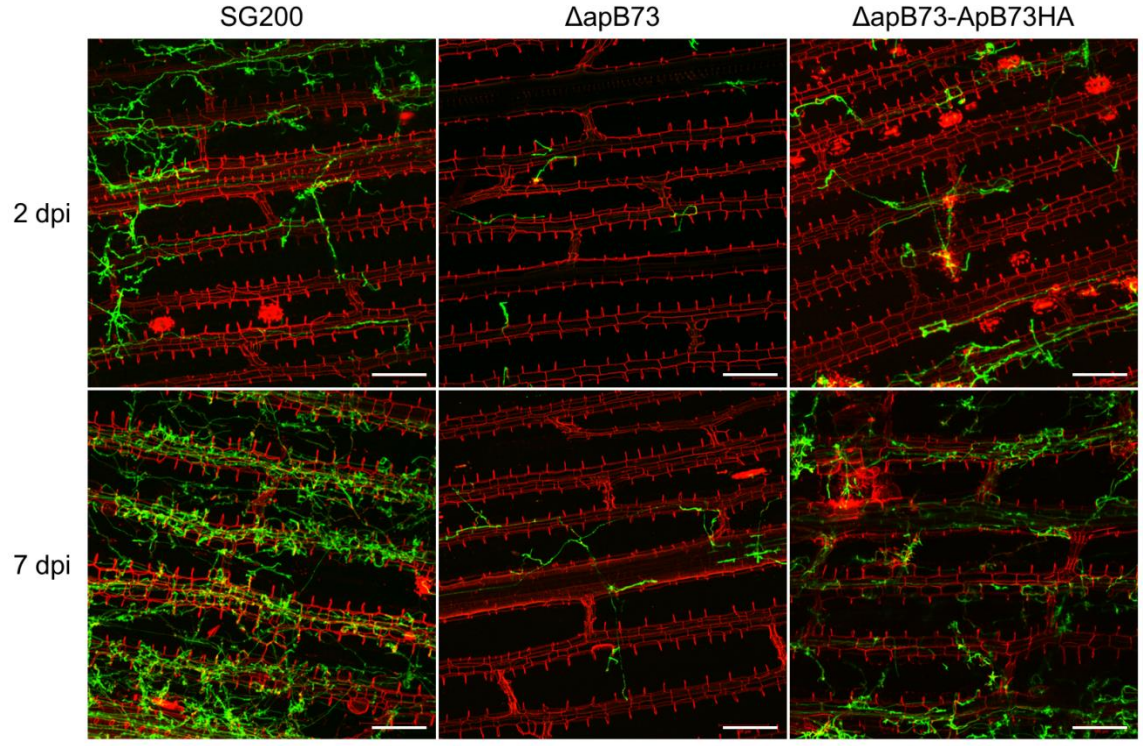

Figure 2.5 Microscopic overview of the ApB73 virulence phenotype on a tissue level.
Seedlings of maize cv. B73 were infected with the progenitor strain SG200, the SG200ΔapB73 deletion strain or the complementation strain SG200ΔapB73-ApB73HA. Infected leaf tissue was harvested two or seven days post infection. Images were taken after staining the tissue with WGA-AF488 (green), to visualize fungal chitin, and propidium iodide (red) to observe plant cell walls. Bar = 100 µm. The SG200ΔapB73 strain is drastically impaired in colonization of the maize tissue. This defect can be complemented by introducing *apB73HA*.

Microscopic analysis shows a situation that is comparable to the disease rating that was conducted on the macroscopic level (Figure 2.4). The maize tissue infected with the mutant strain shows less fungal hyphae in total and the fungal hyphae present do not

seem to be able to proliferate and branch in the same way the progenitor strain and the complementation strain do. The reduced branching and capability to proliferate within new intact cells becomes even more obvious when having a closer look at individual cells (Figure 2.6).

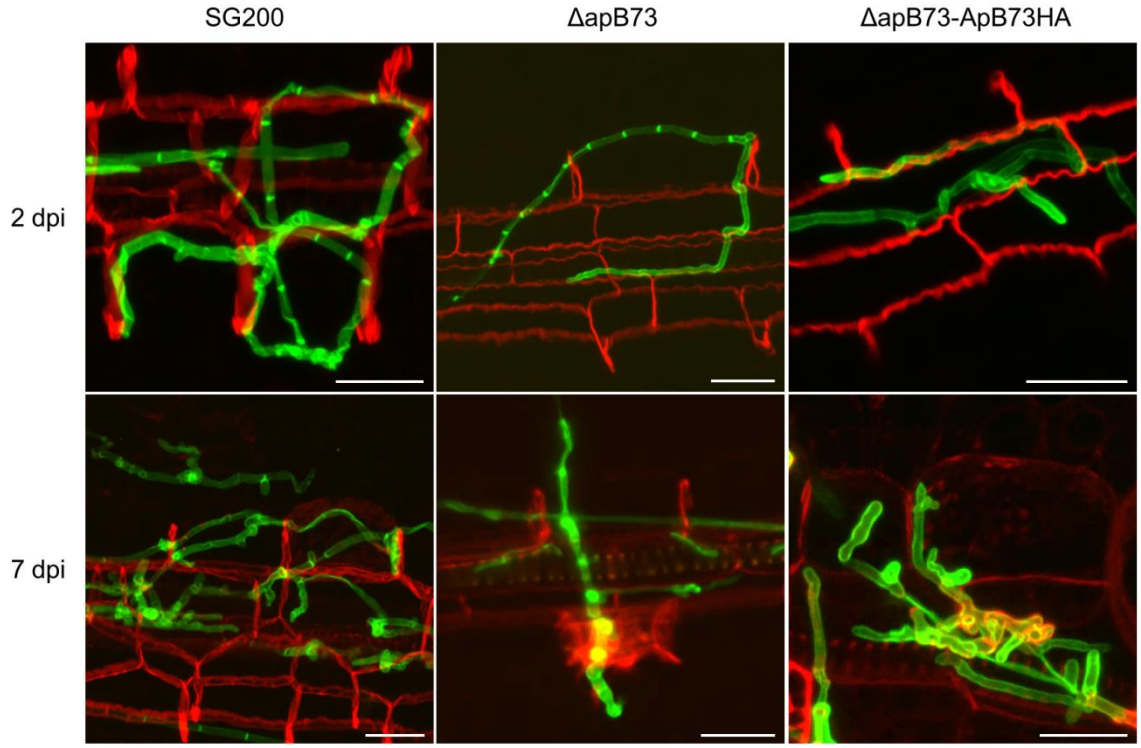

Figure 2.6 Microscopic analysis of the ApB73 virulence phenotype at a cellular level.
Maize seedlings of maize cv. B73 were infected with the progenitor strain SG200, the SG200ΔapB73 deletion strain or the complementation strain SG200ΔapB73-ApB73-HA. The tissue was harvested two or seven days post infection. Images were taken after staining the tissue with WGA-AlexaFluor488 (green) to visualize fungal chitin and propidium iodide (red) to observe plant cell walls. Bar = 20 µm.

Microscopy of infected maize tissue on a cellular level shows, that although the SG200ΔapB73 mutant strain still appears to be capable of forming appressoria and penetrating the plants cuticle, branching and therefore proliferation inside the plant is strongly reduced. To confirm that the formation of appressoria and penetration structures in the *apB73* mutant is comparable to the progenitor strain, a microscopy based assay was conducted comparing appressoria marker induction and penetration efficiency of fluorescently labelled *apB73* mutant and progenitor strains (see Figure 2.7 for representative image).

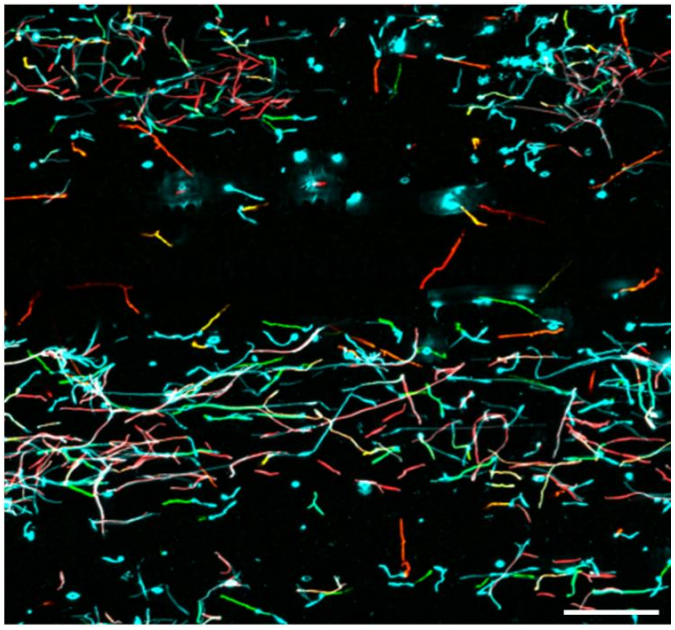

Figure 2.7 Representative picture used to evaluate appressoria marker induction and penetration efficiency of the *apB73* mutant compared to SG200.
Shown are the analysed filaments on an infected maize leaf. For the infection, two strains (SG200AM1-RFP and SG200ΔapB73-AM1) with an OD_{600} = 1 were mixed, infected into maize cv. B73 and stained with Calcofluor white 18-20 hours post infection. SG200AM1 cells appear red (RFP) and blue (Calcofluor white stain), SG200AM1 cells with induced appressoria marker will appear blue/red and green (GFP), SG200ΔapB73-AM1 strains look blue or green/blue after induction of the appressoria marker. Bar = 10µm.

This assay makes use of a promoter specifically induced in appressoria, called AM1 (Appressoria Marker 1, Mendoza-Mendoza *et al.*, 2009), to drive GFP expression. In the shown experiment, the ΔapB73 mutant and SG200 progenitor strain both express AM1-GFP. To be able to differentiate between the two strains, SG200 contains an additional construct constitutively expressing RFP (SG200AM1-RFP, Mendoza-Mendoza *et al.*, 2009). This way, the two strains can be simultaneously infected into the same plant, allowing the comparison of appressoria formation of the two strains in the same tissue (red and green hyphae vs. green hyphae). Additionally, the infected tissues were stained with Calcofluor white, a substance staining fungal hyphae by binding to chitin, to evaluate the total number of hyphae. This also permits the evaluation of penetration efficiency, as cytosolic GFP will also be visible in penetrated hyphae, whereas calcofluor white only stains fungal hyphae on the leaf surface. The results comparing the induction of the appressoria marker and penetration efficiency of the ΔapB73 mutant and SG200 are shown in Figure 2.8.

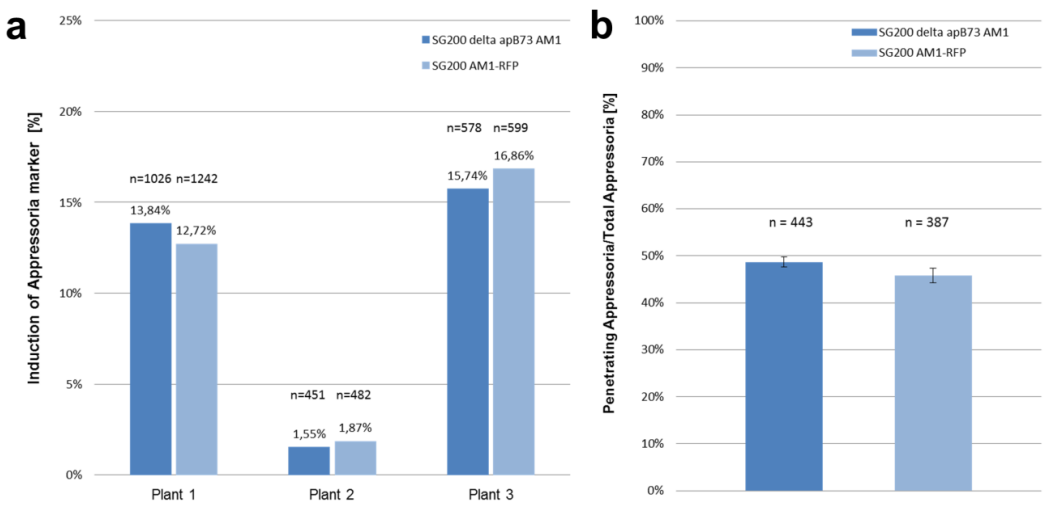

Figure 2.8 Appressoria marker induction and penetration efficiency are not impaired in the *apB73* mutant strain.
(a) Comparison of the induced appressoria marker in SG200AM1-RFP or SG200ΔapB73-AM1. Three independent plants were analysed, as efficiency greatly varies depending on the analysed area and plant. The experiment was repeated two times with similar results. **(b)** Penetration efficiency of the formed appressoria in SG200AM1-RFP or SG200ΔapB73-AM1. Penetrated hyphae expressing cytoplasmic GFP cannot be stained by Calcofluor white allowing the quantification of penetration efficiency (ratio of green vs. blue/green hyphae). Error bars indicate standard deviation.

The results show, that the rates for appressoria formation and penetration efficiency of the *apB73* mutant are progenitor-strain like. Similar observations have been made previously when investigating the microscopic virulence phenotype of the *U. maydis* Δpit1 mutant, a non-secreted membrane protein (Doehlemann *et al.*, 2011). Summarizing these observations, the *apB73* mutant strain appears to be constrained in effectively colonizing the maize leaf tissue after initial penetration, rather than showing a defect in penetration itself.

2.6. ApB73 mutant strains are impaired in sporogenesis

Dealing with such a severe virulence phenotype implies the question if the deletion of *apB73* is actually evolutionary lethal for the fungus, or differently, if lacking ApB73, leads to a defect that does not allow for the formation of spores, ergo the completion of the biotrophic phase of *U. maydis'* life cycle.

As the formation of spores requires the karyogamy of diploid cells, the solopathogenic strain SG200 was not used for this experiment, but rather the two compatible haploid wildtype strains FB1 and FB2 (Banuett & Herskowitz, 1989). Deletion mutants of *apB73* were generated via homologous recombination in the FB1 and FB2 background, respectively. After confirming the successful deletion of *apB73* by Southern blot analysis, the obtained strains were tested for their capability to mate. Mating, as a prerequisite for *U. maydis* in establishing infection on *Z. mays* (Kahmann & Kämper, 2004), could have been affected by the deletion of *apB73.* The wildtype progenitor

strains FB1 and FB2, as well as two independent *apB73* mutants of FB1 and FB2 respectively, were spotted individually and in a 1:1 mixture on charcoal plates (Figure 2.9a). The results show that the deletion of *apB73* does not have an influence on the formation of dikaryotic filaments.

To test for the formation of spores, the male reproductive organs (tassels) of maize cv. Gaspe Flint were infected. Gaspe Flint was used here for several reasons. As a dwarf *Z. mays* cultivar, it completes its life cycle in only 30-35 days with a floral switch as early as 15 days. Accordingly, it is more eligible for early tassel infections. 15 day old maize plants of cv. Gaspe Flint were infected using FB1xFB2 and FB1ΔapB73 xFB2ΔapB73 and symptoms were observed 18 days post infection (Figure 2.9a).

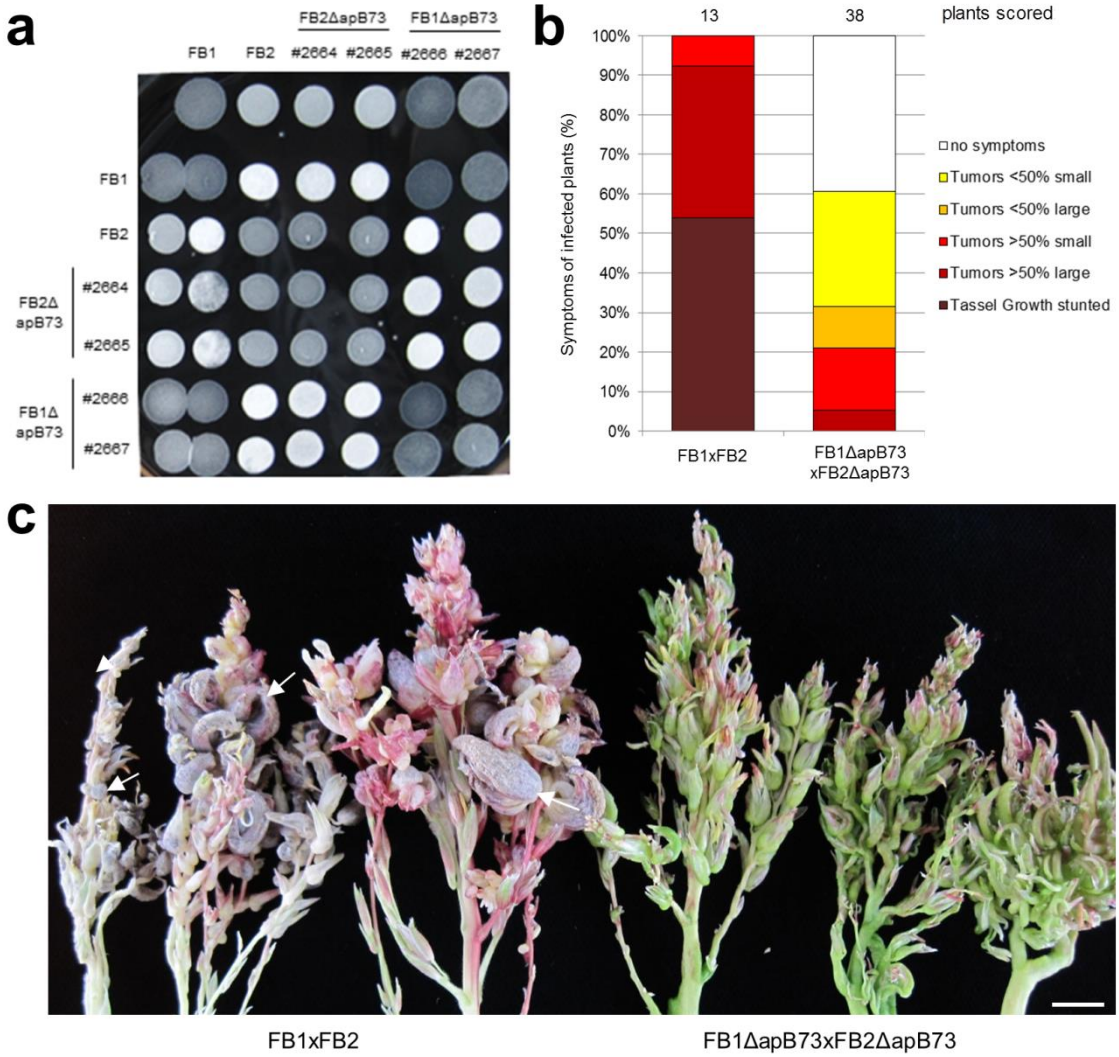

Figure 2.9 ApB73 is required for spore formation.
(a) Mating assay on charcoal plates. The wildtype strains FB1 and FB2, as well as, two independent *apB73* mutants of FB1 and FB2 were spotted onto charcoal containing plates to test for mating and subsequent filament formation. Picture was taken after 24h. **(b)** Disease scoring of tassel infections. Maize cv. Gaspe Flint was infected using either FB1xFB2 or FB1ΔapB73xFB2ΔapB73 and symptom formation on female floral organs was observed 18 days post infection. Disease scores are shown on the right and the total number of infected plants is indicated above the respective columns. **(c)** Tassel phenotype of maize plants infected with FB1xFB2 or FB1ΔapB73xFB2ΔapB73. Representative tassels were chosen to illustrate symptom development of the used strains. Picture was taken 18 dpi. The white arrows indicate greyish areas resulting from encased black teliospores. Bar = 1 cm.

Although both strain combinations were able to cause tumors, symptoms were more severe for the infection with the wildtype strains FB1xFB2. However, the induction of tumorous structures does not seem to be sufficient to allow spore formation. A closer look at the infected tassel tissue shows that the FB1xFB2 combination was able to form a substantial amount of spores (Figure 2.9c, white arrows indicating greyish looking tissue as a result of encased black teliospores). In contrast, the *apB73* deletion strains seem to fail to produce spores (Figure 2.9c, all tassel tissue is green or pinkish). To clarify this, the tissue was investigated microscopically by staining infected tassel material with WGA-AlexaFluor488 (Figure 2.10).

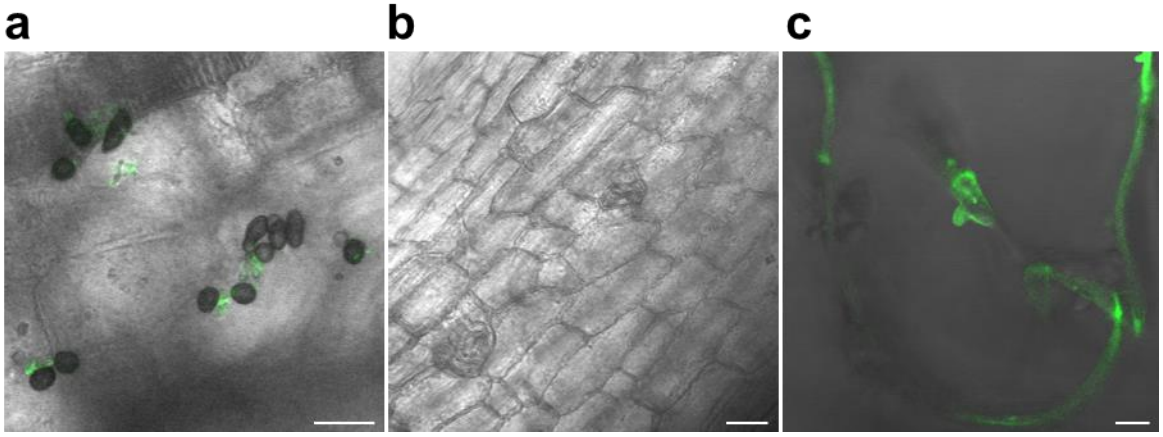

Figure 2.10 Microscopy of infected tassels stained with WGA-AlexaFluor488.
Representative pictures from infected tassel material. Maize cv. Gaspe Flint was infected using either FB1xFB2 or FB1ΔapB73xFB2ΔapB73 and infected male floral organs were observed 18 days post infection. Bar = 20 µm. **(a)** Germinating spores observed in tassel infected with FB1xFB2. **(b)** Tumorous tissue without signs of *U. maydis* infection observed on tassels infected with FB1ΔapB73xFB2ΔapB73. **(c)** Fungal hyphae of *U. maydis* on tassels infected with FB1ΔapB73xFB2ΔapB73.

The pictures show that in the tassels infected with FB1xFB2, germinating spores can be abundantly detected (Figure 2.10a), whereas the FB1ΔapB73xFBΔapB73 infected tassels do not show any spores, but rather undisturbed flower material (Figure 2.10b) or intracellularly branched fungal hyphae (Figure 2.10c).

Another possibility would be that it takes the mutant strains longer to complete their life cycle, however, even 40 days post infection no spores could be observed, whereas the FB1xFB2 infected flowers show first signs of spores as early as 12 dpi (data not shown, Banuett & Herskowitz, 1996). This result indicates that lack of ApB73 directly or indirectly inhibits fungal growth and development on its host plant maize to an extent that completion of the biotrophic phase of the *U. maydis* life cycle is no longer possible.

2.7. Virulence phenotype in different maize accessions

The tassel infection experiments conducted on the maize cv. Gaspe Flint were revealing in many ways. Not only, because they show that ApB73 seems to be important for spore formation, but also because the FB1/FB2 mutant strains still seem to be able to induce

tumor formation (at a strongly reduced rate) on Gaspe Flint. In contrast, when infecting cv. B73 using the SG200ΔapB73 strain, tumor formation was completely abolished (Figure 2.4). Even though it is known that infections performed with the FB1/FB2 dikaryon are much more pathogenic than infections with the solopathogenic strain SG200, I also wanted to test if the difference in infection severity was affected by the used host accession.

As a result, virulence defects of the mutant strain were analysed in the most commonly used maize cultivar in the *Ustilago maydis* field, the sweet corn Early Golden Bantam (EGB). To have a direct comparison between accessions, maize cv. EGB and B73 were simultaneously infected with SG200 and the mutant strain ΔapB73 (Figure 2.11).

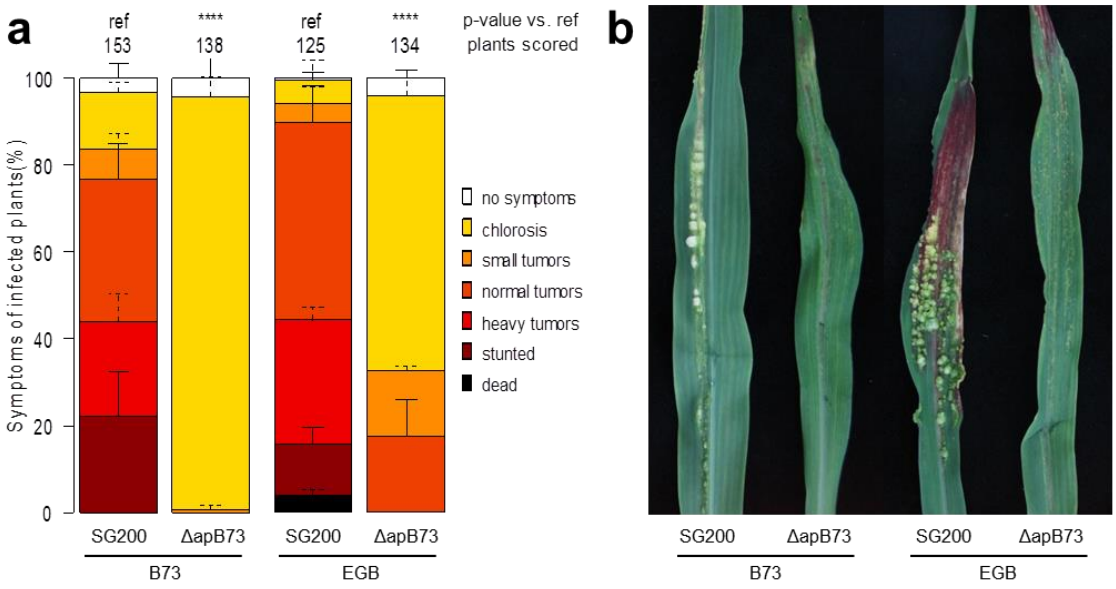

Figure 2.11 The effect of ApB73 on virulence varies in different maize accessions.
(a) Virulence assay of the SG200 and the ΔapB73 mutant using maize cultivar B73 or EGB. Seedlings were infected seven days after germination and scored for symptoms 12 dpi. Disease scores are shown on the right. Mean values of three independent infections are depicted and the total number of infected plants is indicated above the respective columns. Mean and standard deviation of relative counts from replicates are displayed. For clarity, only positive error bars are shown. P-values were calculated by Fisher's exact test. ****, P <0.0001. **(b)** Representative pictures of EGB and B73 maize leaves infected with SG200 or ΔapB73. Seedlings were infected seven days after germination and observed 12dpi.

Interestingly, and in contrast to maize cv. B73, the SG200ΔapB73 deletion strain is capable of inducing tumor formation on maize cv. EGB but at a lower rate (tumor rate 65% reduced in EGB in contrast to a 99% reduction in B73). This shows that different maize accessions respond differently to infection with *U. maydis apB73* mutant strains.

2.8. Localization of ApB73

The previously described data shows that *apB73* is specifically upregulated during biotrophic growth of *U. maydis,* and that ApB73 is involved in the pathogenic

development of the fungus on its host plant *Z. mays*. This indicates that the ApB73 protein is a virulence factor of *U. maydis.* However, the question remains whether ApB73 qualifies as an effector. Virulence factors are proteins capable of affecting the performance of a pathogen in its pathogenic life style. Effectors, a sub-class of virulence factors, are proteins that directly or indirectly interact with the host during the establishment of an interaction. One hallmark of *U. maydis* effectors, and the first prerequisite that needs to be matched, is their secretion into the apoplastic space: the biotrophic interface.

2.8.1. ApB73 fusion proteins localize to the biotrophic interface

To test for the secretion of ApB73, fusion proteins of ApB73 and mCherry were generated. The construct, encoding for ApB73-mCherryHA under the native *apB73* promoter, was ectopically integrated into the *ip* locus of the SG200ΔapB73 mutant. Five days after seedling infection of maize cv. B73, the infected tissues were observed microscopically (Figure 2.12).

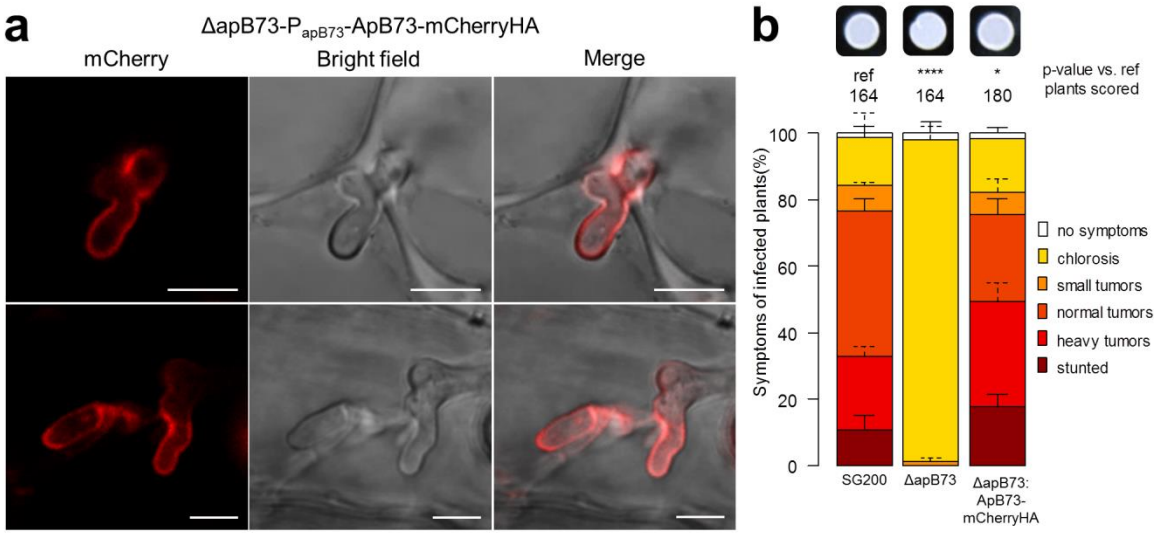

Figure 2.12 The ApB73-mCherryHA fusion protein localizes around the hyphae and complements the mutant phenotype.
(a) Secretion of ApB73-mCherryHA in infected maize plants. Leaves were infected with SG200ΔapB73-P$_{apB73}$-ApB73$_{1-709}$-mCherryHA and fluorescence was observed five days post infection. Bar = 5 µm. **(b)** Virulence assay confirming the functionality of the ApB73-mCherryHA fusion protein. Seven day old maize seedlings of cv. B73 were infected and twelve days later symptoms caused by a strain expressing ApB73-mCherryHA, under the control of the native *apB73* promoter, were compared to the deletion strain ΔapB73 and the progenitor strain SG200. In the top row, pictures of the respective strain are shown after growing on filamentation inducing charcoal plates for 24h. Disease scores are shown on the right. Mean values of three independent infections are depicted and the total number of infected plants is indicated above the respective column. Mean and standard deviation of relative counts from replicates are displayed. For clarity, only positive error bars are shown. P-values were calculated using Fisher's exact test. *, P<0.05; ****, P<0.0001.

Microscopy of maize leaves infected with a strain expressing ApB73-mCherryHA, shows that the fusion protein primarily localizes around the fungal hyphae and that the mCherry signal seems stronger at the hyphal tip, the main place of fungal secretion

(Figure 2.12a, Bielska *et al.*, 2014). To ensure, that this observation is no artefact and that the fusion protein retains the function of ApB73, a virulence assay was performed (Figure 2.12b). It shows that the mutant strain expressing ApB73-mCherryHA fully complements the mutants' virulence phenotype, indicating the functionality of the fusion protein. Attempts to biochemically detect the full length protein by immunoprecipitation and Western blot analysis failed, likely due to weak expression from the *apB73* promoter.

2.8.2. ApB73 is not detectable in supernatant assays

The localization of the ApB73-mCherryHA fusion protein around the fungal hyphae is a good indication that ApB73 might be secreted. However, due to the fact that the full length protein could not be detected using Western blot analysis, the microscopy results should be confirmed using a different technique.

Supernatant assays where Western blot analysis is performed on secreted proteins are widely used to examine protein secretion. These assays are based on the idea that fungi grown axenically should secrete proteins into the surrounding culture medium. These proteins are precipitated using Trichloroacetic acid (TCA)/Sodium deoxycholate (DOC) and can be finally detected by Western blot analysis. As there is no specific antibody available for ApB73, HA-tagged proteins were used for this experiment.

Within the life cycle of the fungus, secretion is of special importance on the plant leaf, as this is the time when the fungus needs to suppress plant defence responses with the help of secreted effector proteins. To be able to conduct this experiment on a developmental stage normally only present on the plant leaf, I made use of the genetically modified strain AB33 (Spellig *et al.*, 1996; Brachmann *et al.*, 2001). AB33 expresses a heterodimeric transcription factor that is responsible for filamentation in the context of pathogenic development, under a nitrate inducible promoter (P_{nar}).

Accordingly, a AB33 strain was generated expressing ApB73 under the control of the *otef* promoter (Spellig *et al.*, 1996), which is constitutively active in axenic culture, and a supernatant assay was performed (Figure 2.13). Cell extracts and supernatants of the background AB33 strain were included to ensure specificity of the antibody. To confirm that only the supernatant, ergo the medium, is precipitated without any remnant cells, actin was detected as a lysis control. In the lysis control, bands can only be seen for whole cell extracts. Previous experiments showed that, although using identical culture volumes, the protein yield of Cmu1-HA is higher in comparison to ApB73-HA. Accordingly, compared to Cmu1-HA, five times as much protein extract, obtained from the precipitated supernatant of strain AB33-P_{otef}-ApB73-HA, was loaded.

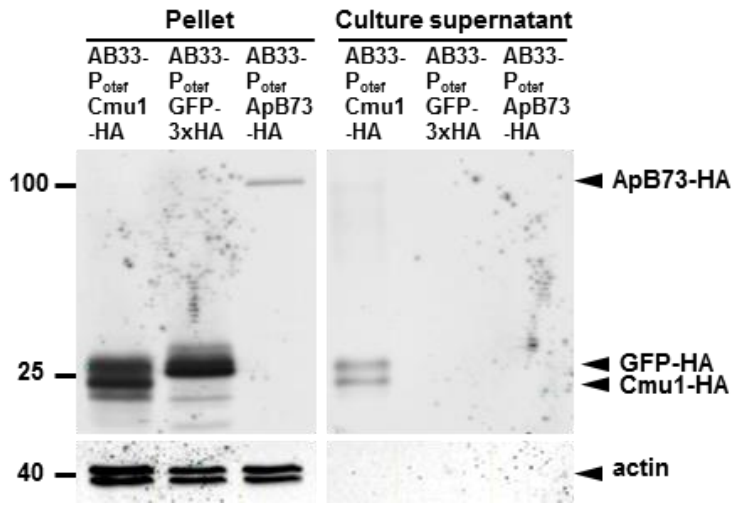

Figure 2.13 ApB73-HA is not detectable in culture supernatants.
Ustilago maydis strains AB33 and AB33-P_{otef}-ApB73-HA were harvested after shifting the fungal cells to nitrate-containing medium for six hours to induce filamentation. AB33-P_{otef}-Cmu1-HA was used as a positive control and AB33-P_{otef}-GFP-3xHA as a negative control. Supernatants were collected; the present proteins were TCA/DOC precipitated and subjected to western blot analysis using anti-HA and anti-actin antibodies. Compared to Cmu1-HA, five times more precipitated supernatant derived proteins of ApB73-HA were loaded. Numbers on the left indicate protein size in kDa.

In contrast to the *in planta* microscopy data (Figure 2.12), the supernatant assay fails to demonstrate free secretion of ApB73.

2.8.3. Function of the signal peptide

The conflicting results of the microscopy experiment and the secretion assay require a functional confirmation of the predicted N-terminal signal peptide of ApB73. To this end, different constructs were cloned, where either the ApB73 SP was removed or exchanged by the SP of the previously characterized effector Pit2 (Doehlemann *et al.*, 2011). Considering observations from previous experiments (Figure 2.12), i.e. that the C-terminal fusion of mCherry to ApB73 results in a fusion protein capable of fully complementing the mutant phenotype, and additionally, keeping in mind that immunoprecipitation/Western blot experiments from infected maize tissue are not successful with the native *apB73* promoter, a C-terminal mCherry fusion was generated in all used constructs. This allows for the microscopic detection of fusion proteins. The respective constructs were ectopically integrated in the *ip* locus of the SG200ΔapB73 deletion strain and challenged to a virulence assay in B73 (Figure 2.14).

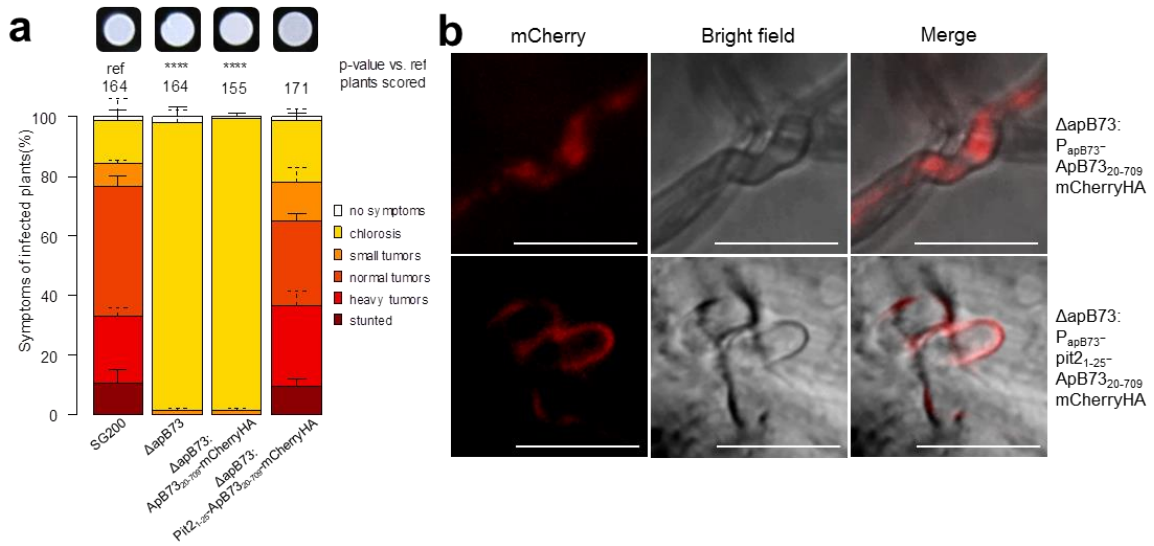

Figure 2.14 The ApB73 secretion signal is essential for protein function.
(a) Virulence assay confirming the essential role of the ApB73 signal peptide (SP). Strains expressing ApB73 without SP (ApB73$_{20-709}$) and with a different SP (Pit2$_{1-25}$-ApB73$_{20-709}$), both expressed under the native *apB73* promoter, were compared to the deletion strain ΔapB73 and the progenitor strain SG200 in a seedling infection assay performed with maize cv. B73. Symptoms were scored at 12 dpi. In the top row, pictures of the respective strain are shown after spotting them on filamentation inducing charcoal plates for 24h. Disease scores are shown on the right. Mean values of three independent infections are depicted, and the total number of infected plants is indicated above the respective column. Mean and standard deviation of relative counts from replicates are displayed. For clarity, only positive error bars are shown. P-values were calculated by Fisher's exact test. ****, P <0.0001. **(b)** Microscopy of different complementation strains to show expression of fusion proteins. Maize seedlings were infected with ΔapB73 strains expressing either ApB73$_{20-709}$-mCherryHA or Pit2$_{1-25}$-ApB73$_{20-709}$-mCherryHA both under the native *apB73* promoter. Fluorescence was observed at 5 dpi. Bar = 10 µm.

The results of the disease rating show that the strain without SP is not able to induce tumor formation when infecting B73 maize seedlings. On the contrary, exchanging the ApB73 SP with the SP of *U. maydis* effector Pit2, results in a strain inducing tumors at a similar rate to the progenitor strain SG200. This shows that the ApB73 SP is not only essential for the function of ApB73, but also interchangeable with SP of other proteins.

2.8.4. The function of ApB73 is not fulfilled in the fungal ER

The previous experiments show that the SP of ApB73 is essential for its role in virulence. Accordingly, it is necessary for ApB73 to enter the ER-Golgi, the common route of secreted *U. maydis* proteins. One possibility, as a consequence of the presented conflicting data about secretion, would be that ApB73 does not act in the biotrophic interface or within the host cells, but rather in the fungal ER.

To address this question, the ER retention signal HDEL was used (Pelham, 1990; Wedlich-Soldner, 2002). This short motif ensures that translated protein entering the ER will remain in the ER, rather than being translocated to the Golgi apparatus and then consequently loaded into vesicles to be transported out of the cell. To achieve this,

strains were generated expressing ApB73-mCherryHA-HDEL under the native *apB73* promoter in the ΔapB73 background, and a virulence assay, as well as, microscopy on infected leaf tissue was performed (Figure 2.15).

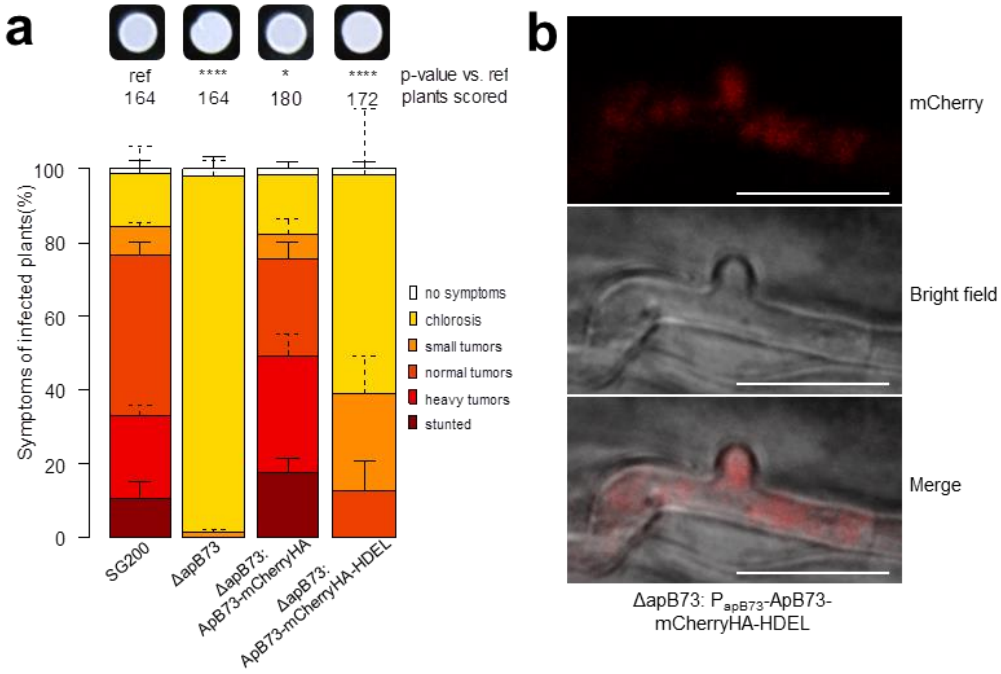

Figure 2.15 ApB73 does not function solely in the ER.
(a) Virulence assay addressing possible role of ApB73 in the ER. Strains expressing ApB73 with the ER retention signal HDEL (ApB73$_{1-709}$-mCherryHA-HDEL) and a strain expressing ApB73-mCherryHA under the native *apB73* promoter were compared to the deletion strain ΔapB73 and the progenitor strain SG200 in a seedling assay using maize cv. B73. In the top row, pictures of the respective strain are shown after growth on filamentation inducing charcoal plates for 24h. Disease scores obtained 12 dpi are shown on the right. Mean values of three independent infections are depicted and the total number of infected plants is indicated above the respective columns. Mean and standard deviation of relative counts from replicates are displayed. For clarity, only positive error bars are shown. P-values were calculated by Fisher's exact test. *, P <0.05; ****, P<0.0001. **(b)** Microscopy of ApB73-mCherryHA-HDEL to show expression of the fusion protein. Maize seedlings of cultivar B73 were infected with a ΔapB73 strain expressing ApB73-mCherryHA-HDEL under the native *apB73* promoter. Fluorescence was observed at 5 dpi. Bar = 10 µm.

The results of the virulence assay illustrate that the ApB73-mCherryHA-HDEL fusion protein, in contrast to a fusion protein without HDEL, is incapable of fully restoring the virulence defect of the mutant strain caused by the *apB73* deletion. However, small and medium sized tumors can be observed to a low extent. This is likely due to the fact that the HDEL motif is not able to withhold all translated fusion protein efficiently. Despite the fact that some plants developed small tumors, indicating leakiness of the ER-retention signal, no mCherry signal was observable around the fungal hyphae using confocal microscopy. Instead, the microscopy shows that all detectable protein is found within the fungal cell walls, probably in the ER.

2.8.5. ApB73 is enriched in the fungal plasma membrane

The results of the last few experiments demonstrate that ApB73 needs a functional signal peptide to perform its role in virulence. However, the results of the microscopy (signal outside of the hyphae indicating secretion) and the secretion assay (no secreted protein detectable) are conflicting. As a function solely in the ER was ruled out, the most straight forward explanation would be that ApB73 is secreted, but stays attached to the fungal plasma membrane or fungal cell wall. To further investigate this possibility, experiments were conducted to enrich PM from fungi expressing a tagged version of ApB73. This would allow me to examine a possible enrichment of ApB73 in the PM by Western blot analysis.

The method that was used aims to isolate the PM from a microsomal membrane fraction by two-phase partitioning, a methodology utilizing the different surface properties of membranes. This method first involves homogenization of fungal pellets, which are then centrifuged to pellet unbroken cells and debris. The supernatant (input) is then subject to further centrifugation to create the microsomal pellet, which is purified to yield the PM fraction. To look at enrichment, the different intermediate products generated over the course of the procedure were kept. If ApB73 is retained in the PM, one would expect the ApB73-HA signal to be stronger in the PM fraction. Accordingly, the pellet fraction, the Input (without cell walls/debris), the supernatant of the microsomal pellet and the final enriched PM were compared using Western blot analysis (Figure 2.16). For this experiment, a SG200 strain was used that ectopically expresses ApB73-HA-Strep under the in axenic culture strong constitutive *oma* promoter (Flor-Parra, 2006).

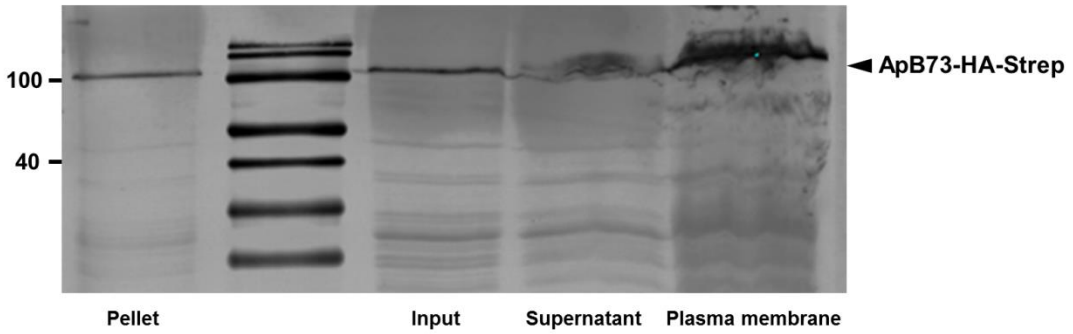

Figure 2.16 Plasma membrane enrichment using *U. maydis* strain SG200-P_{oma}-ApB73-HA-Strep.
Plasma membrane enrichment was performed using a SG200 strain expressing ApB73-HA-Strep under the constitutive *oma* promoter. Intermediate products within the protocol were kept and compared using Western blot analysis. The fractions were: a sub-fraction of the original pellet (Pellet), a sub-fraction of the supernatant obtained after cell disruption (Input), the supernatant after the first ultracentrifugation (Supernatant), where the microsomal pellet is obtained and finally the end product of enriched plasma membrane (Plasma membrane). An anti-HA antibody was used for detection. Numbers on the left indicate protein size in kDa.

Western blot analysis of the different fractions obtained during PM enrichment indicates that the signal for ApB73 is getting enriched over the proceedings of the protocol. The faint band seen in the supernatant after the first ultracentrifugation is most likely overspill from the final lane. Despite the fact that this result indicates that ApB73 might be enriched in the fungal PM, no final conclusion can be made, as certain controls are lacking.

2.8.6. ApB73-mCherry remains at the fungal membrane *in planta*

Analysis of plasma membrane enrichment by itself was inconclusive, leading me to question the use of the method in this context. One potential problem could arise from attempting to solve this question in axenic culture. Considering that secretion of virulence factors is part of *U. maydis*' pathogenic development that occurs *in planta*, conducting experiments that are closer to the natural system could produce more meaningful results.

To this end, plasmolysis experiments on infected plant tissue were conducted. The rationale here is that secreted proteins should freely diffuse within the biotrophic interspace, in contrast to proteins that remain attached to the fungal membrane or the cell wall. Plasmolysis is necessary, as without treatment the biotrophic interspace is a very narrow space, making it indistinguishable from the fungal membrane/cell wall itself. This approach has been used before to show free diffusion of effector fusion proteins like Pep1-mCherry and Pit2-mCherry (Doehlemann *et al.*, 2009; Doehlemann *et al.*, 2011).

Accordingly, microscopy was performed on maize seedlings infected with the ΔapB73 mutant strain expressing ApB73-mCherry-HA under the constitutively active *otef* promoter. The infected maize tissue was harvested three days after infection and treated with 1M mannitol to induce plasmolysis. To exclude differences that may arise when fusing mCherry N- or C-terminally to ApB73, a second strain was generated expressing $ApB73_{1\text{-}19}$-mCherry3xHA-$ApB73_{20\text{-}709}$-3xmyc under the *otef* promoter in the mutant background. Another control strain was also included that expresses mCherryHA fused to the SP of ApB73 ($ApB73_{1\text{-}19}$). This was done to investigate if the SP itself has a membrane anchoring function.

For the $ApB73_{1\text{-}19}$-mCherryHA control construct, clear secretion of the fusion protein was observed (Figure 2.17, top panel). The signal is evenly distributed within the area of the biotrophic interface, suggesting free diffusion. Looking at the fusion protein of full length ApB73-mCherryHA on the other hand, a very different picture can be observed. Although the fusion protein also appears to be clearly secreted by the fungus, the mCherry signal remains associated to the fungal membrane and is not evenly

distributed within the biotrophic interface (Figure 2.17, middle panel). Surprisingly, when conducting the same experiment with an N-terminal mCherry fusion, diffusion of the ApB73$_{1-19}$-mCherry3xHA-ApB73$_{20-709}$-3xmyc fusion protein in the biotrophic interface can be observed (Figure 2.17, bottom panel).

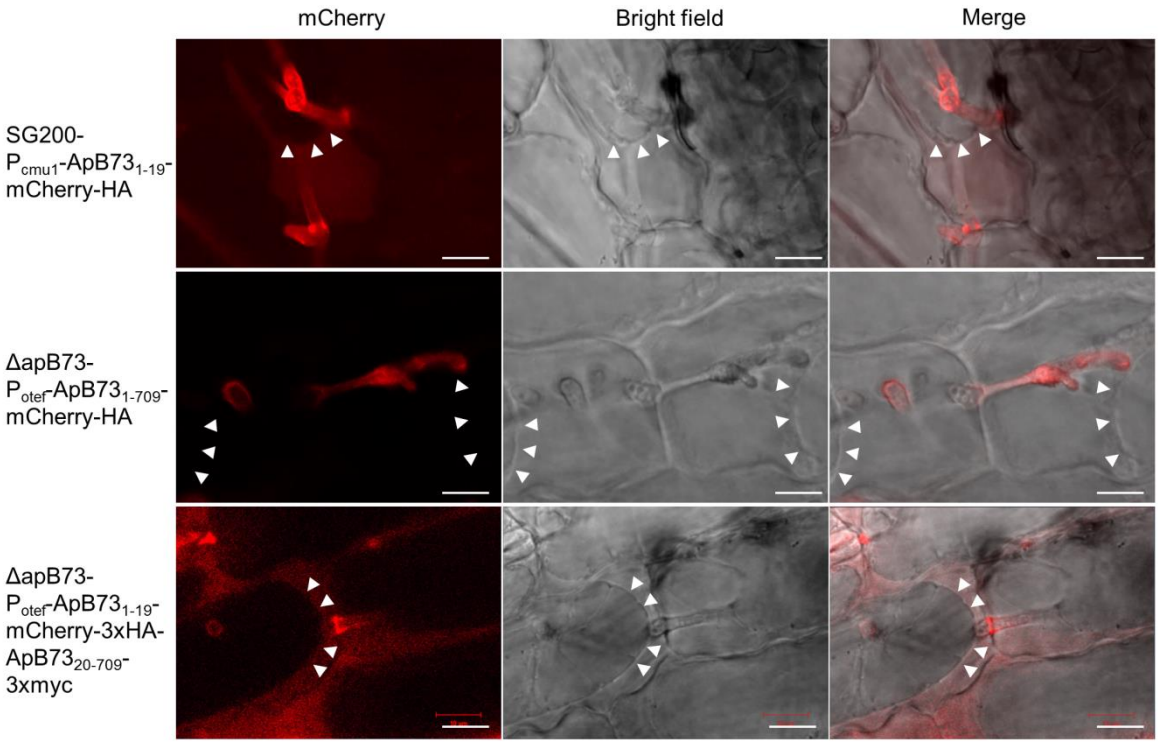

Figure 2.17 Effect of plasmolysis to the localization of ApB73 fusion proteins.
Maize seedlings of cv. B73 were infected with different *U. maydis* strains expressing either a C- or N-terminal fusion of mCherry to ApB73 (ApB73-mCherry-HA or ApB73$_{1-19}$-mCherry-3xHA-ApB73$_{20-709}$-3xmyc) under the *otef* promoter or mCherry in fusion with the ApB73 SP (ApB73$_{1-19}$mCherry-HA) under the biotrophy-specific *cmu1* promoter. The material was harvested three days post infection and treated with 1M mannitol. Arrowheads indicate the plant plasma membrane pulling back from the cell wall. Bar = 10 µm.

These results could indicate that *in planta* ApB73 is processed after secretion into the biotrophic interface, resulting in the cleavage of the N-terminal part including the mCherry protein. Another explanation could be that the N-terminal mCherry protein sterically hinders the association of ApB73 to the fungal membrane resulting in the observed unbound protein. Both the C- and the N-terminal version complement the mutant phenotype (Figure 2.18).

The successful complementation of the ApB73 mutant phenotype implies that if mCherry is actually blocking association of ApB73 to the fungal surface, this attachment cannot be critical for the function of ApB73. The second mentioned possibility is that ApB73 is processed, resulting in free diffusion of the N-terminal part. This remains a valid option, although similar observations implying that ApB73 is processed, were not made when conducting Western blot analysis of axenically grown cultures. Here, ApB73 was only detected as a full length protein (e.g. Figure 2.13).

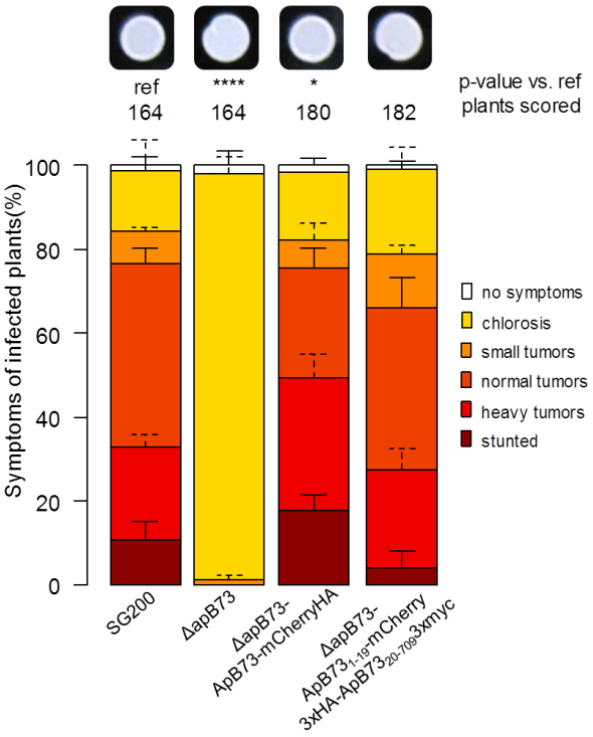

Figure 2.18 Virulence assay to test for complementation of mCherry fusion proteins. Virulence assay showing complementation of the C- and N-terminal fusions to mCherry. Strain SG200ΔapB73-P_{apB73}-ApB73-mCherryHA and SG200ΔapB73-P_{otef}-ApB73$_{1-19}$mCherry3xHA-ApB73$_{20-709}$-3xmyc, were compared to the deletion strain (ΔapB73) and the progenitor strain SG200. In the top row, pictures of the respective strain are shown after growing on filamentation inducing charcoal plates for 24h. Disease scores obtained 12 dpi are shown on the right. Mean values of three independent infections are depicted and the total number of infected plants is indicated above the respective columns. Mean and standard deviation of relative counts from replicates are displayed. For clarity, only positive error bars are shown. P-values were calculated by Fisher's exact test. *, P <0.05; ****, P <0.0001.

To clarify this, an attempt was made to address processing of ApB73 biochemically by performing immunoprecipitation/Western blot analysis of infected plant material. Unfortunately, due to the weak promoter strength of the ApB73 promoter, no specific bands were obtained. The usage of other promoters, with stronger expression patterns of their corresponding genes during all biotrophic stages, namely of *stp1* and *pit2* (Daniel Lanver, personal communication), were neglected due to the fact that the respective strains cannot fully complement the virulence phenotype, implicating that expression with these promoters does not allow ApB73-mCherry-HA to fulfil its function (Figure 2.19a). Expression and secretion of the fusion proteins of the constructed strains was confirmed using microscopy (Figure 2.19b).

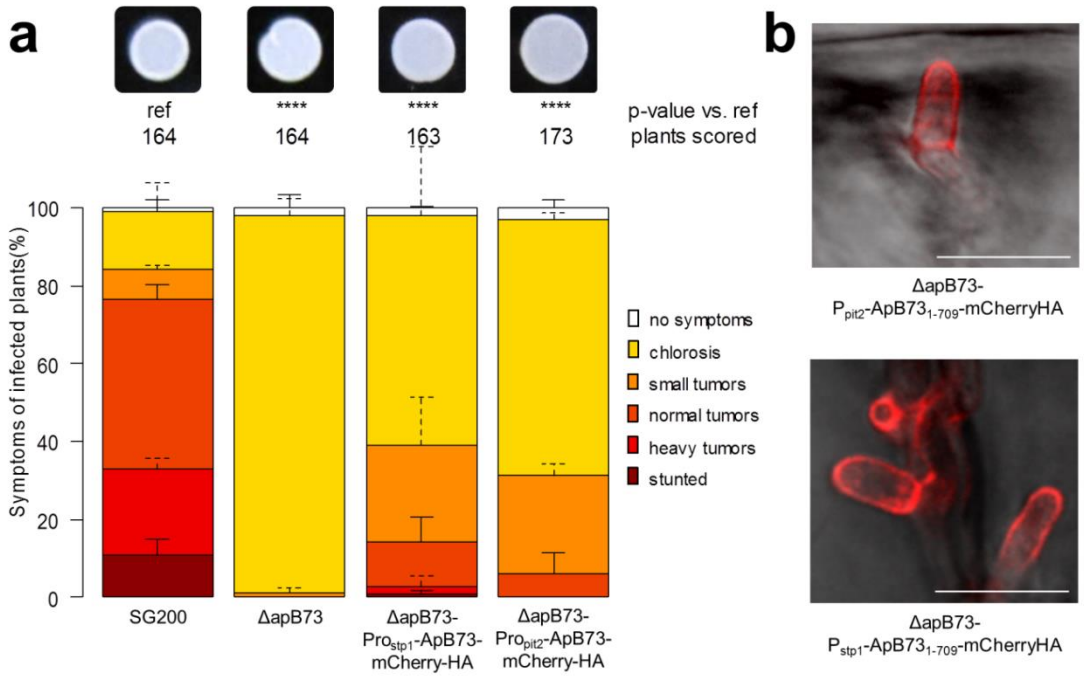

Figure 2.19 Virulence assay and microscopy of ApB73 using promoters strongly upregulated during biotrophy.
(a) Disease rating of ApB73 expressed under different promoters in the ΔapB73 mutant. The mutant was transformed with a construct expressing ApB73-mCherry-HA under two biotrophy-specific promoters of the effector genes *stp1* and *pit2* (Schipper, 2009; Doehlemann *et al.*, 2011). Seedlings were infected seven days after germination and scored for symptoms at 12 dpi. In the top row, pictures of the respective strain are shown after growing on filamentation inducing charcoal plates for 24h. Disease scores are shown on the right. Mean values of three independent infections are depicted and the total number of infected plants is indicated above the respective columns. Mean and standard deviation of relative counts from replicates are displayed. For clarity, only positive error bars are shown. P-values were calculated by Fisher's exact test, ****, P <0.0001. **(b)** Microscopy to show expression of fusion proteins. Maize seedlings were infected with ΔapB73 strains expressing ApB73-mCherry-HA under either the *pit2* or *stp1* promoter. Fluorescence was observed at five days post infection. Bar = 10 µm.

2.8.7. ApB73 co-localizes with the membrane protein Pit1

From the previous experiments, it remained unclear if ApB73 is localized to the fungal PM or cell wall. Therefore, co-localization experiments were conducted. ApB73-mCherry-HA was co-expressed with a known *U. maydis* membrane protein, Pit1, fused to GFP (Figure 2.20; Doehlemann *et al.*, 2011). Both cassettes were expressed under the native *apB73* promoter to avoid differences in expression levels.

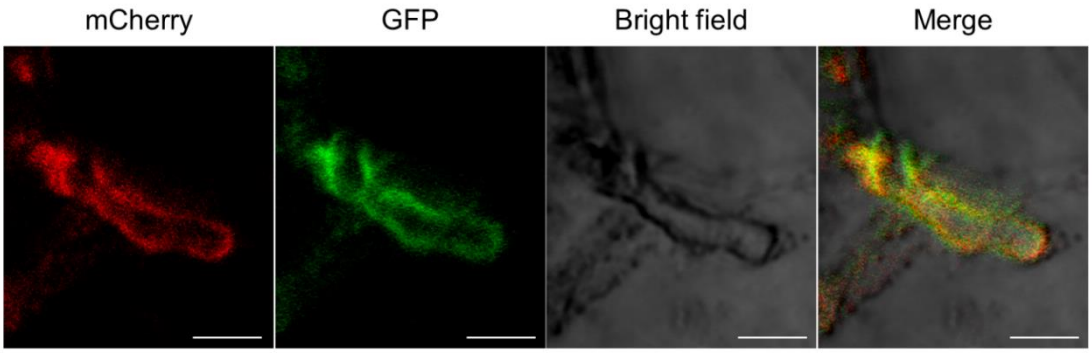

Figure 2.20 Localization of Pit1-GFP and ApB73-mCherry-HA in infected maize leaves.
Seven day old maize seedlings of cv. B73 were infected with a ΔapB73 strain co-expressing ApB73-mCherry-HA and Pit1-GFP both under the native *apB73* promoter. Fluorescence was observed by confocal microscopy three days post infection. Bar = 5 µm.

The microscopy images show co-localization of ApB73-mCherry-HA and Pit1-GFP, supporting the idea that ApB73 might be localizing to the fungal plasma membrane. However, it should be considered that the two structures in question might be too close to another to be confidently separated using light microscopy. Attempts to generate a cell wall marker in *U. maydis* to substantiate the results were unsuccessful (Simon Uhse, personal communication).

2.8.8. Localization in *Nicotiana benthamiana*

The observed possible processing gives an indication that parts of the ApB73 protein may be cleaved off *in planta*. This allows the speculation that ApB73 (or more likely parts of it) may be translocated into the plant cell.

To figure out if ApB73 has a specific localization *in planta*, the gene was overexpressed in *Nicotiana benthamiana* plants using *Agrobacterium tumefaciens* mediated transient transformation. Expression constructs were generated without the N-terminal SP. The reasoning here is that the SP is cleaved off by the fungus before secretion ergo no fungal proteins bearing a secretion signal should ever enter a plant cell. As a control, leaves were infiltrated with an *A. tumefaciens* strain expressing cytosolic YPF. The results are shown in Figure 2.21.

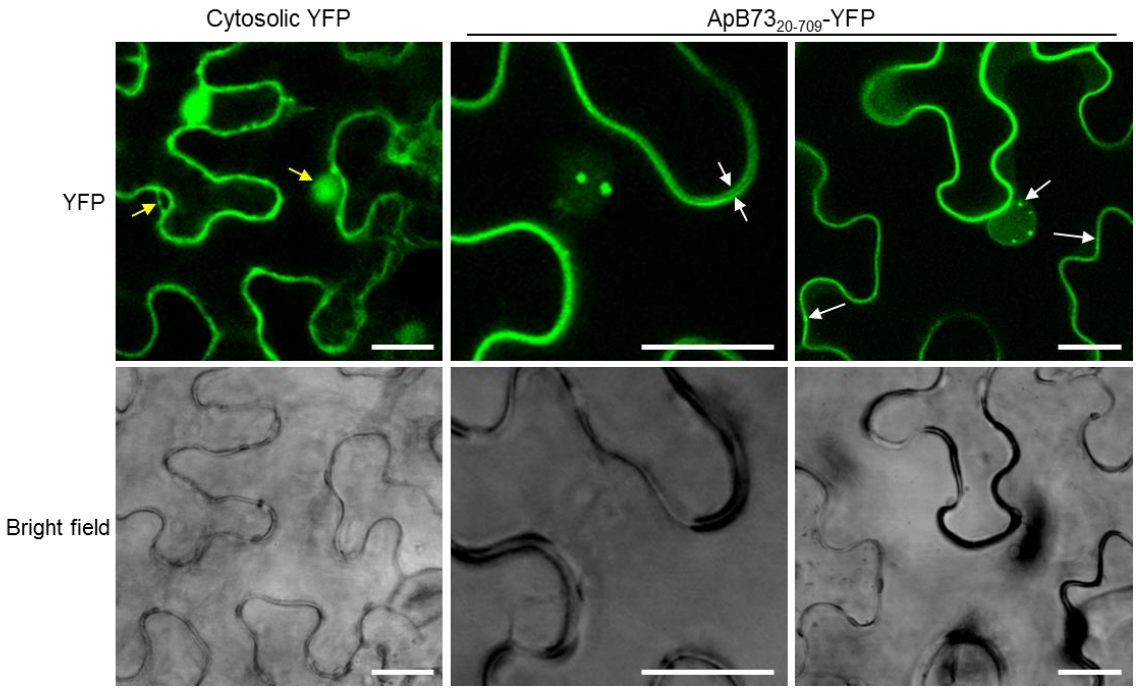

Figure 2.21 Transient expression of ApB73$_{20-709}$-YFP in *Nicotiana benthamiana*.
Agrobacterium strains, expressing either YFP or ApB73$_{20-709}$–YFP under the strong 35S Promoter, were used for transient expression experiments in *N. benthamiana*. Tobacco plants were infiltrated and observed three days later. Yellow arrows underline cellular localizations of YFP. White arrows emphasize localization of ApB73$_{20-709}$-YFP signal different to the signal observed for YFP. Bar = 25µm.

The microscopy data shows that YFP alone seems to localize to the cytoplasm indicated by cytoplasmic strands (yellow arrow, Figure 2.21). As nuclear pores allow free diffusion of proteins up to at least 60 kDa, YFP signal can be also observed in a round structure probably displaying the nucleus (yellow arrow, Figure 2.21). Compared to YFP alone, ApB73$_{20-709}$-YFP shows a different localization pattern. Although the surroundings of the cell show a signal similar to YFP, one cannot observe cytoplasmic strands indicating that the observed signal does not come from the cytoplasm, but rather from the plasma membrane. Additionally, the signal of ApB73$_{20-709}$-YFP appears to localize to vesicle-like structures in the cell periphery and within a structure that is most likely the nucleus.

Despite the fact that fungal proteins with a secretion signal should not be ending up in plant cells, constructs were generated expressing full length ApB73 in fusion with YFP to see where full length ApB73 would localize (Figure 2.22).

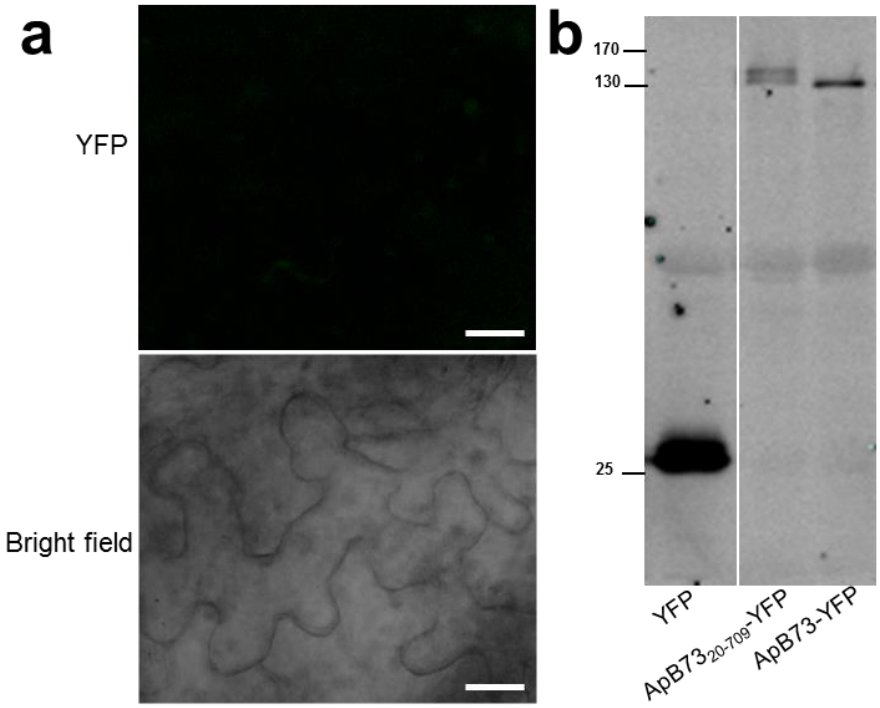

Figure 2.22 Transient overexpression of ApB73-YFP in tobacco.
(a) *Agrobacterium tumefaciens* strain expressing ApB73-YFP under the strong 35S promoter was infiltrated into *Nicotiana benthamiana* plants and infiltrated tissue was observed three days later. Bar = 25 µm. **(b)** Western blot analysis of Agrobacterium infected *Nicotiana benthamiana* leaf extracts (leaves harvested three days post infiltration) were performed. Three different *A. tumefaciens* strains were used expressing either YFP alone, ApB73$_{20-709}$-YFP or ApB73-YFP under the 35S promoter. Anti-GFP antibodies were used for detection. Numbers on the left indicate protein size in kDa.

Surprisingly, no YFP signal was detectable for ApB73-YFP (Figure 2.22a). As YFP is known to be pH sensitive (Llopis *et al.*, 1998), and the pH in the apoplast of plants is reportedly in the range of pH5 (Felle *et al.*, 2004), Western blot analysis was conducted. Thereby one can investigate the possibility that, although ApB73-YFP is successfully expressed, the fusion protein is secreted into the apoplast and, because of the low pH, not visible (Figure 2.22b). The Western blot shows that all three proteins (YFP, ApB73$_{20-709}$-YFP and ApB73-YFP) are expressed implicating that ApB73-YFP is secreted, but due to the low pH outside the cell, not detectable. Interestingly, the fusion protein without signal peptide results in two bands on the Western blot, suggesting a processing of ApB73$_{20-709}$-YFP in tobacco. As the additional band is bigger than the band observed for ApB73-YFP, it seems like the fusion protein is not cleaved.

Taken together, expression of ApB73 in *N. benthamiana,* results in a specific localization of both fusion proteins with and without signal peptide. ApB73-YFP appears to be secreted into the tobacco apoplast, whereas ApB73$_{20-709}$-YFP localizes to vesicle-like structures and the cell periphery. To confirm the assumptions about the localization of the fusion proteins, the mentioned strains were co-transformed with other strains expressing fusion proteins known to localize to specific cell organelles. The constructs

used here, were BFP fused to a ER signal sequence and the ER retention signal HDEL (secBFP-HDEL; Lampropoulos *et al.*, 2013), cytosolic mCherry, and a secreted as well as a non-secreted pH sensitive version of GFP (pHLuorin and sec-pHLuorin; Sankaranarayanan *et al.*, 2000). As the secreted version of ApB73-YFP is pH sensitive, full length ApB73 was fused to C-terminal mCherry. First, it was tested if ApB73$_{20\text{-}709}$-YFP co-localizes with the markers for the cytosol or the ER (Figure 2.23).

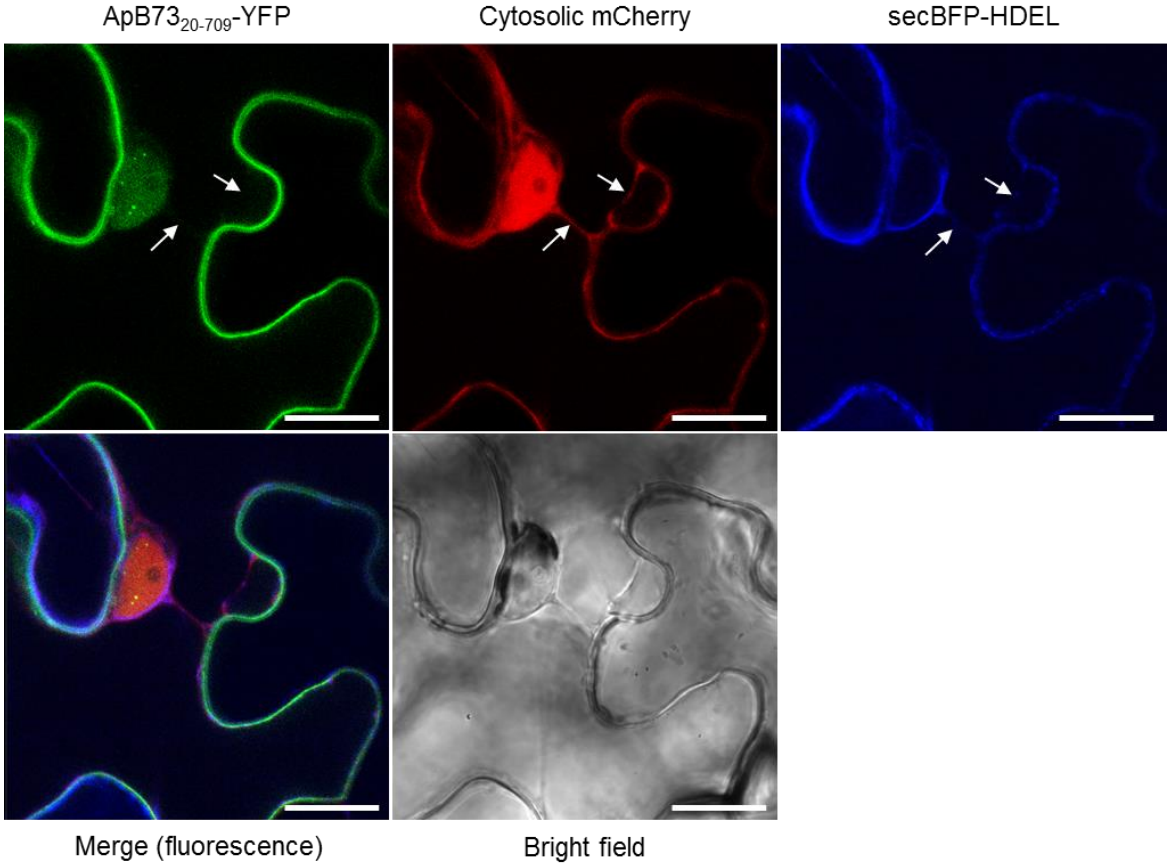

Figure 2.23 Co-localization of ApB73$_{20\text{-}709}$-YFP with ER- and cytosolic markers in *N. benthamiana*. Agrobacterium strains, expressing either ApB73$_{20\text{-}709}$–YFP, mCherry or secBFP-HDEL under the strong 35S Promoter, were used for transient expression experiments in *N. benthamiana*. Tobacco plants were infiltrated and observed three days later. Arrows emphasize signal differences at specific localizations. Maximum intensity projections. Bar = 20 µm.

The co-localization images show that ApB73$_{20\text{-}709}$-YFP does not localize to areas specific for the ER, i.e. around the nucleus. The same is true for cytoplasmic strands, also stained by the ER marker as they contain parts of the ER, were ApB73$_{20\text{-}709}$-YFP does not localize. An area where all shown constructs give signal is the cell periphery. However, as ApB73$_{20\text{-}709}$-YFP fails to localize to the ER/cytoplasmic strands, one can assume that it does not localize to those compartments. This would mean that the ApB73$_{20\text{-}709}$-YFP signal at the periphery is probably not displaying localization to the ER/ cytoplasm but rather localization to a different compartment (e.g. the plasma membrane).

And as the PM/cell wall is spatially so closely located next to the ER/cytoplasm, it is not possible to obtain distinct signals using light microscopy.

Next, I aimed to confirm the initial experiments implying that full length ApB73, ergo with the fungal secretion signal, is secreted in this heterologous system of Agrobacterium mediated transformation of *N. benthamiana*. To this end, ApB73-mCherry was co-transformed with two versions of a pH sensitive Version of GFP (pHLuorin), once without a tag and once with an ER signal sequence (Lampropoulos *et al.*, 2013) targeting it to the secretory system (sec-pHLuorin, Figure 2.24).

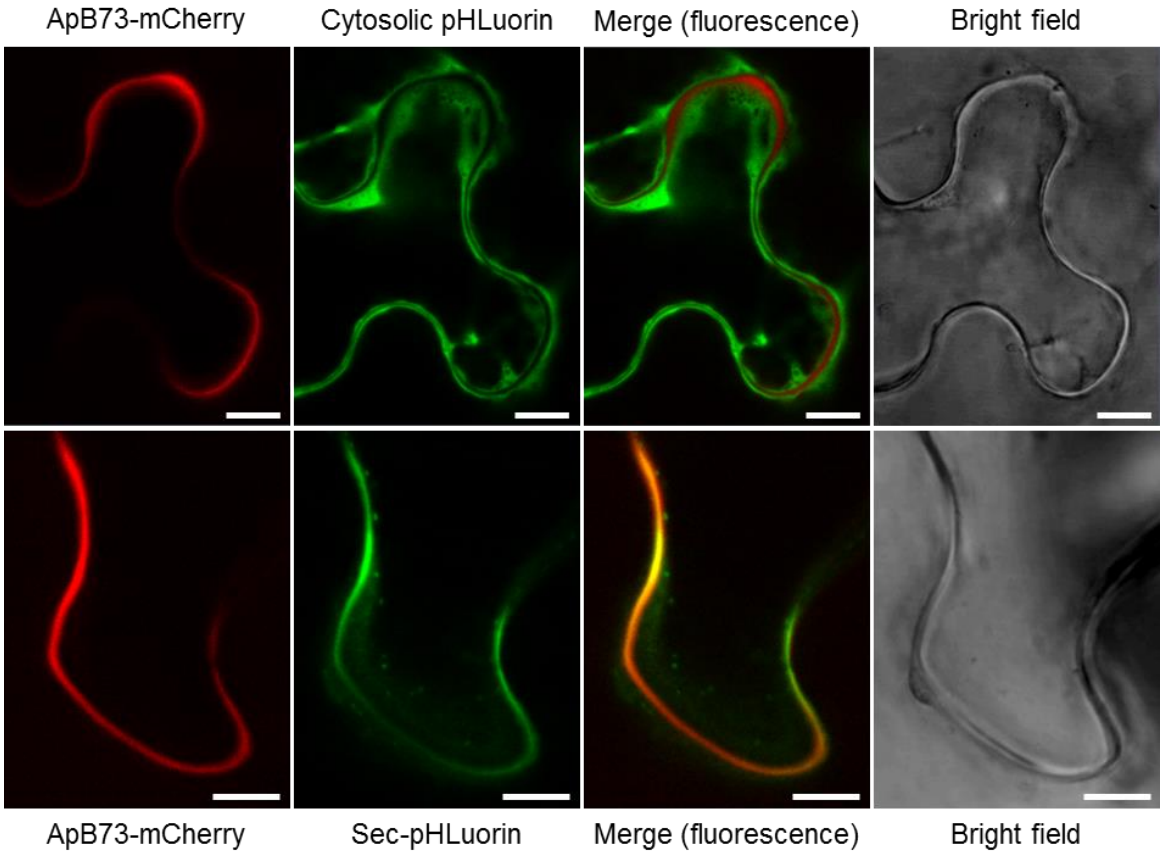

Figure 2.24 Co-localization pf ApB73-mCherry and secreted/non-secreted pHLuorin in tobacco. Agrobacterium strains expressing ApB73–mCherry were infiltrated together with strains expressing either cytosolic pHLuorin or sec-pHLuorin, all of them under the 35S promoter, were used for transient expression experiments in *N. benthamiana*. Tobacco plants were infiltrated and observed three days later. Bar = 5 µm.

The microscopy pictures show that ApB73-mCherry does not co-localize with cytosolic pHLuorin, however, there is a clear co-localization with sec-pHLuorin. This indicates that ApB73 is secreted in this heterologous system, meaning that the ApB73 secretion signal is also functional in *N. benthamiana*.

2.9. Membrane association of ApB73 *in vitro*

To characterize the observed membrane association of ApB73, I attempted to purify the protein and test it for its solubility *in vitro*. Therefore, ApB73 was expressed under the

oma promoter in the *U. maydis* progenitor strain SG200. For detection, both a HA (YPYDVPDYA) and a strep tag (WSHPQFEK) were C-terminally fused to ApB73. As it was unknown under which conditions purification of ApB73 would work best, and if purification was possible at all - considering the membrane association observed in infected plant tissue - various conditions were tested (buffers, different pH values and addition of detergents; Figure 2.25).

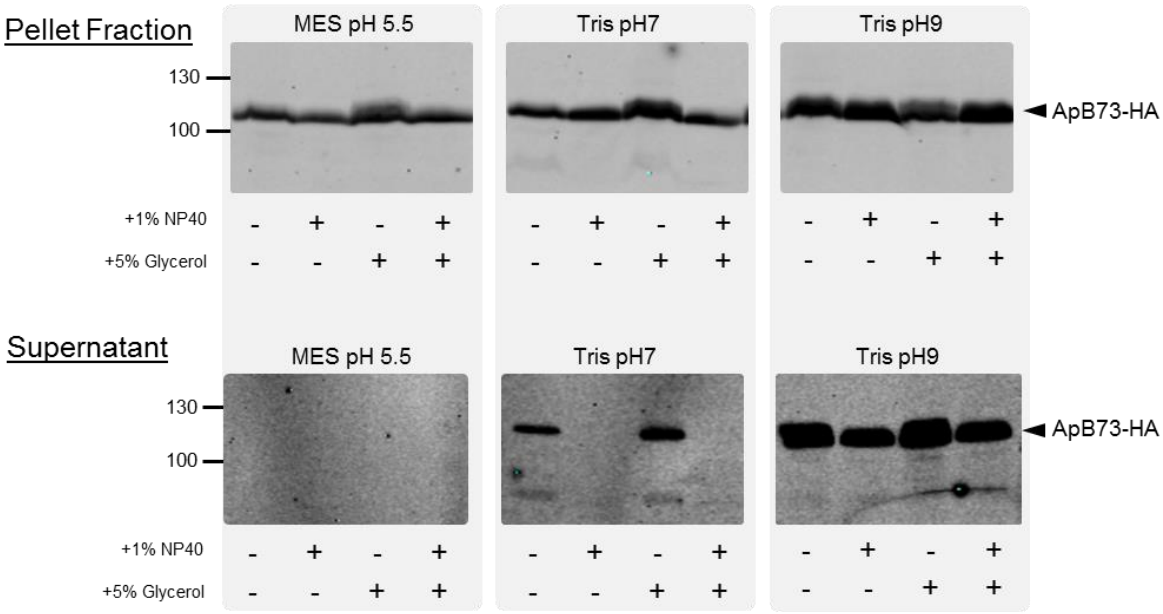

Figure 2.25 Expression of ApB73-HA-Strep protein in *U. maydis* strain SG200.
ApB73-HA-Strep under the strong *oma* promoter was expressed in SG200. Various conditions during cell disruption were used, including different buffers (MES pH5.6, Tris pH7 and pH9) and addition of different detergents (either none, 1% NP-40, 5%Glycerol or both). Denatured proteins from supernatant- and pellet fractions were loaded and detected using Western blot analysis and anti-HA antibodies. Numbers on the left indicate the protein size in kDa.

Interestingly, a dramatic difference can be observed in the solubility of the ApB73-HA-strep protein upon changing the buffer constitution. Overall, it can be stated that soluble protein was only obtained using buffers with pH7 or pH9. However, when using Tris pH 7 during cell disruption, ApB73-HA-strep is only soluble without addition of NP40. The addition of 5% Glycerol or the use of no detergent at all did not have an impact. Under high pH conditions the fusion protein remains soluble, independent of the detergent used. The question arising here is, if this observation could actually hint to something important for the function of the ApB73 protein during the establishment of biotrophy in the pathosystem *U. maydis – Z. mays*.

From the literature it is known that upon pathogenic attack the apoplastic pH undergoes dramatic changes. In barley, for example, it was shown that the apoplastic pH after addition of the PAMP molecule chitooctaose, a chitin derivative, increases more than one unit from pH4.8 to pH6 (Felle *et al.*, 2004). Although no similar observations are

reported for the interaction between corn and *U. maydis*, it is conceivable that a similar phenomenon takes place. However, as the pH changes are unlikely to result in differences as dramatic as shifts from pH7-pH9, it was investigated if changes in pH of one unit are sufficient to modulate solubility of the ApB73 protein.

To do so the same strain was used to express ApB73-HA-Strep. This time buffers with pH values from pH5.5.-pH7.4 were used and no detergent was added. As the buffer capabilities of MES, as well as Tris, are limited MES buffer was used for pH5.5-6.5 and Tris buffer for pH7-7.4 (Figure 2.26).

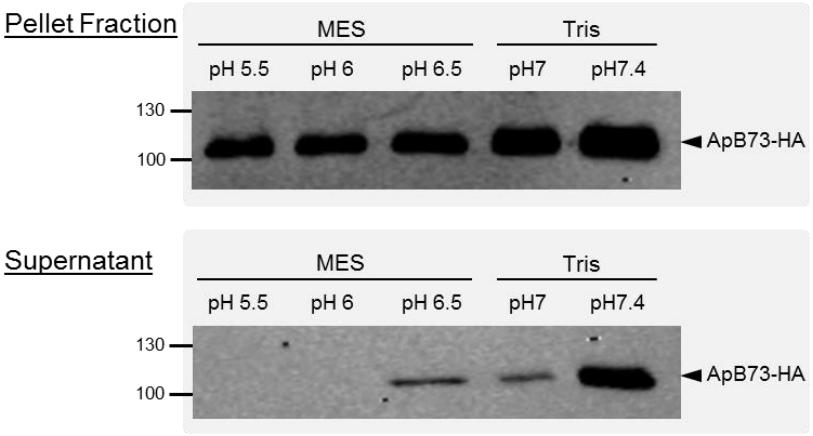

Figure 2.26 Solubility of ApB73-HA-Strep under different pH conditions.
ApB73-HA-strep was expressed in *U. maydis* strain SG200 under the *oma* promoter. Buffers with different pH values (pH5.5-7.4) were used during cell disruption. Supernatant- as well as pellet-fractions were subjected to Western blot analysis using anti-HA antibodies. Numbers on the left indicate protein size in kDa.

The results from this Western blot analysis indicate that the shift in solubility of ApB73-HA-strep happens between pH6 and pH6.5. These values could correspond to pH differences observed in nature. Nevertheless it should be noted that the observed differences may be a feature of other proteins as well. Therefore, it would be beneficial to include control proteins in this assay. Possible candidates here would be Pit1, a fungal membrane protein, as well as, cytosolic GFP and secreted GFP. This way it would be possible to observe, if membrane associated proteins, secreted proteins or proteins in general show a similar behaviour. However, even when including the appropriate controls, this assay is purely based on the behaviour of ApB73 in axenic culture and not on the possible properties of ApB73 after secretion to the biotrophic interface. Accordingly, it was aimed to investigate the solubility of ApB73 under different pH conditions on infected maize leaves.

2.9.1. Plasmolysis using different pH values

The previous experiments show that the solubility of ApB73, when expressed axenically in *U. maydis* strain SG200, is dependent on the pH of the solution used during cell

disruption. Even when conducted with additional controls, these results could be an artefact, rather than displaying a natural property of the protein. As shown before (Figure 2.17), the ApB73-mCherry-HA protein localizes around the fungal hyphae *in planta* and the signal remains in the fungal periphery even after plasmolysis. On the contrary, when fusing mCherry N-terminally to ApB73, the signal freely diffuses within the biotrophic interface upon plasmolysis. To elucidate if the observed change in solubility in axenic culture also happens in nature, the very same plasmolysis experiment with the mentioned strains was conducted. This time either 1M mannitol pH5 or 1M mannitol pH10 was used to simulate shifts in the pH. If the previously observed solubility changes of ApB73, are indeed pH dependent, different behaviours of the fusion protein after plasmolysis should also be observable *in planta* (Figure 2.27).

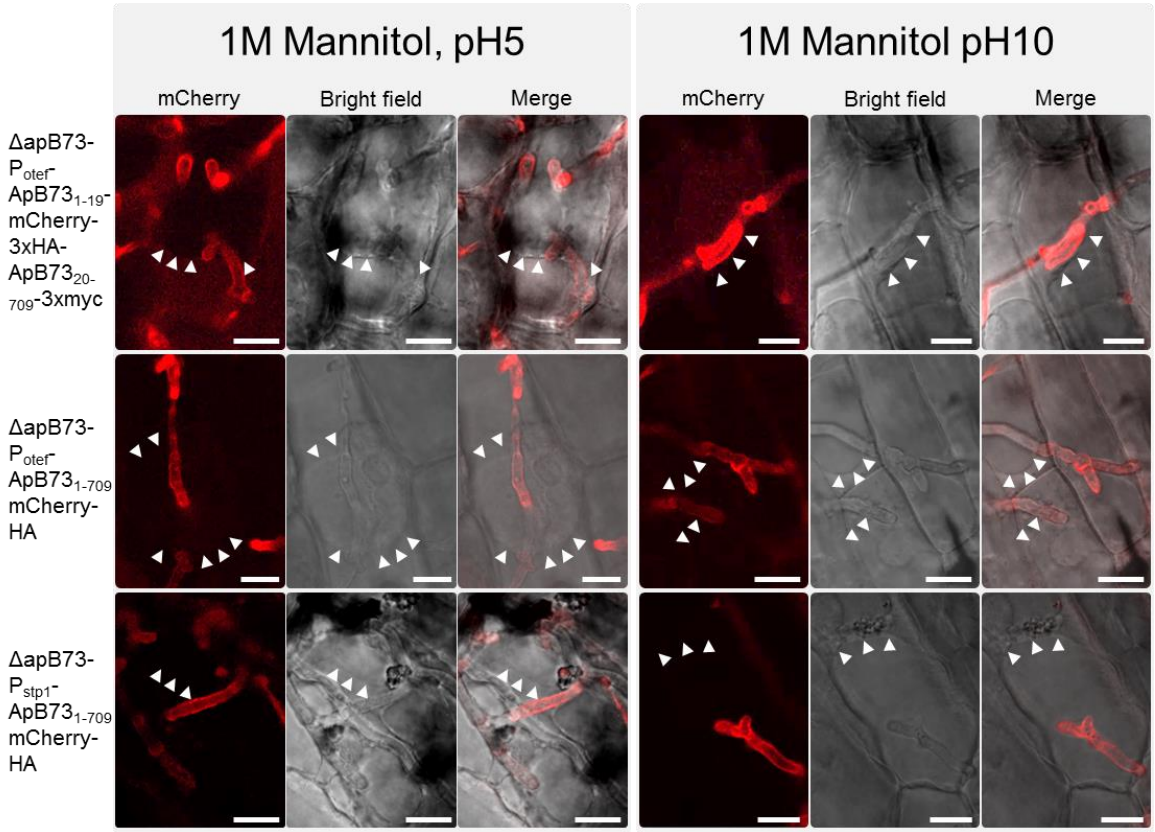

Figure 2.27 Effect of plasmolysis under different pH conditions on the localization of ApB73 fusion proteins.
Maize seedlings were infected with *U. maydis* strains expressing either a C- or N-terminal fusion of mCherry to ApB73 (ApB73-mCherry-HA or ApB73$_{1-19}$-mCherry-3xHA-ApB73$_{20-709}$-3xmyc) under the *otef* promoter or ApB73-mCherry-HA under the biotrophy-specific very strong *stp1* promoter. Material was harvested three days post infection and treated with 1M mannitol with the pH set to either pH5 or pH10. Arrowheads indicate the plant plasma membrane pulling back from the cell wall. Bar = 10µm.

The microscopy images show that, under the tested conditions, no change in solubility of the ApB73 fusion proteins occurs. The N-terminal fusion (Figure 2.27, top panel) stays soluble independent of the pH, whereas the C-terminal fusion of ApB73 and mCherry (Figure 2.27, middle panel) remains exclusively localized around the fungal

hyphae. To exclude a detection problem, the strong biotrophy specific *stp1* promoter was tested (Figure 2.27, bottom panel), however, the signal of the ApB73-mCherry-HA fusion protein remains at the fungal periphery.

Accordingly, it appears that a portion of the N-terminal part of the ApB73 protein is pH independently soluble/unbound (neglecting the possibility that mCherry sterically hinders binding of the N-terminal fusion protein to the fungal surface), whereas a C-terminal moiety of the ApB73 proteins remains pH independently insoluble/bound.

2.10. Orthologs of ApB73

Many proteins have orthologs in closely related species. Looking at them can help to identify regions important for the function of the protein. However, such comparisons can also clarify the specific role of a protein within different pathosystems.

As mentioned earlier (see 2.2 Bioinformatical analysis of ApB73), amino acid blast analysis using the ApB73 sequence revealed that many smut fungi closely related to *U. maydis* encode for proteins orthologous to ApB73. These include different pathogenic species like *U. hordei*, *U. bromivora*, *S. reilianum*, *S. scitamineum* and *M. pennsylvanicum,* but also the non-pathogenic saprophytic fungus *P. aphidis*.

2.10.1. Bioinformatic comparison of the ApB73 orthologs

To get a first impression about the conservation of the orthologous proteins, all sequences were aligned using Clustal O (Figure 2.28). Apart from the *P. aphidis* protein, all mentioned orthologs share an N-terminal SP indicating their secretion (Petersen *et al.*, 2011). Intriguingly, the Pseudozyma ortholog PaApB73 also contains a short stretch of amino acids that would qualify as a SP; however, due to a new methionine 89 aa ahead of the potential SP, the stretch is not located N-terminally and therefore most likely fails to send the protein to the secretory pathway. Otherwise, the alignment shows that there are certain regions very highly conserved (especially at the N-terminus when neglecting the extra 89 aa of PaApB73) among all orthologs, whereas other areas located rather C-terminally seem to be more variable.

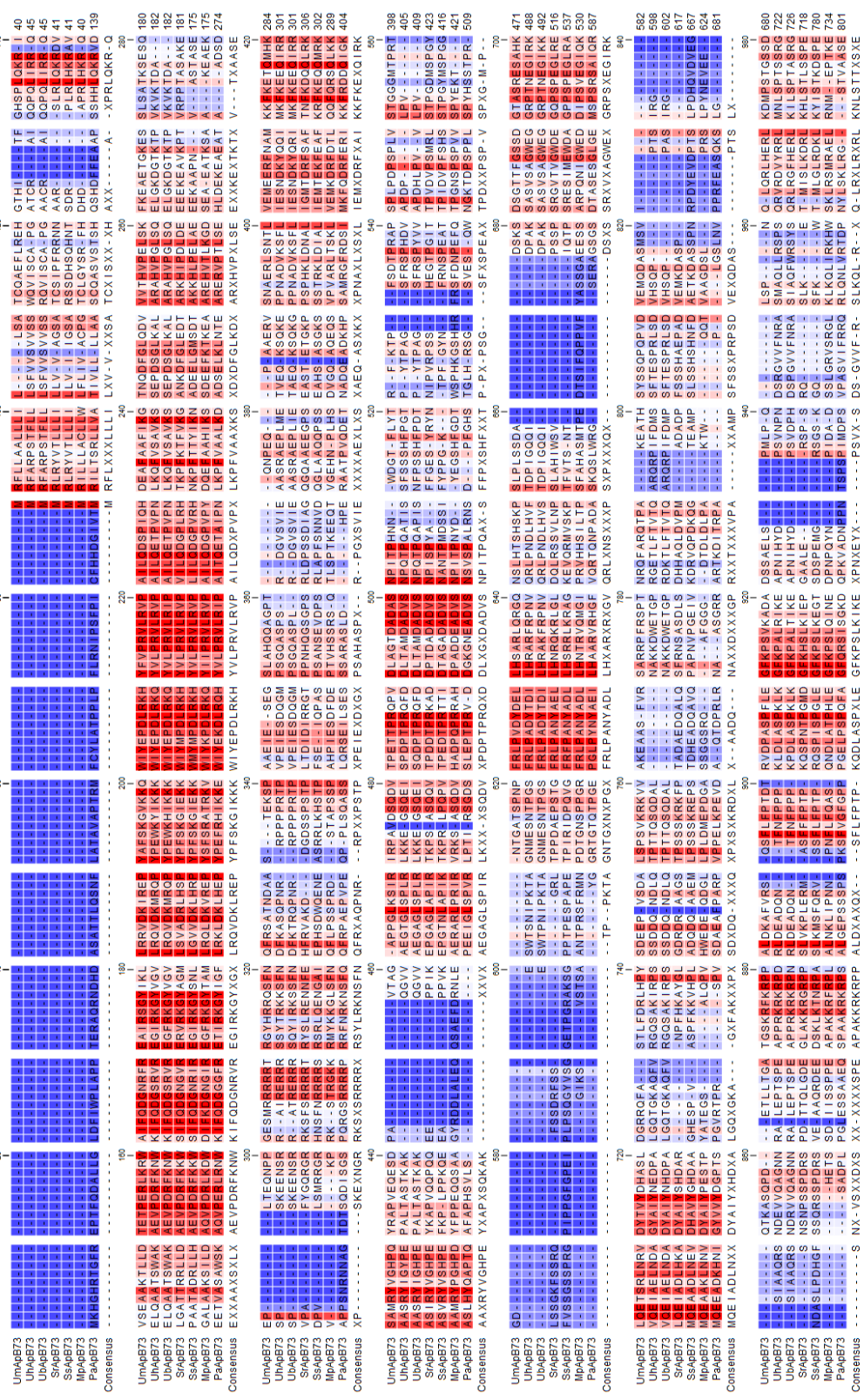

Figure 2.28 Amino acid sequence alignment of ApB73 orthologs from different smuts.
Sequences of the full length proteins from *U. maydis* (UmApB73), *U. bromivora* (UbApB73), *U. hordei* (UhApB73), *S. reilianum* (SrApB73), *S. scitamineum* (ScApB73), *M. pennsylvanicum* (MpApB73) and *P. aphidis* (PaGApB73) were obtained from public databases. Sequence alignment was generated by the multiple sequence alignment program CLUSTAL O in CLC main bench using default parameters. Colour scheme visualizes consensus strength, with red representing the highest and blue the lowest values.

To get a better idea about the conservation of the individual orthologs in comparison to ApB73 from *U. maydis,* identity and similarity values were calculated using the software tool SIAS (Immunomedicine Group, 2015; Table 2.1). Similarity in this context is defined as a more loose definition than identity and takes physical and chemical properties of the analysed amino acids into account.

Table 2.1 Identity and similarity values of the different ApB73 orthologs in respect to UmApB73.
Identity and similarity values of ApB73 orthologs from different smut fungi to the *U. maydis* ApB73 protein. Values were calculated for the protein sequences of the orthologs from *Sporisorium reilianum*, *Melanopsichium pennsylvanicum*, *Ustilago hordei, Ustilago bromivora, Sporisorium scitamineum* and *Pseudozyma aphidis*. Values were calculated using amino acid sequences and feeding them into the software tool SIAS (Immunomedicine Group, 2015).

ApB73	Identity to UmApB73	Similarity to UmApB73
SrApB73 (sr12972)	44.44%	55.02%
MpApB73 (MP05899)	38.88%	48.5%
UhApB73 (UHOR_02986)	38.88%	50.85%
UbApB73 (UBRO_02986)	38.88%	50.42%
SsApB73 (SPSC_03285)	36.75%	46.36%
PaApB73 (PaG03016)	27.5%	36.15%

The calculated identity values among the orthologs of ApB73 range from 27.5-44.5%, the similarities go even up to 55% for the *S. reilianum* ortholog. To examine, if those values correspond to different degrees of functional conservation, certain orthologs were subjected to cross-species complementation assays.

2.10.2. Functional redundancies of the ApB73 orthologs

High identity or similarity values, when comparing the amino acid sequences of orthologous protein, do not imply that the two proteins are also functionally similar. To further investigate the possible functional redundancy of the orthologs, a cross-complementation assay was conducted. In this assay, it was attempted to rescue the ΔapB73 phenotype of *U. maydis* on maize cv. B73 by expressing the different orthologs. Three orthologs were chosen to represent the various orthologs based upon different characteristics. The *S. reilianum* ortholog SrApB73 (sr12972) was used as the pathogen and *U. maydis* share the same host *Z. mays* and are most closely related, the MpApB73 (MP05899) from *M. pennsylvanicum* was selected due to the fact, that *M. pennsylvanicum* is the only smut infecting dicotyledonous plants, and finally UbApB73 (UBRO_02986) from *U. bromivora* was included, a Bromus-infecting smut and very close relative of *U. hordei*. As the ortholog of *P. aphidis* lacks a functional SP and as the SP, as it was already shown, is crucial for the function of UmApB73 (Figure 2.14), the Pseudozyma ortholog was neglected.

To this end, the coding sequences of the orthologous proteins SrApB73, MpApB73 and UbApB73 were ectopically introduced into *U. maydis* ΔapB73 strain. To exclude problems with the strength and timing of the individual promoters, expression of all orthologs was driven by the native *apB73* promoter. The derived transgenic strains, including SG200 and the ΔapB73 mutant as controls, were injected into seedlings of maize cv. B73 and disease symptoms were scored 12 dpi (Figure 2.29a).

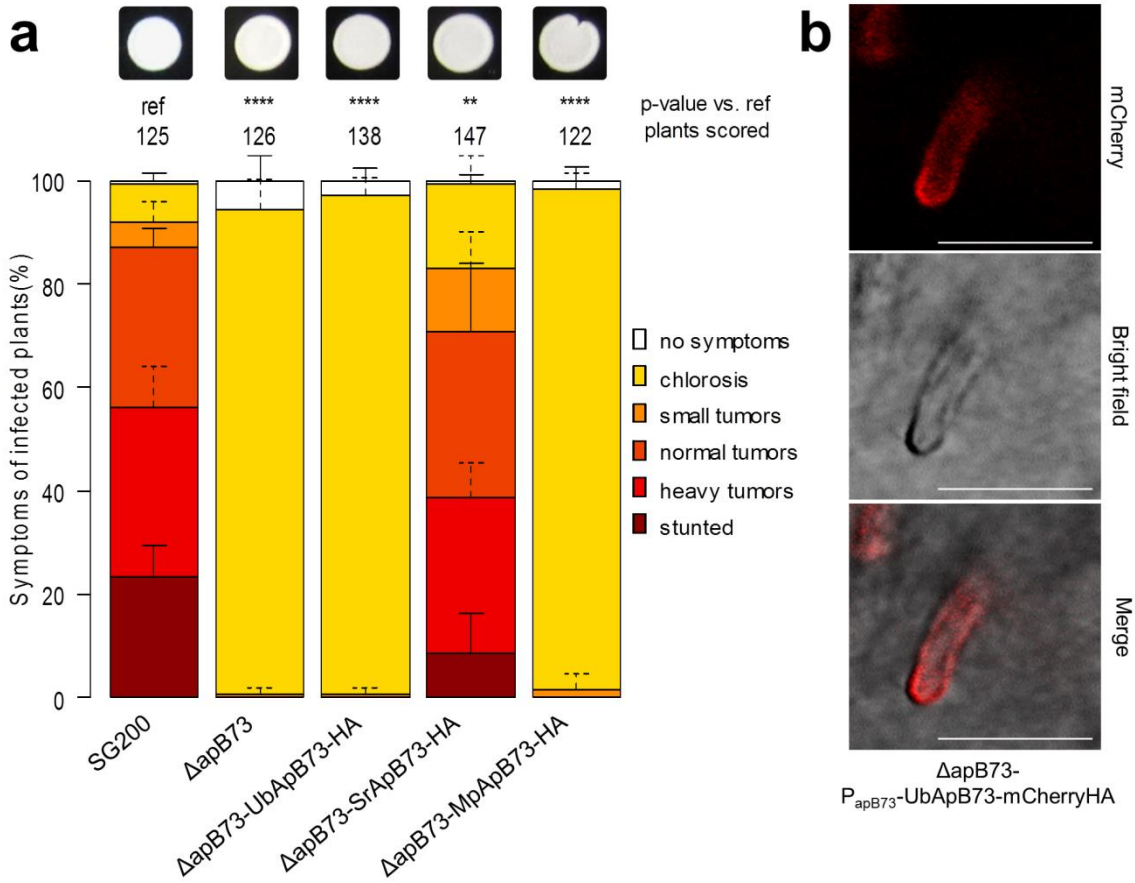

Figure 2.29 Virulence assay and microscopy of ApB73 orthologs.
(a) *U. maydis* strains expressing UbApB73, SrApB73 or MpApB73 under the native *apB73* promoter in the ΔapB73 mutant background were used for a seedling infection assay of maize cv. B73. Plants were infected seven days after germination and scored for symptoms 12 dpi. In the top row, pictures of the respective strain are shown after growing on filamentation inducing charcoal plates for 24h. Disease scores are shown on the right. Mean values of three independent infections are depicted and the total number of infected plants is indicated above the respective columns. Mean and standard deviation of relative counts from replicates are displayed. For clarity, only positive error bars are shown. P-values were calculated by Fisher's exact test. **P, <0.01; ****, P <0.0001. **(b)** Microscopy to show expression of the UbApB73-mCherryHA fusion protein. Maize seedlings were infected with ΔapB73 strains expressing UbApB73-mCherry-HA under the native *apB73* promoter. Fluorescence was observed at three days post infection. Bar = 10 µm.

The results of the virulence assay, using ApB73 orthologs from three different related smut fungi, show that only the *S. reilianum* ortholog SrApB73 complements the *apB73* mutant phenotype. The less conserved orthologs from *M. pennsylvanicum* and *U. bromivora* on the other hand, both sharing the same identity value towards UmApB73, were unable to rescue the virulence defect of the *apB73* deletion strain. To further elaborate if expression problems could be the reason for UbApB73´s inability to

complement the *umapB73* deletion phenotype, a C-terminal mCherry fusion was generated, and expression, as well as, secretion was confirmed by fluorescent microscopy (Figure 2.29b).

2.10.3. Phenotypic rescue using mosaic versions of ApB73

The ApB73 protein of *U. maydis* has many orthologs in related smut fungi. When challenging three of them (SrApB73, MpApB73 and UbApB73) for their capability to rescue the *U. maydis apB73* mutant phenotype, only SrApB73 could rescue it. This distinct behaviour of the orthologous proteins could be used to identify regions within ApB73 that are essential for its function in virulence. The idea here is to substitute certain parts of the *U. maydis apB73* CDS with the corresponding region of the *U. bromivora apB73* CDS. This way, mosaic proteins are generated from a version of the protein unable to rescue the mutant phenotype, and a version that can rescue the phenotype. As shown with the help of bioinformatic comparisons, it is not possible to identify specific domains within the ApB73 protein, the full length CDS of UmApB73 and UbApB73, were therefore divided into three equally sized pieces (Figure 2.30). When doing so, using the Golden Gate cloning technique, it was made sure that the individual domains end on the same amino acid, making it possible to have no extra amino acids in the constructs. Additionally, the SP peptide from UmApB73 was used for all constructs, to rule out that possible differences simply occur as a result of different secretion efficiencies.

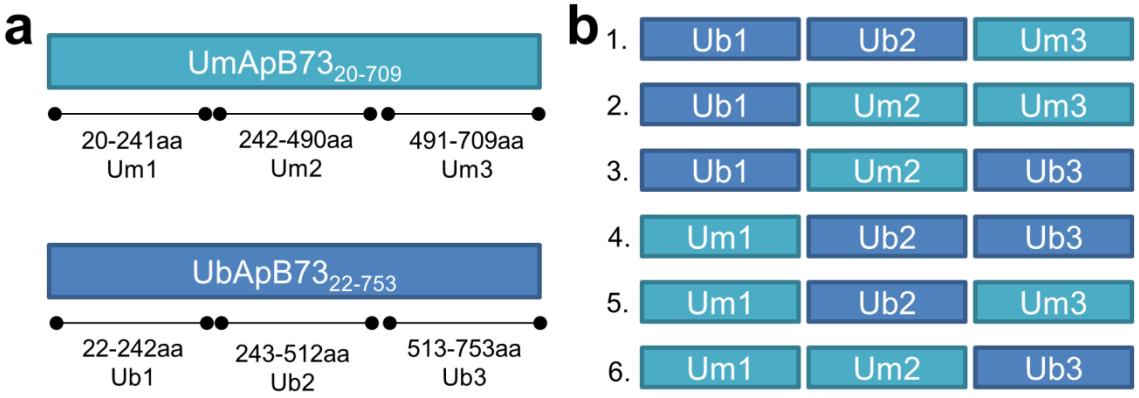

Figure 2.30 Schematic representation of the individual parts of the mosaic ApB73 proteins.
(a) Protein structure of the ApB73 orthologs from *U. maydis* and *U. bromivora.* Shown are the full length proteins (without signal peptide). Underneath the individual proteins the three domains chosen for the creation of mosaic proteins is shown. **(b)** Structure of the six mosaic proteins generated out of the coding sequences of the ApB73 orthologs from *U. maydis* and *U. bromivora*.

The six versions of ApB73, shown in Figure 2.30, were ectopically integrated into strain SG200ΔapB73, each expressed under the native *umapB73* promoter and with the UmApB73 SP. The resulting strains were subjected to a virulence assay in maize cv. B73 (Figure 2.31).

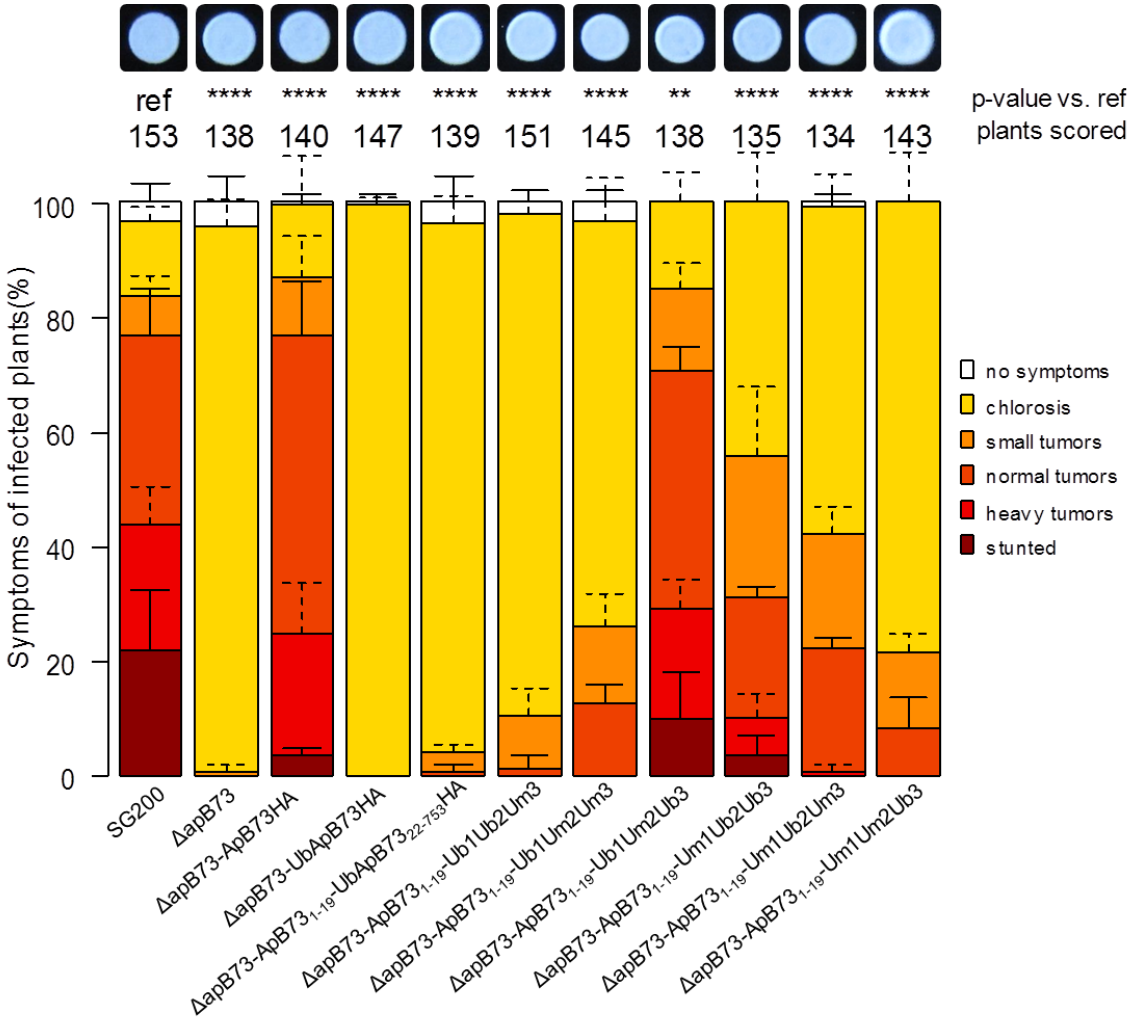

Figure 2.31 Virulence assay comparing mosaic versions of UbApB73 and UmApB73.
Different *U. maydis* strains were used for a seedling infection assay of maize cv. B73. The used strains express mosaic version of UmbApB73 and UmApB73 with the UmApB73 secretion signal (ApB73$_{1-19}$) under the native *apB73* promoter in the ΔapB73 mutant background. They were compared to the wildtype SG200, the mutant ΔapB73, the complementation strain ΔapB73-ApB73-HA and two strains expressing UbApB73 in the ΔapB73 mutant background, either with the native SP or the UmApB73 SP. Plants were infected seven days after germination and scored for symptoms at 12 dpi. In the top row, pictures of the respective strain are shown after growing on filamentation inducing charcoal plates for 24h. Disease scores are shown on the right. Mean values of three independent infections are depicted, and the total number of infected plants is indicated above the respective columns. Mean and standard deviation of relative counts from replicates are displayed. For clarity, only positive error bars are shown. P-values were calculated by Fisher's exact test. **P, <0.01; ****, P <0.0001.

The virulence assay shows that, in comparison to the mutant background, all mosaic versions of the ApB73 protein, display some degree of complementation. This is also true when comparing them to the strains expressing full length UbApB73 or ApB73$_{1-19}$-UbApB73 in the mutant background.

Those that were least successful in complementation included strains expressing Ub1Ub2Um3, Ub1Um2Um3 or Um1Um2Ub3. Intermediate phenotypes were obtained for Um1Ub2Um3 and Um1Ub2Ub3. Ub1Um2Ub3 was able to fully complement the phenotype in a way comparable to UmApB73-HA. As there is no clear pattern indicating which domains are necessary for complementation and which are not, and as the most

simple explanation would be a correlation of the results with amino acid identity/similarity, the overall identity and similarity values of the mosaic proteins in respect to UmApB73 were calculated (Table 2.2).

ApB73	Identity to UmApB73	Similarity to UmApB73	Strength of complementation
Ub1Ub2Um3	52.89%	59.92%	very weak
Ub1Um2Um3	80.57%	83.11%	weak
Um1Um2Ub3	73.06%	74.48%	weak
Um1Ub2Um3	71.65%	74.22%	weak intermediate
Um1Ub2Ub3	48.37%	52.19%	intermediate
Ub1Um2Ub3	54.3%	60.18%	strong

Table 2.2 Identity and similarity values of the six mosaic proteins in respect to UmApB73 protein. Identity and similarity values of the Um-ApB73/UbApB73 mosaic proteins when comparing them to UmApB73. In the right column estimates of the complementation strength of the individual constructs is described. Values were calculated using amino acid sequences and feeding them into the software tool SIAS (Immunomedicine Group, 2015).

The calculated identity values do not correlate with the ability of a strain to complement the *apB73* deletion phenotype. This indicates that the overall identity of the protein is not responsible for its ability to cause virulence, but rather that stretches of specific amino acids result in the proteins' ability to perform the function of ApB73.

2.11. Function of ApB73

2.11.1. Yeast two hybrid screen

One main open question about ApB73 is its molecular function. To get an idea, in which process the protein might be involved in, an attempt was made to identify possible interaction partners of ApB73. The identification of proteins that interact with ApB73 would allow conclusions about the metabolic place of action of ApB73 if these proteins are already characterized or share homologies with characterized proteins.

To this end, a heterologous system was used: the yeast *S. cerevisiae*. In this system, interaction screens, termed yeast two-hybrid (Y2H), are very well established (Young, 1998). The principle of this screen is the activation of reporter genes located downstream of an upstream activating sequence with the help of a transcription factor, here GAL4. The transcription factor is split into two moieties (binding domain, BD and activation domain, AD), and the protein of interest, here $ApB73_{20\text{-}709}$, is typically fused to the BD, whereas the library, containing possible interaction partners, is fused to the AD. As one can assume that ApB73, having a role in virulence, would interact with a maize protein or an *U. maydis* protein expressed during biotrophy, $BD\text{-}ApB73_{20\text{-}709}$ was exposed to a library that was generated out of reverse transcribed RNA isolated from infected

maize plants two and five days post infection respectively (Stratagene Phagemid library from Dr. Christoph Basse; Farfsing, 2004).

To bring those constructs, linked to either BD or AD, together, a mating approach was used. Plasmids that contain genes fused to the BD are transformed into a yeast strain of type a (here AH109), whereas plasmids encoding genes fused to the AD were transformed in a compatible yeast strain of type α (here Y187). Haploid strains of different mating types can fuse to generate diploid cells expressing the selection markers of both haploids.

In the described Y2H setup, some proteins can be 'autoactive', meaning that fusion of these proteins to the BD, results in activation of the reporter genes without the requirement of an interaction partner. To rule out that ApB73 is autoactive, the strain AH109-BD-ApB73$_{20\text{-}709}$ was mated with Y187-AD, a strain expressing the AD alone, as well as the other way around, where Y187-AD-ApB73$_{20\text{-}709}$ was mated with AH109-BD (Figure 2.32). As a positive control, a known autoactive protein Ap1 (Denise Seitner, personal communication) was used.

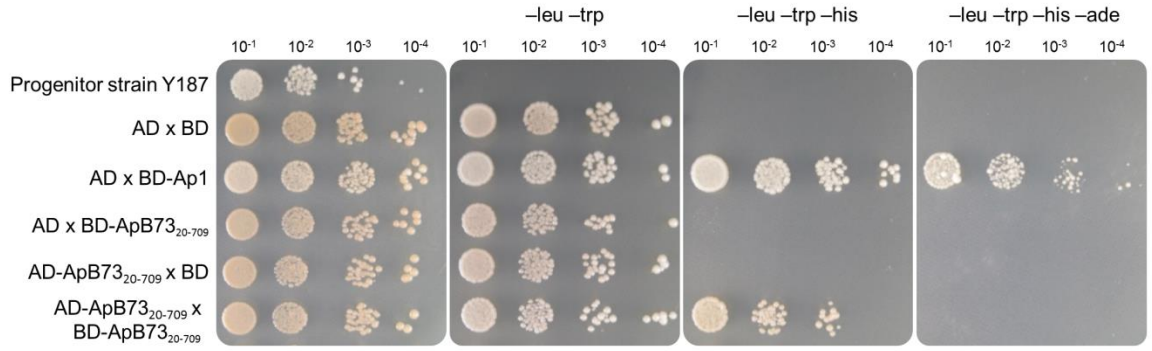

Figure 2.32 Spotting assay of ApB73 in yeast.
ApB73$_{20\text{-}709}$ shows no autoactivity on low or high stringency plates. The respective yeast cultures were spotted on selection media in serial dilutions. BD-Ap1 was used as a positive control. ApB73$_{20\text{-}709}$ can homodimerize, indicate by growth on low stringency medium.

The spotting assay shows that BD-ApB73$_{20\text{-}709}$ is not autoactive. Next, it was investigated if ApB73$_{20\text{-}709}$ might be capable of forming homodimers. To this end, two strains expressing ApB73 fused either to the AD or the BD were mated and spotted (Figure 2.32). The assay shows that ApB73 is capable of homodimerizing, indicated by the growth on low stringency medium (-leu, -trp, -his). However, the interaction does not allow growth on high stringency medium (-leu, -trp, -his, -ade).

The Y2H was performed with the mentioned library transformed into yeast strain Y187. The number of screened library clones was calculated by counting the colony forming units (cfu) on SD –leu plates, ~40000, multiplying them with the total suspension volume, 13 mL, and dividing the resulting number by the plated volume, 100 µL. This

results in a number of $5.2x10^6$ library clones that were screened in this Y2H for interaction with ApB73.

Depicted below are the proteins retrieved from 86 yeast clones found to be capable of growing on high stringency medium, indicating an interaction with ApB73 (Table 2.3).

Table 2.3 Proteins identified in a Y2H performed with ApB73 as bait.
The table below lists all proteins identified from cDNA in yeast clones that grew on high stringency medium in a Y2H screen performed with BD-ApB73 as bait and a cDNA library of *U. maydis* infected maize plants as prey. Additionally listed are specific domains present in the found proteins. Mentioned domains are restricted to those domains that were found in the actual found cDNA clones. Also listed is the number of clones the protein was found in, and the interaction strength of the specific plasmids when mated with either UmApB73 or UbApB73, where 5 indicates strong growth and 1 very limited growth on high stringency medium.

#	*Zea mays* protein	Domains	clone #	Interaction with UmApB73	Interaction with UbApB73
1	LOC103626210 golgin subfamily A member 4-like	**Smc, SMC_prok_B,** PRK05771, TMCO5	13	5	5
2	LOC100272719 uncharacterized protein	PHD_OBE1_like, PRK09173, PHD, DUF1423, PTZ00121, tolA_full, COG2433	13	5	4
3	LOC100193058 uncharacterized protein	ENT domain, LBR_tudor, Agenet, Med15	12	5	5
4	LOC100285243 ATMAP70-2	CENP-Q, TMF TATA binding, **SMC prok B, Smc**, Myosin HC like, PRK03918	5	5	2
5	LOC103643560 myosin-2 heavy chain-like	**Smc, SMC_prok_B**	4	5	5
6	LOC103643830 uncharacterized protein At4g38062	**SMC_prok_B, Smc,** AAA_27, PRK00409	4	5	5
7	LOC100383189 uncharacterized protein	ANK, ANK2	4	5	5
8	LOC100273855 uncharacterized protein	ACD_sHsps-like, BRIGHT, ARID, HSP20, IbpA	4	3	1
9	LOC542638 kinesin-related protein13	Ded_cyto, Kinesin-related, PLN03188, **SMC_prok_B, Smc**	3	5	5
10	LOC100273501 auxin response factor 4	B3_DNA, Auxin_resp, AUX_IAA	3	4	1
11	LOC100382371 uncharacterized protein	KISc_KIF2_like, Kinesin, KISc, KIP1, PLN03188	3	3	1
12	LOC100281506 potyvirus VPg interacting protein	DUF1423, PRK00409	2	4	1
13	LOC103633476 phragmoplast orienting kinesin-1-like	**SMC_prok_B, Smc,** PTZ00121, Macoilin	2	3	3
14	LOC100272566 uncharacterized protein	KISc_KIF2_like, Kinesin, KISc, KIP1, PLN03188	2	2	1
15	LOC100193731 uncharacterized protein	**Smc, SMC_prok_B,** PRK05771, TMCO5	1	5	3
16	LOC103655564 uncharacterized protein	FANCD2, DUF342, ArcA, BAR_SNX2, PTZ00121, Mplasa_alph_rch, **Smc,** Macoilin, Spc7	1	5	5
17	LOC100194064 alpha-taxilin	Taxilin, **SMC_prok_B, Smc**	1	4	4

18	LOC103652610 uncharacterized protein	RNase_HI_RT_Ty1	1	4	4
19	LOC100282725 RNA recognition motif containing protein	PLN03121, PLN03120	1	4	2
20	LOC100381535 uncharacterized protein	no known domains	1	3	2
21	LOC100383507 uncharacterized protein	Mitofilin, PTZ00121	1	3	2
22	LOC100279874 uncharacterized protein	ACE1-Sec16-like, Sec16_C, Atrophin-1, PHA03247, PABP-1234, COG5028, Amelogenin	1	2	1
23	LOC100302578 ATP binding protein	KISc_KIF2_like, Kinesin, KISc, KIP1, PLN03188	1	2	1
24	LOC100274434 uncharacterized protein	TPR_11	1	2	1
25	LOC100274688 uncharacterized protein	RING, zf-C3HC4, **Smc, SMC_prok_B,** rad18, DUF390, PRK02224, PLN03208	1	2	3
26	LOC100274272 uncharacterized protein	Mrs2_Mfm1p-like, CorA, PLN03229	1	2	4

The DNA identified from all shown interaction partners was in-frame with the AD. Mentioned domains found in the identified cDNA clones are domains present in the actual clones, i.e. domains that are part of the corresponding protein but are not in the interacting cDNA are not shown. The domains were identified using BLASTp with an E-value of 0.01 (Marchler-Bauer *et al.*, 2014).

The plasmids of all found candidates were transformed again into yeast strain Y187, mated with AH109-BD-ApB73$_{20\text{-}709}$ and spotted to evaluate and compare their interaction strength. Depending on their ability to grow on high stringency selection plates the interaction partners were categorized into five groups from 1, no growth to 5, very strong growth (Table 2.3).

As mentioned earlier, the ApB73 ortholog from *U. bromivora* UbApB73 is not capable of complementing the virulence phenotype of SG200ΔapB73 in maize (Figure 2.29). This suggests that there are certain differences between those two proteins that result in their functional divergence. Accordingly, UbApB73$_{22\text{-}753}$ was fused to the BD and transformed into AH109 to elucidate its capability to interact with the interaction partners of ApB73 found in the performed Y2H (Table 2.3). Although in some cases there are differences regarding the interaction strength with a certain partner, depending on the usage of UmApB73$_{20\text{-}709}$ or UbApB73$_{22\text{-}753}$, there are no striking correlations with a certain domain.

Interestingly, one domain appears in the sequence of 38% (10/26) of all proteins identified as possible interaction partners, or differently in more than 40% (35/86) of all picked yeast clones, indicating a possible affinity of ApB73 towards this domain (labelled in blue, Table 2.3). In ten identified proteins, a domain resembling a Smc domain

(COG1196) is found, and additionally in nine of these ten proteins, the same domain also resembles the similar SMC_prok_B domain (TIGR02168). Both domains were identified in SMC (structural maintenance of chromosomes) proteins, a large family of chromosome segregation-related ATPases (Milutinovich & Koshland, 2003).

To investigate if this domain is actually responsible for the interaction, one clone of the identified 13 clones encoding for the *Zea mays* protein golgin subfamily A member 4-like (LOC103626210, for simplicity called Golgin from now on) was chosen and cloned with and without the Smc domain into the pGAD vector. Additionally, the SMC region alone was tested for its capability to interact with ApB73. The resulting yeast strains were mated with a strain expressing ApB73-BD and spotted on selection medium (Figure 2.33).

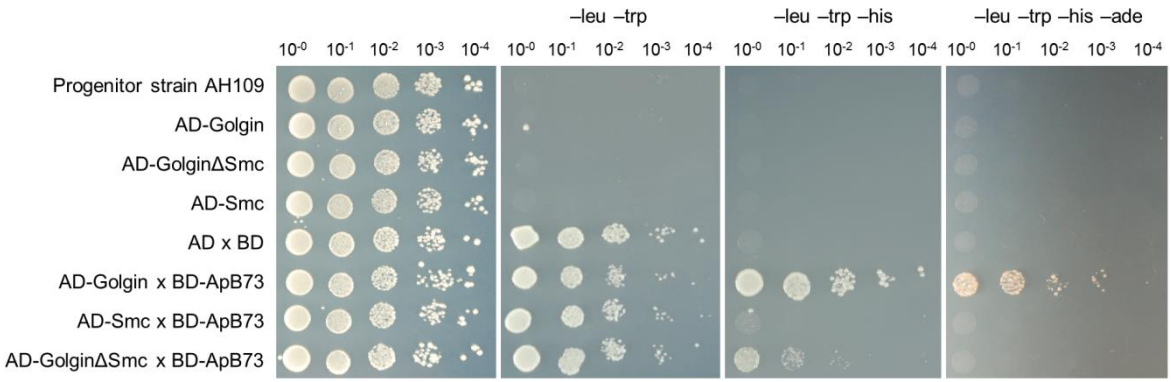

Figure 2.33 Spotting assay to evaluate the role of the Smc domain.
Different yeast strains expressing either Golgin, the SMC domain or GolginΔSMC were tested for their interaction with ApB73. As a control, the unmated strains, empty vector controls and wildtype yeast are shown. Pictures were taken 72 hours after spotting. The mated strain expressing BD-ApB73 and AD-Golgin shows growth on low and high stringency plates, whereas BD-ApB73 mates with AD-SMC only grows on low stringency. The AD-GolginΔSmc does not grow on low or high stringency plates when mated with BD-ApB73. The respective yeast cultures were spotted on selection media in serial dilutions.

Interestingly, the spotting assay shows that without the SMC domain no growth on low or high stringency selection plates can be observed, whereas the SMC domain alone is sufficient to induce growth on low stringency plates. This indicates that the SMC domain is indeed (partially) responsible for the interaction of the two proteins.

Despite the fact that this last shown experiment gives some indication that the Smc domain, identified in many clones that were found to interact with ApB73, may actually be of importance, it is important to mention that this Y2H was performed very early during the study of this protein.

Timewise later on during my PhD, it turned out that ApB73, or parts of it seem to be localizing to the membrane, as a results, it is possible that the conducted Y2H gives arbitrary results. In a Y2H screen, the two proteins tested for their interaction are expressed and localized to the yeast cytosol. Accordingly, this assay probably changes

the accessibility of ApB73 domains dramatically. However, as there are some indications that the N-terminal domain of ApB73 might be cleaved of the protein in the biotrophic interface, it is still conceivable that this Y2H screen found true interaction partners. Ideally, if one can determine the exact part that is split off of ApB73 in the plant, this Y2H should be repeated simply expressing this N-terminal moiety of ApB73 as bait.

3 Discussion

In the last decades it has become more and more evident that virulence factors, including effector molecules, are key players in the establishment of biotrophic interactions between pathogens and plants (Jones & Dangl, 2006). Although research has mainly focused on bacterial proteins, factors from oomycetes and fungi were also characterized shedding light into these complex interactions (de Jonge *et al.*, 2010; Djamei *et al.*, 2011). In this thesis, the *Ustilago maydis* protein and effector candidate ApB73 was investigated.

3.1. The role of ApB73 in biotrophic interactions between *U. maydis* and *Z. mays*

The main objective of this thesis was to elucidate if ApB73 has a role in virulence, qualifies as an effector and, finally, its mode or mechanism of action. The experiments described above show that ApB73 is one of the few secreted molecules crucial to establish biotrophy in the *Ustilago maydis –Zea mays* cv. B73 pathosystem. Deleting *apB73* from the *U. maydis* progenitor strain SG200 abolishes the fungus' ability to induce tumor formation on maize cultivar B73.

In the next few subchapters, I will discuss the specific observations that were made while investigating ApB73, and how these results help to further specify the exact role of ApB73 during virulence.

3.2. Impact of ApB73 is maize cultivar dependent

The abolishment of tumor formation in seedling infection assays on maize cv. B73 seems to be a cultivar specific observation. This changes when other accessions like the most widely used accession of the *U. maydis* field EGB, were infected.

On EGB, a more susceptible maize variety, mutant strains lacking *apB73* are still capable of forming tumors upon infection even though to a very limited extent. These differences in infection strength in response to different maize accessions, is a so far undescribed observation regarding effector mutants in the *U. maydis* field. It shows that the outcome of an infection is not only depending on the strength of the pathogen, but also the susceptibility of its host.

This observation that maize accessions vary in their response to *U. maydis* infection is supported by the comparison of known quantitative resistance loci in maize. The *U. maydis*-maize interaction is not based on gene-for-gene interactions common to other pathosystems. Instead it was shown that the outcome of an infection of *Z. mays*

with *U. maydis* is determined by the interplay of several quantitative trait loci (QTL, Baumgarten *et al.*, 2007). So although there are currently no studies available comparing the genomes of EGB and B73, one can speculate that the differences between those two genomes must affect important quantitative resistance loci decisive over the outcome of an infection with *U. maydis*.

The presented results show that virulence phenotypes caused by deletions of 'weaker' virulence factors can be intensified when tested in maize accession B73 instead of EGB. Considering how many putative effector gene deletions do not result in measurable phenotypes (Kämper *et al.*, 2006), this could help to widen the dynamic range of infection scorings and allow for the detection of minor contributions to virulence from effector candidates. Additionally, this could assist researchers in the field of plant pathogens by making them aware that in some cases it could help to use various host accessions to elucidate the role of an effector candidate.

3.3. *apB73* mutants do not form spores

Another key finding of this thesis is that the *apB73* mutant fails to generate spores in tassel infections on maize cv. Gaspe Flint. This implies that lack of ApB73 finally leads to an evolutionary dead end for the fungus, making ApB73 an essential protein for the sexual reproduction of *U. maydis*. In a less likely scenario, the lack of ApB73 leads to a much delayed formation of spores not covered by the extended time period already given for spore development in tassel tumors in the presented experiments (40 days in contrast to 12-15 days needed for spore formation in the wildtype). Considering that tumor formation on tassels still occurs to a decreased extent, ApB73 is the first secreted protein described that has an impact on sporogenesis without completely depleting the induction of tumor tissue.

The finding that *apB73* mutants induce tumor formation (at a low rate) not only on tassels but also on seedlings of maize cv. EGB, shows that ApB73 is not an organ specific effector. It would be interesting to repeat these experiments on tassels of cv. B73 and EGB to observe how *apB73* mutants perform on reproductive organs of different maize cultivars. Additionally, seedling assays on cv. Gaspe Flint should be conducted to allow for a comparison between infection efficiency on tassels and leaves in different varieties. However, as Gaspe Flint is described as a cultivar with a similar susceptibility rate to *U. maydis* as cultivar EGB (Redkar, 2014), it is to be expected that Gaspe Flint should behave similar to EGB in seedling infection assays, whereas EGB should behave similar to Gaspe Flint in tassel infection assays. Depending on the

outcome, this would allow to further strengthen or actually weaken the observation that ApB73 does not seem to have an organ specific role.

3.4. *apB73* mutants are not impaired in penetration

Next, an attempt was made to determine at which step of infection *apB73* mutants are impaired. In contrast to *pep1* mutants, where growth of *U. maydis* is blocked at a very early stage leaving them unable to penetrate the plant (Doehlemann *et al.*, 2009), *apB73* mutants form appressoria and penetrate the plants epidermis at rates comparable to the progenitor strain SG200. However, they fail to establish biotrophy, indicated by the lack of extensive and branched fungal growth as late as seven days post infection. This shows that expression of *apB73* is crucial for virulence and that the protein is needed, not in the very first steps of the infection process, but later to ensure efficient tumor formation. The shown qPCR data supports the involvement of ApB73 at later stages of infection. Although expression levels of *apB73* increase already after 24h (~10 fold), highest levels are found between two to eight days post infection (>100 fold). This coincides with the biotrophic stages of development of *U. maydis* as shortly after this phase hyphae start to fragment (9 dpi), initiating the first steps towards the formation of spores (Banuett & Herskowitz, 1996). The expression profile is comparable to other known effectors like Pit2 or Tin2 (Doehlemann *et al.*, 2011; Tanaka *et al.*, 2014). Here, deletions also result in strains still capable of penetrating the plants epidermis but then fail to cause progenitor strain-like symptoms.

The observation that some effector mutants of *U. maydis* are still virulent to a certain degree, i.e. are in principle capable of penetrating the plant and also succeed to colonize the next few cells, can be explained by imagining an equilibrium between virulence factors and the host defence machinery. The less efficiently the pathogen suppresses the host defence machinery, for example due to a lack of specific effectors, the more likely it will fail over the long run in the colonization of its host. Vice versa, the less efficiently the host machinery recognizes and reacts to the invader, the more likely it will be overcome by the pathogen. The binary outcome of the mentioned spore formation is therefore a quantitative product of the susceptibility of the host and the virulence of the pathogen.

3.5. Localization of ApB73

After establishing the importance of ApB73 for virulence, one of the major open questions revolved around the localization of the protein during the infection process. This helps to differentiate between proteins qualifying as virulence factors or as effectors.

Although both categories describe molecules important for virulence, the function of effectors, in contrast to virulence factors, is characterized by their direct or indirect interaction with the host during establishment of pathogenicity. Localization to the biotrophic interface would therefore be necessary but not sufficient for ApB73 to qualify as an effector, and would also not rule out the possibility of ApB73 being a virulence factor.

3.5.1. Localization in the biotrophic interface

In vivo microscopy of ApB73-mCherry-HA and complementation attempts without the ApB73 SP show that ApB73 is secreted and that secretion is essential for its function in virulence. However, Western blot analyses on secreted proteins, termed supernatant assays, fail to show secretion of ApB73.

One explanation for this discrepancy could be a quantitative problem. However, even quadrupling the culture volume did not result in a detectable signal using Western blot analysis. Another problem could be the stability of the protein, but if degradation would occur the degradation products should still be visible on a Western blot.

The results of a recent study looking at the involvement of ER stress in secretion might also be relevant to explain the failure to show secretion of ApB73 using secretion assays (Hampel *et al.*, 2016). The authors show that ER stress in *U. maydis* can increase not only transcription but also secretion of certain *U. maydis* effectors. It has been known for a long time that ER stress leads to the accumulation of un- or misfolded proteins, which results in activation of the unfolded protein response (UPR). Specific motifs within promoter sequences, termed unfolded protein response elements (UPRE), play a role in the expression of UPR target genes. In *U. maydis* these UPRE motifs are also present in the promoter sequences of many effectors, e.g. *tin1-1* and *pit2*. As a result, the *pit2* promoter under ER stress leads to stronger expression of a specific gene than with the in axenic culture constitutively active *otef* promoter (Hampel *et al.*, 2016). Additionally, they show that UPR leads to stronger secretion and/or more efficient processing of genes expressed under an UPRE responsive promoter. The promoter sequence of ApB73 also contains a sequence qualifying for an UPRE, however, in contrast to *tin1-1* and *pit2;* no transcriptional induction (<2 fold) upon ER stress in *U. maydis* was found (Hampel *et al.*, 2016). However, it is possible that ApB73 is less than 2 fold induced and, additionally, secretion of ApB73 might still be enhanced in ER stressed cells. Accordingly, it would be interesting to repeat the secretion assay using an ER-stress inducible strong promoter (e.g. *pit2* promoter). Also Hampel *et al.* observed a role of ER stress in post-translational processes which might apply to ApB73 as well, and

could possibly result in misleading results in axenic culture conditions (Hampel *et al.*, 2016).

Another previously mentioned explanation for the failure to show secretion of ApB73 in supernatant assays would be that ApB73, after passing the secretory pathway, stays attached to the fungal membrane or cell wall.

Indications that this is actually the case come, for example, from the plasma membrane enrichment experiment where ApB73 seems to be enriched in the PM fraction. However, as all secreted proteins pass the endomembrane system and the protocol is enriching membranes in general, rather than just the PM, it is conceivable that all secreted proteins get enriched. Therefore, this experiment should be repeated including the appropriate controls, like for example a strain overexpressing a tagged secreted protein known to not associate to the PM (e.g. Cmu1, Djamei *et al.*, 2011) and a strain expressing a positive control, like the membrane protein Pit1 (Doehlemann *et al.*, 2011). Another drawback of this experiment is that it is performed on axenic cultures rather than infecting fungal filaments. Therefore, instead of repeating this experiment, other experiments were designed in an attempt to answer the question if ApB73 localizes to the PM *in planta*.

To this end, co-expression studies of ApB73-mCherry-HA with the known membrane protein Pit1 fused to GFP were performed. Microscopy shows a clear overlay of the two signals indicating co-localization of the two proteins. However, as the fungal PM and cell wall are compartments that are localized very close to each other, it is difficult to separate signals coming from those two compartments using light microscopy. As, unfortunately no protein was available localizing to the cell wall of the fungus and all attempts to generate one failed (Simon Uhse, personal communication), no data is shown confirming this assumption.

Additionally, attempts were made to fuse ApB73 to known transmembrane domains (Pit1, Doehlemann *et al.*, 2011). The idea behind this approach was to determine if ApB73 retains its functionality if N-terminally attached to the membrane. Unfortunately, none of the cloned transmembrane (TM) domains allowed secretion and membrane attachment of the fusion protein (e.g. TM1-ApB73$_{20\text{-}709}$-mCherry, tested using microscopy, data not shown).

One approach successfully used to show localization of effectors within the interaction zone of *Ustilago maydis* and *Zea mays* is immunoelectron microscopy. Here, differentiation between signals coming from the PM or the cell wall will still be challenging, but it should be possible to see an overall prevailing accumulation in either

compartment. The more problematic issues regarding this approach for ApB73 are more fundamental regarding primarily expression. In general, expression levels should be relatively high to ensure detection of a sufficient number of molecules. This is supported by the studies published within the field so far, where biotrophic promoters with strong expression levels were used, especially when comparing the expression levels of the used promoters to those of the *apB73* promoter (Djamei *et al.*, 2011, Redkar *et al.*, 2015a, Daniel Lanver, personal communication). Despite these possible difficulties, it would be interesting to determine the localization of ApB73 using immunoelectron microscopy, as the exact place of action would help in designing experiments aimed at identifying possible interaction partners.

Finally, plasmolysis experiments of infected maize plants were conducted using mCherry fusions to ApB73. A C-terminal fusion of ApB73 to mCherry results in a fluorescent signal localizing around the fungal hyphae that does not diffuse within the biotrophic interface during plasmolysis. In contrast, free diffusion of ApB73 fusion proteins was observed *in planta*, when conducting plasmolysis experiments with $ApB73_{1-19}$-mCherry-3xHA-$ApB73_{20-709}$3xmyc. This either shows a possible processing of ApB73 or steric hindrance of its membrane attachment due to the N-terminal mCherry. However, as the mentioned construct complements the virulence phenotype of the *apB73* mutant strain steric hindrance seems unlikely. Processing of this unusually large protein might be an important step that could either change the function of the protein or possibly release an active moiety in order to fulfil its function. We do not know if ApB73 is only cut once, or eventually, multiple times.

Summarizing the observations that: 1. secretion is happening (shown by *in vivo* microscopy) and necessary (as complementation attempts without SP fail), 2. ApB73 is enriched in the PM of axenic culture, 3. ApB73 is not detectable in *in vitro* supernatant assays and 4. ApB73-mCherry does not freely diffuse in the biotrophic interface, but mCherry-ApB73 does, shown *in vivo* using plasmolysis, it seems well supported to conclude that ApB73 is secreted and (partially) localizes to the fungal surface.

3.5.2. Localization of ApB73 *in vitro* is pH dependent

Another set of experiments conducted on axenic cultures indicated a possible influence of the pH on the localization of ApB73.

To investigate if this might be relevant for the biological role of ApB73, the shown experiments should be repeated including the controls mentioned in the results section, i.e. the effector protein Cmu1 and the membrane protein Pit1. The inclusion of these proteins would make it possible to differentiate if we are dealing with a specific property

of ApB73, or with a phenomenon that is true for all secreted or all membrane proteins. If this observation is reproducible and the controls indicate that pH dependent solubility is indeed a characteristic of ApB73 in particular, there still remains the result obtained *in planta*. Here, in contrast to axenic culture, plasmolysis of infected maize leaves with different pH solutions failed to show solubility changes of ApB73-mCherry. However, there are several possibilities why this experiment may did not show a pH dependent effect on solubility of ApB73. It is possible that the used solutions were not potent enough to induce changes in the local pH of the infected leaf tissue or, that microscopy is simply not sensitive enough to show low amounts of soluble protein. It is also conceivable that the conducted experiments were performed too late within the time course of biotrophy to show the effect of a pH change. The fact that changes in pH can actually happen at very early time points of infection was shown for other pathosystems. In barley, exposure to PAMPs resulted in changes of one pH unit within only a few minutes (Felle *et al.*, 2004). Unfortunately, this cannot be tested with the current protocol, as protein expression, and ergo fluorescence, with the used promoters is not strong enough at early time points.

This could also explain the results obtained in the plasmolysis experiments *in planta*, where C-terminal tagged ApB73-mCherry remains bound, whereas N-terminal tagged mCherry-ApB73 always appears soluble. If changes in pH, happening very early during infection, allow a certain moiety of the N-terminal part of ApB73 to be released, only the result, i.e. solubilised, processed protein, is observed in infected leaves. This means that N-terminally tagged ApB73 proteins seem freely diffusing, whereas C-terminally tagged proteins appear to remain membrane bound.

Approaches to address this question by tagging ApB73 C-terminally with mCherry and adding an N-terminal GFP failed, as the GFP signal was not detectable (data not shown). Another interesting possibility here could be to use ‘click chemistry’ for the addition of dual-colour fluorophores to modified terminal amino acids after translation and secretion (Nikić *et al.*, 2014). As this to my knowledge has never been done before in the Ustilago maize system, it would possibly require some modifications. However, the advantage would be that the ApB73 protein could be expressed and translated without additional tags, reducing the chance of possible artefacts. Afterwards, plasmolysis experiments of infected maize leaves could illustrate if the N-terminal part is indeed processed and freely diffusible, whereas the C-terminal part remains associated to the fungal surface.

Additionally, it is conceivable that this trigger – changes in pH – is actually necessary for the now released protein moieties to function. The trigger would be the

signal meaning the apoplast is prepared for the role of processed ApB73. Considering that this protein would be much smaller now, it may even be translocated into the plant cell.

3.5.3. Localization in the heterologous system *N. benthamiana*

To address the possibility that ApB73 might be translocated into the plant cell, localization studies were conducted expressing ApB73 in the heterologous system *N. benthamiana*. When expressing the protein as a mCherry or YFP fusion without the native signal peptide it reproducibly localizes to the PM, as well as, to round structures, possibly vesicles, in the cytosol and around the nucleus. Although the localization looks very interesting, one has to keep in mind that these results come from a heterologous system and could be an artifact.

Despite this, the microscopy data from tobacco confirms that ApB73 seems to have a general affinity towards membranes. The dual localization, however, might be an artefact of the expression of the full length protein. As descried earlier, there are some indications that ApB73 might be processed *in planta* resulting in the 'release' of an N-terminal moiety. It would be interesting to test different C-terminally truncated versions of ApB73 to observe if localization in tobacco is affected. It is conceivable, for example, that a C-terminal part of ApB73 shows localization to the PM, whereas a truncated protein harboring only the N-terminus of ApB73 localizes solely to the observed putative vesicles. In combination with complementation attempts in the *U. maydis*/*Z. mays* system, it might be possible to draw conclusions about the distinct functions of individual parts of the protein by either expressing individual truncated proteins or simultaneously co-expressing the N- and C-terminal moieties. Whereas a C-terminal portion might fulfill a function at the PM, an N-terminal portion might be translocated to the plant cell.

In case a suitable strong promoter was identified that still complements the deletion phenotype the translocation into the plant cell of ApB73 or just the mentioned N-terminal or C-terminal portion could be tested by immunoelectron microscopy tagging. This could include either the whole full length protein or the N-terminal/C-terminal part of the protein. Additionally, if one could show with the earlier described experiments that the two moieties function independently, transgenic maize plants could be generated expressing either part to test them for *in trans* complementation of the virulence phenotype. The individual parts of ApB73 should additionally be fused to a nuclear localization signal, as well as, a nuclear export signal to elucidate if localization to the nucleus which was observed in *N. benthamiana* is actually relevant.

3.5.4. Complementation of the virulence defect using different promoter sequences

The ΔapB73 virulence phenotype can be complemented by reintroducing *apB73* ectopically. Although complementation success does not seem to be influenced by the addition of N- or C-terminal tags (e.g. HA or mCherry), the usage of certain promoters seems to be critical. Whereas usage of the native *apB73* promoter results in full complementation, even when expressing *apB73* ectopically, usage of the strong biotrophic promoters of *stp1* and *pit2* does not result in complementation of the phenotype.

Expression patterns of *stp1*, *pit2* and *apB73* are comparable as expression of all genes is enhanced over the biotrophic stages of infection (Schipper, 2009; Doehlemann *et al.*, 2011). However, when having a closer look at timing and strength of expression, striking differences can be observed (Daniel Lanver, unpublished). Expression profiles of *stp1* seem very similar to *apB73* at a first glance. Both expression patterns peak at two days post infection and then slow but steadily decrease till 12dpi. In contrast, *pit2* expression has its highest peaks at 4 dpi and then decreases more rapidly. Absolute expression values of *stp1,* however, are 4-7 times higher when comparing them to *apB73* and values for *pit2* 30-50 times higher (based on RNAseq data, Daniel Lanver, unpublished). And even though comparing mRNA levels might be misleading as certain transcripts might differ in their stability, it is fair to speculate that *apB73* expression levels 4-50 times higher than under native conditions might be the cause for the unsuccessful complementation attempts with these biotrophy specific promoters.

Another possible reason could be basal expression levels of *apB73* under these different promoters, as expression under the *apB73* promoter in axenic culture seems to be 7-8 times higher compared to the *stp1* or *pit2* promoter. Accordingly, it seems feasible that certain levels of *apB73*, while still very low compared to levels during biotrophic stages, might be needed within the first few hours of infection. At this point expression levels that are reached with the *apB73* promoter still exceed those of the *pit2* or *stp1* promoter.

Summarizing these observations it can be stated that timing and strength of *apB73* expression seem critical for its role in virulence. This is very interesting, but makes possible downstream assays, like e.g. immunoprecipitation (IP) or protein complex immunoprecipitation (Co-IP) harder, as protein levels using the native *apB73* promoter are below the detection limit. However, it is still possibly to identify a strong promoter that

is capable of complementing the *apB73* deletion phenotype, if more different promoters would be screened.

3.6. Conservation of ApB73 in other smut fungi

Among the 485 predicted effector candidates (Jason Bosch, personal communication), ApB73 belongs to a group of candidates (212/485, Jason Bosch, personal communication) where orthologs can be found in all the smut genomes sequenced so far. However, that does not imply that the predicted orthologs are also functionally redundant. From the literature it is known that certain effectors, like *MC69* from the rice pathogen *Magnaporthe oryzae*, share pathogenicity relevant orthologs with other species, like *MC69* from the cucumber pathogen *Colletotrichum orbiculare.* This means that orthologs from the same effector can be important for monocotyledonous and dicotyledonous hosts (Saitoh *et al.*, 2012). Accordingly, I attempted to elucidate if the ApB73 mutant phenotype can be complemented using orthologous proteins from closely related smuts.

It was observed that neither the ortholog from *M. pennsylvanicum* nor the one from *U. bromivora* can complement the phenotype. However, the ortholog from *S. reilianum* almost fully restores virulence. This shows that pure size of the protein is not sufficient for its function, although it should be considered that differences in the SP could matter. One reason, why only the ortholog from *S. reilianum* can complement the phenotype, could be that both fungi are infecting the same host ergo both of them may have evolved to interact with a certain maize protein. It would be interesting to conduct plasmolysis experiments with a mCherry tagged version of SrApB73 to see if this protein also localizes to the PM. A more simple explanation could be the fact that UmApB73 and SrApB73 share the highest identity values. For other effectors, studies of orthologous proteins were also conducted. For Pep1, for example, a well-characterized effector of *U. maydis*, all complementation attempts using orthologs from various other smuts were successful (Hemetsberger *et al.*, 2015). The reason here is likely the very high overall conservation (identities of 51-64% compared to only 27-44.5% for ApB73). In line with this, complementation attempts for the effector See1 with its *U. hordei* ortholog were not successful with identity values of 34% (Redkar *et al.*, 2015b).

These results - some orthologs fully complement the phenotype and others do not - allowed for the attempt to narrow down specific regions within the 709aa large ApB73 protein by generating ‘mosaic’ versions of UmApB73 and UbApB73. The coding sequences of the two proteins were cut into three equal parts and then shuffled with each other generating six different fusion protein versions. The resulting strains were

used for complementation attempts of the *umapB73* mutant phenotype. Interestingly, all versions show some degree of complementation with one version (Ub1Um2Ub3) almost fully complementing the mutant phenotype. At first this sounded very exciting, as it implies that there is a feature in the second module of UbApB73, where if it gets exchanged with the UmApB73 version, the protein can suddenly complement the phenotype. However, this scenario seems not very likely as mosaic protein versions like Um1Um2Ub3 barely complement the mutant phenotype. The overall identity values of the generated mosaic proteins to UmApB73 also do not provide any further insight as there is no correlation between identity and ability to functionally complement. Another possibility would be that the 3D structure of the protein is more important than the simple amino acids, meaning that the exchange of one amino acid in e.g. module 1 requires the exchange of a certain corresponding amino acid in, e.g. module 3, to result in an again functional protein. However, from the results and the sequence analysis of the proteins, no hints towards or against this idea can be deduced leaving this purely speculative. Accordingly, the question if a mosaic protein can complement the *apB73* mutant phenotype seems to be more much complex than initially imagined.

3.7. Interaction partners of ApB73

One of the key questions regarding ApB73 is the specific mechanism of its function. The performed virulence assays clearly show, that ApB73 is important for the fungus to establish the interaction with its host maize. Additionally, one can exclude that ApB73 is needed for the penetration event itself. The shown data regarding localization of ApB73 indicate that after secretion of ApB73 by the fungus, the protein localizes to either the fungal cell wall or the fungal plasma membrane.

However, although these results narrow down the place of action of ApB73, it is completely unknown if the protein has any interaction partners or how specifically it helps the fungus to establish biotrophy.

To address this question, a Y2H screen was performed, using ApB73 as a bait protein. ApB73 was tested for its interaction with proteins expressed from a cDNA library obtained from maize plants infected with *U. maydis*. This assay resulted in the identification of 26 possible interaction partners. Interestingly 10 of them contained a domain termed Smc domain (COG1196) and 9 out of these 10 proteins also showed resemblance to the SMC_prok_B domain (TIGR02168). These domains are found in SMC (structural maintenance of chromosomes) proteins, a large family of chromosome segregation-related ATPases, important for different aspects of chromosome dynamics and organization (Milutinovich & Koshland, 2003). Proteins carrying such domains might

be involved in any of the activities known to characterize SMC proteins including: hydrolase activity, nucleic acid binding and chromatin binding.

Interesting to mention here is that the second most prevalent domain found among the possible interaction partners of ApB73 in the Y2H screen is a kinesin domain (found three times), and kinesins are also known to bind and hydrolyze ATP. Accordingly, it is feasible that ApB73 interacts with a protein that exhibits ATPase activity. Also possible would be the interaction with a nucleic acid binding protein. This theory would be strengthened by the observation that overexpression of $ApB73_{20\text{-}709}$ in *N. benthamiana* results in localization to speckles in the nucleus, as well as the plasma membrane. This nuclear localization might be the result of an interaction with a DNA binding protein.

In any case, possible interaction partners found in Y2H screens could also be misleading. This is based on, for example, the observation a recent study made that post-translational modifications are needed for the activity and/or stability of certain effectors (Fernández-Álvarez *et al.*, 2012). As a result, possible interaction partners might not be identifiable when using heterologous systems.

Another possibility to identify interaction partners would be a Co-IP of infected maize or even tobacco plants. Unfortunately, as promoter strength of the *apB73* promoter is weak and expression of ApB73 under the control of the tested other (stronger) promoter sequences cannot complement the virulence phenotype, conducting this experiment in maize is not feasible. In tobacco the problem lies in the artificiality of the system. This situation becomes even more complex when considering that ApB73 could be processed. Due to this possibility one cannot even be sure which part of ApB73 should be pulled down or which part is actually interacting with another protein. The most straight forward experiment to try here would be to do several Co-IP experiments with a C- or N-terminally tagged protein. However, the mentioned problems with expression strength make this infeasible.

3.8. Conclusions and Outlook

Virulence factors have been shown to be mayor players in shaping the interaction between *Ustilago maydis* and its host plant *Zea mays*. In recent years, more and more of these factors are being functionally characterized, shedding light into this fascinating interaction.

Within this thesis, the so far uncharacterized protein ApB73 was shown to be one of these factors highly important for this interaction. The shown experiments illustrate

that the role of ApB73 is restricted to the biotrophic phase of the fungus. The ApB73 protein is secreted to the biotrophic interface and localizes to the fungal surface, and the lack of it finally results in loss of sporogenesis. Additionally, it was shown that the protein is conserved among sequenced smut fungi however functional redundancy was only shown for the *S. reilianum* ortholog.

Although a possible domain was identified potentially relevant for ApB73s interaction with other proteins, the identification of specific interaction partners, its exact localization and mechanism of action though will require further investigations. The possibility of a processing of ApB73 makes the design of these experiments even more challenging.

Only assumptions can be made about the mechanistic role of ApB73 during biotrophy. Considering the size of the protein, ApB73 may (first) have a shielding function. Selective positioning of ApB73 could make the fungus less obvious to the plant's defence system or shield the fungal membrane against possible defence proteins secreted by the plant. Similar roles are known for virulence factors from other pathogens including *Cladosporium fulvum* (Avr4, van den Burg *et al.*, 2006; van Esse *et al.*, 2007) and *Mycosphaerella graminicola* (Mg3LysM, Marshall *et al.*, 2011). Avr4 as well as Mg3LysM protect/shield fungal chitin against hydrolysis by plant chitinases. Apart from this putative shielding function of ApB73, its possible *in planta* processing may allow other functions.

So, although it was demonstrated that ApB73 is an important and functionally conserved secreted virulence factor among some of the tested smuts, the elucidation of its mechanistic role during biotrophy is still enigmatic and awaits future research.

4 Material

4.1. Chemicals, enzymes and antibodies

The chemicals used for this thesis were primarily obtained from the following companies: Merck, Roche, PanReac AppliChem, Qiagen, CenticBiotec, Analytik Jena, Sigma-Aldrich, Life technologies and Carl-Roth. The lytic enzyme Glucanex was obtained from Sigma-Aldrich. Cloning reagents (restriction enzymes, polymerases, ligases etc.) were primarily obtained from New England Biolabs. Size standards for agarose gel electrophoresis were 1 kb and 2 log ladder (New England Biolabs). For SDS poly-acrylamide gel electrophoresis the size standard Page Ruler Prestained Protein Ladder (Thermo Fisher Scientific) was used. Primary antibodies used are mouse-anti HA (Sigma-Aldrich) and mouse anti-actin (Thermo Pierce); as secondary antibodies IRDye® 800CW Goat anti-Mouse (Licor) and anti-Digoxigenin-AP (Roche) were used.

4.2. Buffers and solutions

Most buffers and solutions used in this thesis were prepared as described previously (Sambrook *et al.*, 1989;Ausubel *et al.*, 2003). In case special buffers and solutions were required, they are mentioned within the corresponding method. If necessary, solutions were autoclaved at 121°C for 5 minutes. Heat sensitive solutions were filter sterilised using filters with a pore size of 0.2 µm.

4.3. Kits

Table 4.1 Kits used for this thesis

Name	Purpose	Manufacturer
InnuPrep Doublepure	Purification of DNA fragments from PCR or Agarose gels	Analytik Jena
Plasmid Isolation	DNA isolation from *E. coli*	Qiagen (Buffers), Centic Biotec (columns)

4.4. Bacterial strains

Different strains of *Agrobacterium tumefaciens* and *Escherichia coli* were used during the course of the work for this thesis (Table 4.2).

Table 4.2 Bacterial strains used during this thesis

Strain	Glycerol -stock # / DNA #	Genotype	Resistance	Reference
E. coli Mach1™ $T1^R$	#1455	F– Φ80lacZΔM15 ΔlacX74 *hsd*R(r_K^-, m_K^+) ΔrecA1398 *end*A1 *ton*A	none	Invitrogen
A. tumefaciens Gv3101pMP90		C58C1: pGv3101 Rif^R; pTiC58 ΔT-DNA $Gent^R$	Rif^R $Gent^R$	Koncz & Schell, 1986
A. tumefaciens Gv3101pMP90 RK		C58C1: pGv3101 Rif^R; pTiC58 ΔT-DNA $Gent^R$ Kan^R	Rif^R $Gent^R$ Kan^R	Koncz & Schell, 1986

A. tumefaciens Gv3101pMP90 pSoup	#1980	C58C1: pGv3101 Rif^R; pTiC58 ΔT-DNA Gent^R; pSoup Tet^R	Rif^R Gent^R Tet^R	Koncz & Schell, 1986; Hellens *et al.*, 2000
A. tumefaciens Gv3101pMP90 pSoup pGreenII-35S-Tl-ApB73$_{20-709}$-YFP	#1892 / #2859	C58C1: pGv3101 Rif^R; pTiC58 ΔT-DNA Gent^R; pSoup Tet^R; pGreenII-35S-Tl-ApB73$_{20-709}$-YFP Kan^R	Rif^R Gent^R Tet^R Kan^R	This thesis
A. tumefaciens Gv3101pMP90 pSoup pGreenII-35S-Tl-ApB73-YFP	#1993 / #2955	C58C1: pGv3101 Rif^R; pTiC58 ΔT-DNA Gent^R; pSoup Tet^R; pGreenII-35S-Tl-ApB73-YFP Kan^R	Rif^R Gent^R Tet^R Kan^R	This thesis
A. tumefaciens Gv3101pMP90 RK pPCV-H_35S-YFP	#2002	C58C1: pGv3101 Rif^R; pTiC58 ΔT-DNA Gent^R Kan^R; pPCV-H_35S-YFP Carb^R	Rif^R Gent^R Kan^R Carb^R	Janos Bindics
A. tumefaciens Gv3101pMP90 pSoup pGG-35S-Ω-mCherry-UBQ10-HygR	#2068 / #2995	C58C1: pGv3101 Rif^R; pTiC58 ΔT-DNA Gent^R; pSoup Tet^R; pGG-35S-Ω-mCherry-UBQ10-HygR Spec^R	Rif^R Gent^R Tet^R Spec^R	This thesis
A. tumefaciens Gv3101pMP90 pSoup pGG-35S-sec-BFP-HDEL-UBQ10-HygR	#2071 / #2998	C58C1: pGv3101 Rif^R; pTiC58 ΔT-DNA Gent^R; pSoup Tet^R; pGG-35S-sec-BFP-HDEL-UBQ10-HygR Spec^R	Rif^R Gent^R Tet^R Spec^R	This thesis
A. tumefaciens Gv3101pMP90 pSoup pGG-35S-Ω-ApB73-linker-mCherry-HA-UBQ10-HygR	#2073 / #3005	C58C1: pGv3101 Rif^R; pTiC58 ΔT-DNA Gent^R; pSoup Tet^R; pGG-35S-Ω-ApB73-linker-mCherry-HA-UBQ10-HygR	Rif^R Gent^R Tet^R Spec^R	This thesis
A. tumefaciens Gv3101pMP90 pSoup pGG-35S-Ω-supereclipticpHLuorin-UBQ10-HygR	#2080 / #3017	C58C1: pGv3101 Rif^R; pTiC58 ΔT-DNA Gent^R; pSoup Tet^R; pGG-35S-Ω-supereclipticpHLuorin-UBQ10-HygR	Rif^R Gent^R Tet^R Spec^R	This thesis
A. tumefaciens Gv3101pMP90 pSoup pGG-35S-sec-supereclipticpHLuorin-UBQ10-HygR	#2081 / #3018	C58C1: pGv3101 Rif^R; pTiC58 ΔT-DNA Gent^R; pSoup Tet^R;	Rif^R Gent^R Tet^R Spec^R	This thesis

4.5. *Ustilago maydis* strains

Different *Ustilago maydis* strains were used when conducting the work for this thesis. They are listed in Table 4.3.

Table 4.3 *Ustilago maydis* strains used in this study.

Strain	Glycerol stock # / DNA #	Genotype	Resistance	Reference
AB33	#189	*a2 P$_{nar}$:bW2, bE1*	Phleo^R	Brachmann *et al.*, 2001
FB1	#262	*a1 b1*	-	Banuett & Herskowitz, 1989
FB2	#2702	*a2 b2*	-	Banuett & Herskowitz, 1989
SG200	#261	*a1 mfa2 bE1 bW2*	Phleo^R	Kämper *et al.*, 2006
SG200AM1-RFP	#28	*a1 mfa2 bE1 bW2 ip^r[P$_{um01779}$:3xeGFP]ip^s P$_{otef}$:2RFP*	Phleo^R CBX^R	Mendoza-Mendoza *et al.*, 2009
AB33-p123-P$_{otef}$-GFP-3xHA #	#2263/ #3062	*a2 P$_{nar}$:bW2, bE1 ip^r[P$_{otef}$:GFP_1xHA]ip^s*	Phleo^R CBX^R	Denise Seitner
AB33-p123-P$_{otef}$-Cmu1-HA #	#1583	*a2 P$_{nar}$:bW2, bE1 ip^r[P$_{otef}$:um05731_1xHA]ip^s*	Phleo^R CBX^R	Djamei *et al.*, 2011
AB33-p123-P$_{otef}$-UmApB73-HA #	#1700/ #2680	*a2 P$_{nar}$:bW2, bE1 ip^r[P$_{otef}$:um02011_1xHA]ip^s*	Phleo^R CBX^R	This thesis
FB1ΔapB73-1 ##	#2666/	*a1 b1 Δum02011*	Hyg^R	This thesis

	pUKO PI G9			
FB1ΔapB73-2 ##	#2667/ pUKO PI G9	*a1 b1 Δum02011*	Hyg^R	This thesis
FB2ΔapB73-1 ##	#2664/ pUKO PI G9	*a2 b2 Δum02011*	Hyg^R	This thesis
FB2ΔapB73-2 ##	#2665/ pUKO PI G9	*a2 b2 Δum02011*	Hyg^R	This thesis
SG200-p123-P_{oma}-UmApB73-HA-Strep #	#1882/ #2827	*a1 mfa2 bE1 bW2 ip^r[P_{oma}:um02011_1xHA_1xStrep]ip^s*	Phleo^R CBX^R	This thesis
SG200-pUG-P_{cmu1}-ApB73$_{1-19}$-mCherry-3xHA #	#2139/ #3036	*a1 mfa2 bE1 bW2 ip^r[P_{cmu1}:um02011$_{1-19}$_1xHA_1xStrep]ip^s*	Phleo^R CBX^R	This thesis
SG200ΔapB73 ##	pUKO81-11/PIG9	*a1 mfa2 bE1 bW2 Δum02011*	Phleo^R Hyg^R CBX^R	This thesis
SG200ΔapB73-p123P_{apB73}-UmApB73-HA #	#1686/ #2705	*a1 mfa2 bE1 bW2 Δum02011 ip^r[$P_{um02011}$:um02011_1xHA]ip^s*	Phleo^R Hyg^R CBX^R	This thesis
SG200ΔapB73-p123P_{apB73}-UbApB73-HA #	#1688/ #2657	*a1 mfa2 bE1 bW2 Δum02011 ip^r[$P_{um02011}$:ub02986_1xHA]ip^s*	Phleo^R Hyg^R CBX^R	This thesis
SG200ΔapB73-p123-P_{apB73}-UmApB73-mCherry-HA #	#1735/ #2748	*a1 mfa2 bE1 bW2 Δum02011 ip^r[$P_{um02011}$:um02011_mCherry_1xHA]ip^s*	Phleo^R Hyg^R CBX^R	This thesis
SG200ΔapB73-p123-P_{apB73}-UmApB73$_{20-709}$-mCherry-HA #	#1861/ #2817	*a1 mfa2 bE1 bW2 Δum02011 ip^r[$P_{um02011}$:um02011$_{20-709}$_mCherry_1xHA]ip^s*	Phleo^R Hyg^R CBX^R	This thesis
SG200ΔapB73-p123-P_{apB73}-SrApB73-HA #	#2051/ #2956	*a1 mfa2 bE1 bW2 Δum02011 ip^r[$P_{um02011}$:sr12972_1xHA]ip^s*	Phleo^R Hyg^R CBX^R	This thesis
SG200ΔapB73-p123-P_{apB73}-MpApB73-HA #	#2089/ #3019	*a1 mfa2 bE1 bW2 Δum02011 ip^r[$P_{um02011}$:MP05899_1xHA]ip^s*	Phleo^R Hyg^R CBX^R	This thesis
SG200ΔapB73-pUG-P_{otef}-ApB73$_{1-19}$ -mCherry-3xHA-UmApB73$_{20-709}$-linker-3xmyc #	#2435/ #3215	*a1 mfa2 bE1 bW2 Δum02011 ip^r[P_{otef}:um02011$_{1-19}$_mCherry_3xHA_um02011$_{20-709}$_linker_3xmyc]ip^s*	Phleo^R Hyg^R CBX^R	This thesis
SG200ΔapB73-pUG-P_{apB73}-Pit2$_{1-25}$-UmApB73$_{20-709}$-linker-mCherryHA #	#2481/ #3289	*a1 mfa2 bE1 bW2 Δum02011 ip^r[$P_{um02011}$:um01375$_{1-25}$_um02011$_{20-709}$_mCherry_1xHA]ip^s*	Phleo^R Hyg^R CBX^R	This thesis
SG200ΔapB73-pUG-P_{apB73}-UmApB73-mCherryHA-HDEL#	#2651/ #3422	*a1 mfa2 bE1 bW2 Δum02011 ip^r[$P_{um02011}$:um02011_mCherry_1xHA_HDEL]ip^s*	Phleo^R Hyg^R CBX^R	This thesis
SG200ΔapB73-pUG-P_{otef}-UmApB73-linker-mCherry-HA #	#2158/ #3041	*a1 mfa2 bE1 bW2 Δum02011 ip^r[P_{otef}:um02011_linker_mCherry_1xHA]ip^s*	Phleo^R Hyg^R CBX^R	This thesis
SG200ΔapB73-pUG-P_{stpI}-UmApB73-linker-mCherry-HA #	#2476/ #3288	*a1 mfa2 bE1 bW2 Δum02011 ip^r[P_{stpI}:um02011_linker_mCherry_1xHA]ip^s*	Phleo^R Hyg^R CBX^R	This thesis
SG200ΔapB73-pUG-P_{pit2}-UmApB73-linker-mCherry-HA #	#2484/ #3290	*a1 mfa2 bE1 bW2 Δum02011 ip^r[P_{pit2}:um02011_linker_mCherry_1xHA]ip^s*	Phleo^R Hyg^R CBX^R	This thesis
SG200ΔapB73-pUG-P_{apB73}-ApB73$_{1-19}$-UbApB73$_{22-753}$-mCherry-HA #	#2179/ #3046	*a1 mfa2 bE1 bW2 Δum02011 ip^r[P_{apB73}:um02011$_{1-19}$_ub02986$_{22-753}$_mCherry_HA]ip^s*	Phleo^R Hyg^R CBX^R	This thesis
SG200ΔapB73-pUG-P_{apB73}-ApB73$_{1-19}$-UmApB73$_{20-241}$ UbApB73$_{243-512}$ UmApB73$_{491-709}$ #	#2508/ #3331	*a1 mfa2 bE1 bW2 Δum02011 ip^r[P_{apB73}:um02011$_{1-19}$_um02011$_{20-241}$ub02986$_{243-512}$um02011$_{491-709}$]ip^s*	Phleo^R Hyg^R CBX^R	This thesis
SG200ΔapB73-pUG-P_{apB73}-ApB73$_{1-19}$-UmApB73$_{20-241}$ UbApB73$_{243-512}$ UbApB73$_{513-753}$ #	#2514/ #3333	*a1 mfa2 bE1 bW2 Δum02011 ip^r[P_{apB73}:um02011$_{1-19}$_um02011$_{20-241}$ub02986$_{243-512}$ub02986$_{513-753}$]ip^s*	Phleo^R Hyg^R CBX^R	This thesis
SG200ΔapB73-pUG-P_{apB73}-ApB73$_{1-19}$-UbApB73$_{22-242}$	#2518/ #3334	*a1 mfa2 bE1 bW2 Δum02011 ip^r[P_{apB73}:um02011$_{1-}$*	Phleo^R Hyg^R CBX^R	This thesis

UmApB73$_{242-490}$ UbApB73$_{513-753}$ #		*19_ub029862$_{22-242}$um02011$_{242-490}$ub02986$_{513-753}$]ip^{s}*		
SG200ΔapB73-pUG-P$_{apB73}$-ApB73$_{1-19}$-UbApB73$_{22-242}$ UbApB73$_{243-512}$ UmApB73$_{491-709}$ #	#2523/ #3335	*a1 mfa2 bE1 bW2 Δum02011 ip^{r}[P$_{apB73}$:um02011$_{1-19}$_ub029862$_{22-242}$ub02986$_{243-512}$um02011$_{491-709}$]ip^{s}*	Phleo^{R} Hyg^{R} CBX^{R}	This thesis
SG200ΔapB73-pUG-P$_{apB73}$-ApB73$_{1-19}$-UbApB73$_{22-242}$ UmApB73$_{242-490}$ UmApB73$_{491-709}$ #	#2525/ #3336	*a1 mfa2 bE1 bW2 Δum02011 ip^{r}[P$_{apB73}$:um02011$_{1-19}$_ub029862$_{22-242}$um02011$_{242-490}$um02011$_{491-709}$]ip^{s}*	Phleo^{R} Hyg^{R} CBX^{R}	This thesis
SG200ΔapB73-pUG-P$_{apB73}$-ApB73$_{1-19}$-UmApB73$_{20-241}$ UmApB73$_{242-490}$ UbApB73$_{513-753}$ #	#2554/ #3332	*a1 mfa2 bE1 bW2 Δum02011 ip^{r}[P$_{apB73}$:um02011$_{1-19}$_um02011$_{20-241}$um02011$_{242-490}$ub02986$_{513-753}$]ip^{s}*	Phleo^{R} Hyg^{R} CBX^{R}	This thesis
SG200ΔapB73-pUG-P$_{apB73}$-ApB73-linker-mCherry-HA-NosT-P$_{apB73}$-pit1-linker-GFP-NosT #	#2941/ #3728	*a1 mfa2 bE1 bW2 Δum02011 ip^{r}[P$_{um02011}$:um02011_mCherry_1xHA_P$_{um02011}$:um01375_GFP]ip^{s}*	Phleo^{R} Hyg^{R} CBX^{R}	This thesis
SG200ΔapB73-AM1 #	#2870/ #304	*a1 mfa2 bE1 bW2 Δum02011 ip^{r}[P$_{um01779}$:3xeGFP]ip^{s}*	Phleo^{R} Hyg^{R} CBX^{R}	This thesis

Plasmids were integrated into the *ip* locus of *U. maydis*. Correct integration into the *ip* locus was confirmed by PCR.
Deletion was confirmed by Southern blot analysis.

4.6. *Saccharomyces cerevisiae* strains

Table 4.4 *Saccharomyces cerevisiae* strains used in this study.

Strain	Glycerol-stock # / DNA #	Genotype	Marker	Reference
AH109	#394	*MATa, ura3-52, trp1-901, leu2-3, 112, his3-200, gal4Δ, gal80Δ, LYS2::GAL1$_{UAS}$-GAL1$_{TATA}$-HIS3, MEL1, GAL2$_{UAS}$-GAL2$_{TATA}$-ADE2, URA3::MEL1$_{UAS}$-MEL1$_{TATA}$-lacZ*		Clontech
Y187	#1564	*MATα, ura3-52, trp1-901, leu2-3,112, his3-200, ade2-101, gal4Δ, gal80Δ, met–, URA3::GAL1$_{UAS}$–Gal1$_{TATA}$–lacZ, MEL1*		Clontech
Y187 pAD cDNA library		*MATα, ura3-52, trp1-901, leu2-3,112, his3-200, ade2-101, gal4Δ, gal80Δ, met–, URA3::GAL1$_{UAS}$–Gal1$_{TATA}$–lacZ, MEL1; pAD*	*LEU2*	Stratagene
AH109 pGBKT7	#1662/ #112	*MATa, ura3-52, trp1-901, leu2-3, 112, his3-200, gal4Δ, gal80Δ, LYS2::GAL1$_{UAS}$-GAL1$_{TATA}$-HIS3, MEL1, GAL2$_{UAS}$-GAL2$_{TATA}$-ADE2, URA3::MEL1$_{UAS}$-MEL1$_{TATA}$-lacZ; pGBKT7*	*TRP1*	Franziska Rabe
Y187 pGADT7	#1675/ #19	*MATα, ura3-52, trp1-901, leu2-3,112, his3-200, ade2-101, gal4Δ, gal80Δ, met–, URA3::GAL1$_{UAS}$–Gal1$_{TATA}$–lacZ, MEL1; pGADT7*	*LEU2*	This thesis
AH109 pGBKT7-N-um12197-STOP	#952/ #1721	*MATa, ura3-52, trp1-901, leu2-3, 112, his3-200, gal4Δ, gal80Δ, LYS2::GAL1$_{UAS}$-GAL1$_{TATA}$-HIS3, MEL1, GAL2$_{UAS}$-GAL2$_{TATA}$-ADE2, URA3::MEL1$_{UAS}$-MEL1$_{TATA}$-lacZ; pGBKT7-N-um12197-STOP*	*TRP1*	Franziska Rabe
AH109 pGBKT7-ApB73$_{20-709}$	#1660/ #2632	*MATa, ura3-52, trp1-901, leu2-3, 112, his3-200, gal4Δ, gal80Δ, LYS2::GAL1$_{UAS}$-GAL1$_{TATA}$-HIS3, MEL1, GAL2$_{UAS}$-GAL2$_{TATA}$-ADE2, URA3::MEL1$_{UAS}$-MEL1$_{TATA}$-lacZ; pGBKT7-ApB73$_{20-709}$*	*TRP1*	This thesis
AH109 pGBKT7-UbApB73$_{22-753}$	#1802/ #2794	*MATa, ura3-52, trp1-901, leu2-3, 112, his3-200, gal4Δ, gal80Δ, LYS2::GAL1$_{UAS}$-GAL1$_{TATA}$-HIS3, MEL1, GAL2$_{UAS}$-GAL2$_{TATA}$-ADE2, URA3::MEL1$_{UAS}$-MEL1$_{TATA}$-lacZ; pGBKT7-UbApB73$_{22-753}$*	*TRP1*	This thesis
Y187 pGADT7-UmApB73$_{20-709}$	#1803/ #2792	*MATα, ura3-52, trp1-901, leu2-3,112, his3-200, ade2-101, gal4Δ, gal80Δ, met–, URA3::GAL1$_{UAS}$–Gal1$_{TATA}$–lacZ, MEL1; pGADT7-UmApB73$_{20-709}$*	*LEU2*	This thesis
Y187 pGADT7-	#3098/ #3778	*MATα, ura3-52, trp1-901, leu2-3,112, his3-200, ade2-101, gal4Δ, gal80Δ, met–, URA3::GAL1$_{UAS}$–*	*LEU2*	This thesis

ZmGolgin		*Gal1$_{TATA}$–lacZ, MEL1; pGADT7-LOC103626210 _ZmGolgin*		
Y187 pGADT7-ZmGolgin ΔSMC	#2614/ #3326	*MATα, ura3-52, trp1-901, leu2-3,112, his3-200, ade2-101, gal4Δ, gal80Δ, met–, URA3::GAL1$_{UAS}$–Gal1$_{TATA}$–lacZ, MEL1; pGADT7-LOC103626210 _ZmGolginΔSMC*	*LEU2*	This thesis
Y187 pGADT7-SMC	#3097/ #3777	*MATα, ura3-52, trp1-901, leu2-3,112, his3-200, ade2-101, gal4Δ, gal80Δ, met–, URA3::GAL1$_{UAS}$–Gal1$_{TATA}$–lacZ, MEL1; pGADT7-LOC103626210 _SMC*	*LEU2*	This thesis

4.7. Plants

Several different plant species were used during the course of this thesis (Table 4.5). *Zea mays* cultivars were used to access the virulence of a number of *Ustilago maydis* strains, whereas *Nicotiana benthamiana* plants were used to study the localization of fusion proteins.

Table 4.5 Used plants in this study.

Name	Description	Obtained from
Zea mays cv. B73	used for virulence assays and microscopy, commercial variety, sequenced genome (Schnable *et al.*, 2009)	Prof. Dr. Alfons Gierl (Wissenschaftszentrum Weihenstephan, Freising-Weihenstephan)
Zea mays cv. Early Golden Bantam (EGB)	used for virulence assays, sweet corn variety	Olds Seeds, Madison, USA
Zea mays cv. Gaspe Flint	Dwarf plant with early floral switch (15d)	Prof. Dr. Regine Kahmann (Max Planck Institute of Terrestrial Microbiology, Marburg)
Nicotiana benthamiana	used for transient expression assays	Anneliese Auer, GMI

4.8. Oligonucleotides

To amplify DNA fragments using polymerase chain reaction different oligonucleotides were used (6.4 Oligonucleotides). Oligonucleotides (Primer) are single-stranded DNA-fragments, generated by the MWG Eurofins Operon.

4.9. Plasmids

Plasmids used in this study are shown below. For many plasmids obtained using Golden Gate the Green Gate system or published Green Gate modules were used (Lampropoulos *et al.*, 2013). The coding sequence for superecliptic pHluorin (Addgene) including the BsaI sites compatible with the Green Gate system was ordered as a string. Complete vector maps of all mentioned constructs can be obtained upon request.

Table 4.6 List of used plasmids and their characteristics.

#	Plasmid	Resistance in *E. coli*	DNA #	Cloning strategy	Note	Origin
1	pUKO-Um02011	Spec^R	pUKO Box PlateI G9	Golden Gate (SapI) into modified p123	For generation of mutant strain in SG200/FB1/FB2	This study

2	p123-P_{oma}-UmApB73-HA-Strep	Amp^R	#1882	Golden Gate (BsaI) into p123	To generate over-expressor in SG200	This study
3	p123-P_{apB73}-UmApB73-HA	Amp^R	#2705	NdeI NotI into p123	To generate complementation strain in SG200ΔapB73	This study
4	p123-P_{apB73}-UmApB73-mCherry-HA	Amp^R	#2748	SacI NotI into #3	To generate complementation strain in SG200ΔapB73	This study
5	p123-P_{otef}-UmApB73-HA	Amp^R	#2680	NcoI NotI into p123	For constitutive over expression of ApB73-HA in AB33	This study
6	pUG-P_{cmu1}-$ApB73_{1-19}$-mCherry-3xHA	$Spec^R$	#3036	Golden Gate (BsaI)	For visualization of protein secretion in SG200	This study
7	pUG-P_{otef}-UmApB73-linker-mCherry-HA	$Spec^R$	#3041	Golden Gate (BsaI)	For visualization of protein secretion in SG200ΔapB73	This study
8	pUG-P_{otef}-$ApB73_{1-19}$-mCherry-3xHA-$UmApB73_{20-709}$-linker-3xmyc	$Spec^R$	#3215	Golden Gate (BsaI)	For visualization of protein secretion in SG200ΔapB73	This study
9	p123-P_{apB73}-$UmApB73_{20-709}$-mCherry-HA	Amp^R	#2817	NcoI NotI into p123	To generate complementation strain in SG200ΔapB73	This study
10	pUG-P_{apB73}-$Pit2_{1-25}$-$UmApB73_{20-709}$-linker-mCherry-HA	$Spec^R$	#3289	Golden Gate (BsaI)	To generate complementation strain in SG200ΔapB73	This study
11	pUG-P_{apB73}-UmApB73-mCherry-HA-HDEL	$Spec^R$	#3422	Golden Gate (BsaI)	To generate complementation strain in SG200ΔapB73	This study
12	p123-P_{apB73}-UbApB73-HA	Amp^R	#2657	NcoI NotI into #3	To generate complementation strain in SG200ΔapB73	This study
13	p123-P_{apB73}-SrApB73-HA	Amp^R	#2956	NcoI NotI into #3	To generate complementation strain in SG200ΔapB73	This study
14	p123-P_{apB73}-MpApB73-HA	Amp^R	#3019	NcoI NotI into #3	To generate complementation strain in SG200ΔapB73	This study
15	pUG-P_{stpI}-UmApB73-linker-mCherry-HA	$Spec^R$	#3288	Golden Gate (BsaI)	To generate complementation strain in SG200ΔapB73	This study
16	pUG-P_{pit2}-UmApB73-linker-mCherry-HA	$Spec^R$	#3290	Golden Gate (BsaI)	To generate complementation strain in SG200ΔapB73	This study
17	pUG-P_{apB73}-$ApB73_{1-19}$-$UbApB73_{22-753}$-mCherry-HA	$Spec^R$	#3046	Golden Gate (BsaI)	To generate complementation strain in SG200ΔapB73	This study
18	pUG-P_{apB73}-$ApB73_{1-19}$-$UmApB73_{20-241}$$UbApB73_{243-512}$$UmApB73_{491-709}$	$Spec^R$	#3331	Golden Gate (BsaI)	For expression of UmApB73/UbApB73 mosaic proteins in SG200ΔapB73	This study
19	pUG-P_{apB73}-$ApB73_{1-19}$-$UmApB73_{20-241}$$UbApB73_{243-512}$$UbApB73_{513-753}$	$Spec^R$	#3333	Golden Gate (BsaI)	For expression of UmApB73/UbApB73 mosaic proteins in SG200ΔapB73	This study
20	pUG-P_{apB73}-$ApB73_{1-19}$-$UbApB73_{22-242}$$UmApB73_{242-490}$$UbApB73_{513-753}$	$Spec^R$	#3334	Golden Gate (BsaI)	For expression of UmApB73/UbApB73 mosaic proteins in SG200ΔapB73	This study
21	pUG-P_{apB73}-$ApB73_{1-19}$-$UbApB73_{22-242}$$UbApB73_{243-512}$$UmApB73_{491-709}$	$Spec^R$	#3335	Golden Gate (BsaI)	For expression of UmApB73/UbApB73 mosaic proteins in SG200ΔapB73	This study
22	pUG-P_{apB73}-$ApB73_{1-19}$-$UbApB73_{22-242}$$UmApB73_{242-}$	$Spec^R$	#3336	Golden Gate (BsaI)	For expression of UmApB73/ UbApB73 mosaic	This study

	$_{490}$UmApB73$_{491-709}$				proteins in SG200ΔapB73	
23	pUG-P_{apB73}-ApB73$_{1-19}$-UmApB73$_{20-241}$UmApB73$_{242-490}$UbApB73$_{513-753}$	Spec^R	#3332	Golden Gate (BsaI)	For expression of UmApB73/ UbApB73 mosaic proteins in SG200ΔapB73	This study
24	pGreenII 0029 2x35S Tl VCP1-YFP	Kan^R	#40		Backbone vector	Armin Djamei
25	pGreenII-35S-Tl-ApB73$_{20-709}$-YFP	Kan^R	#2859	NcoI NotI into #24	For transient expression in tobacco	This study
26	pGreenII-35S-Tl-ApB73-YFP	Kan^R	#2955	NcoI NotI into #24	For transient expression in tobacco	This study
27	pGG-35S-Ω-mCherry-UBQ10-HygR	Spec^R	#2995	Golden Gate (BsaI)	For transient expression in tobacco	This study
28	pGG-35S-sec-BFP-HDEL-UBQ10-HygR	Spec^R	#2998	Golden Gate (BsaI)	For transient expression in tobacco	This study
29	pGG-35S-Ω-ApB73-linker-mCherry-HA-UBQ10-HygR	Spec^R	#3005	Golden Gate (BsaI)	For transient expression in tobacco	This study
30	pGG-35S-Ω-supereclipticpHLuorin-UBQ10-HygR	Spec^R	#3017	Golden Gate (BsaI)	For transient expression in tobacco	This study
31	pGG-35S-sec-supereclipticpHLuorin-UBQ10-HygR	Spec^R	#3018	Golden Gate (BsaI)	For transient expression in tobacco	This study
32	pGBKT7	Spec^R	#112	-	For Y2H	Armin Djamei
33	pGADT7	Amp^R	#19	-	For Y2H	Armin Djamei
34	pGBKT7-ApB73$_{20-709}$	Spec^R	#2632	Gateway	For Y2H	This study
35	pGBKT7-UbApB73$_{22-753}$	Spec^R	#2794	Gateway	For interaction test in yeast	This study
36	pGADT7-UmApB73$_{20-709}$	Amp^R	#2792	Gateway	For interaction test in yeast	This study
37	pGADT7-ZmGolgin	Amp^R	#3778	Gateway	For interaction test in yeast	This study
38	pGADT7-ZmGolginΔSMC	Amp^R	#3326	Gateway	For interaction test in yeast	This study
39	pGADT7-SMC	Amp^R	#3777	Gateway	For interaction test in yeast	This study
40	pAM1	Amp^R	#304	-	To quantify formation of appressoria	Mendoza-Mendoza *et al.*, 2009
41	pUG-P_{apB73}-ApB73-linker-mCherry-HA-NosT-P_{apB73}-pit1-linker-GFP-NosT	Spec^R	#3728	Golden Gate (BsaI)	To test for co-localization	This study

The pUKO vector and the pUG vector (no BsaI sites) are modifications of the vector p123. GoldenGate reactions are based on the GreenGate system (Lampropoulos *et al.*, 2013).

4.10. Software

Gene and protein sequences of *U. maydis*, *S. reilianum* and *U. hordei* were taken from MUMDB/MUHDB and MSRDB respectively (https://www.helmholtz-muenchen.de/en/ibis/ institute/ groups/ fungal-microbial-genomics/ resources/ ustilaginaceae/index.html).

Sequences of *M. pennsylvanicum* and *P. aphidis* were taken from NCBI. *U. bromivora* sequences were identified by Sanger sequencing of PCR products obtained with degenerated *U. hordei* primers on *U. bromivora* genomic DNA. Homology analyses were performed by using BLAST (Basic Local Alignment Search Tool). Homologous amino acid sequences were compared by using CLC Main Workbench 7 (Qiagen). Signal peptide prediction was performed with the program SignalP4.1 (http://www.cbs.dtu.dk/services/SignalP/; Petersen *et al.*, 2011). Identity and similarity values of protein sequences were calculated using the tool SIAS (Immunomedicine Group, 2015). To optimize pictures the program ZEN 2012 (Zeiss) and Microsoft© Office© 2010 were used.

4.11. Confocal laser scanning microscopy (CLSM)

All microscopy images shown within this work were obtained using the LSM780 Axio Observer (inverted) microscope from Zeiss. Pictures were taken using various lasers and excitation wave lengths (Table 4.7).

Table 4.7 Used Lasers, their settings and purpose.

Laser	Excitation	Beam splitter	Emission maxima	Detection
Argon 30mW	488nm	MBS 488/561	519 nm	WGA-AF488, GFP
DPSS 15mW	561nm	MBS 458/561	610 nm	Propidium iodide, mCherry
Laser Diode 25mW	405nm	MBS -405	455 nm	BFP, Calcofluor White

5 Methods

5.1. Cultivation of bacteria

Bacteria were grown under aerobe conditions at 28°C (*A. tumefaciens*)/37°C (*E. coli*) in LB (Luria-Bertani) broth (tubes) or on LB agar (plates). To avoid the growth of untransformed or foreign bacteria, certain antibiotics were added (Table 5.1).

Table 5.1 Antibiotics used for bacterial cultures and their characteristics.

Name	Stock solution	Final concentration	Dissolvent	Notes
Ampicillin (Amp)	100 mg/mL	100 mg/L	Water (Filter sterilize)	store at -20°C
Carbenicillin (Carb)	50 mg/mL	100 mg/L	Water (Filter sterilize)	store at -20°C
Chloramphenicol (ChlA)	10 mg/mL	10- 40 mg/L	Ethanol (Filter sterilize)	store at -20°C
Gentamycin (Gent)	10 mg/mL	40 mg/L	Water (Filter sterilize)	store at 4°C
Kanamycin (Kan)	100 mg/mL	50 mg/L	Water (Filter sterilize)	store at -20°C
Rifampicin (Rif)	50 mg/mL	100 mg/L	Methanol (Filter sterilize)	store at -20°C
Spectinomycin (Spec)	50 mg/mL	100 mg/L	Water (Filter sterilize)	store at -20°C
Tetracyclin (Tet)	5 mg/mL	5 mg/L	Ethanol (Filter sterilize)	store at -20°C

LB medium

1.0 % (w/v) Tryptone
0,5 % (w/v) Yeast extract
1.0 % (w/v) NaCl
[optional for plates: 1.5 % (w/v) Agar]

- pH7, NaOH
- autoclave

5.1.1. Overnight cultures

The cultivation of bacteria in liquid media was done using LB broth containing required antibiotics. To re-grow bacteria, stored at -80°C as a glycerol stock, small amounts of the glycerol culture were streaked onto LB plates containing appropriate antibiotics and cultivated overnight (ON) at 28°C (*A. tumefaciens*) or 37°C (*E. coli*).

5.1.2. Bacterial glycerol stocks

Aliquots (750 µL) from fresh ON cultures of bacterial strains were combined with an equal volume of sterile 50% v/v glycerol in tubes, incubated for 15 min at RT and stored at -80 °C.

5.1.3. Transformation of bacteria

Transformation, in the context of recombinant DNA, means the uptake of DNA in a cell.

5.1.3.1. Preparation of *Agrobacterium tumefaciens* electro-competent Cells

1. Inoculate 5 mL of LB (including antibiotics) with 10 µL liquid culture or a large colony of *A. tumefaciens.* Shake at 28 °C to prepare ON culture.
2. Inoculate two flasks containing 50 mL of LB media with 5 ml of *A. tumefaciens* ON culture and shake at 28 °C with 200 rpm for 4-6 hours.
3. Measure the bacterial density. Adjust OD_{600} to 0.5.
4. Pour the suspension into falcon tubes. Centrifuge the suspensions for 10 min at 3500 rpm at 4 °C. Discard the supernatant.
5. Re-suspend the bacteria gently with 25 mL cold sterile water.
6. Centrifuge for 15 min (5000 rpm, 4°C). Discard the supernatant.
7. Repeat steps 5.-6. four more times. It is very important to wash the cells with excess water to remove salts.
8. Discard supernatant and re-suspend in 2.5 mL cold-sterile 10% glycerol. Combine the solution of all tubes into one cold centrifuge tube. Centrifuge for 10 min (3500 rpm, 4°C).
9. Discard supernatant and finally re-suspend cells completely but gently in 4 mL cold 10% glycerol.
10. Divide solution into 50 µL aliquots by pipetting the cells into pre-cooled micro-centrifuge tubes. Put them into liquid nitrogen immediately and store them at -80 °C.

5.1.3.2. Transformation of electro-competent *Agrobacterium tumefaciens* cells (Mattanovich *et al.*, 1989)

Competent Agrobacterium cells were transformed using electroporation. Aliquots of frozen cells were thawed on ice, DNA was added (0.1-1 µg) and the mixture was pipetted into a pre-cooled electroporation cuvette (Eppendorf). The voltage of the electroporation device (Gene Pulser Xcell from BioRad) was set to 1700 V. After electroporation, the cuvette was removed from the machine and 1 mL of SOC medium was added immediately. For recovery of the cells, the solution was transferred to a micro centrifuge tube and rotated for two to four hours at 28°C. Finally, 100 µL of the cell solution were applied to LB agar plates with suitable antibiotics and incubated at 28°C for two days.

SOC medium

2 % w/v bacto-tryptone
0.5 % w/v bacto-yeast extract
10 mM NaCl
2.5 mM KCl
10 mM $MgCl_2$
20 mM glucose
- autoclave

5.1.3.3. Preparation of chemo-competent *Escherichia coli* cells

1. Inoculate 5 mL of LB (including antibiotics) with a large colony of *E. coli.* Shake at 37°C to prepare ON culture.
2. Inoculate 100 mL of LB media supplemented with 10mM $MgCl_2$ and 10mM $MgSO_4$ with 2 mL of the *E. coli* ON culture and shake at 37 °C with 200 rpm until OD_{600} 0.4-0.6 is reached.
3. Transfer the cells to cold centrifuge bottles and incubate on ice for 30 min.
4. Centrifuge the suspensions for 10 min at 3000 rpm at 4 °C. Discard the supernatant.
5. Re-suspend the cells gently in 33 mL cold RFI solution. Incubate on ice for 30 min.
6. Centrifuge for 10 min (3000 rpm, 4°C). Discard the supernatant.
7. Re-suspend the bacteria gently in 5-8 mL cold RFII solution and chill the cells on ice for at least 30 min.
8. Divide solution into 50 µL aliquots by pipetting the cells into pre-cooled micro-centrifuge tubes. Freeze aliquots in liquid nitrogen and store them at -80 °C.

RF I solution

100 mM RbCl
50 mM $MnCl_2$ x 4 H_2O
30 mM potassium acetate
10 mM $CaCl_2$ x 2 H_2O
15 % glycerol (w/v)
- pH5.8, 0.2M acetic acid
- filter sterilize and store at 4°C.

RF II solution

10 mM MOPS
10 mM RbCl
75 mM $CaCl_2$ x 2 H_2O
15 % glycerol (w/v)
- pH6.8, NaOH
- filter sterilize and store at 4°C.

5.1.3.4. Chemical transformation of *Escherichia coli*

Vials of frozen *E. coli* competent cells were thawed on ice. Under sterile conditions about 5 µL of the ligation solution were added to the bacteria and mixed well. The vials were incubated on ice for 15 min, followed by heat shock at 42°C for 30 seconds and incubation on ice for 1-2 min.

The *E. coli* cells were recovered by adding 800 µL SOC medium to the cells and incubating them at 37°C (200 rpm) for one hour. During this time the potential transformants are able to express the resistance markers. Without recovery the transformants would be killed or their growth would be inhibited after the first contact with the antibiotic. Finally, about 100 µL of the cells were spread on plates with selection markers and incubated ON at 37°C.

5.1.3.5. Preparation of electro-competent *Escherichia coli* cells

To prepare electro-competent *E. coli* cells the protocol described below was employed.

1. Inoculate 5 mL LB medium with a single colony and shake culture at 37°C, ON.
2. Inoculate 250 mL LB medium with 2.5 mL of the fresh ON culture. Grow the cultures at 37°C, shaking, for about two hours until they reach OD_{600} 0.4 – 0.6.
3. Transfer cells to cold centrifuge bottles and let them chill on ice for 30 min
4. Spin cells for 15 min, 4.000 rpm at 4°C and discard the supernatant.
5. Wash the cells in 250 mL ice-cold ddH_2O.
6. Wash the cells in 250 mL ice-cold 10% Glycerol.
7. Wash cells two times using 10 mL ice-cold 10% Glycerol.
8. Re-suspend cells in 1-2 mL ice-cold 10% Glycerol.
9. Aliquot cells à 50 µL in micro-centrifuge tubes, then shock-freeze them in liquid nitrogen and store the cells at -80°C.

5.1.3.6. Transformation of electro-competent *Escherichia coli*

1. Thaw vials of frozen electro-competent cells on ice and place electroporation cuvettes on ice (1 mm or 2 mm).
2. Add about 3-4 µL DNA of your ligation reaction to the cells and mix gently.
3. Transfer solution to the electroporation cuvette.
4. For electroporation the Gene Pulser Xcell (Bio-Rad) was used with the preset setting for *E. coli* transformation. Place cuvette into the machine and press pulse. Check pulse parameters, the time constant should be close to 5 milliseconds.
5. Quickly add 1 mL SOC medium to the cuvette and transfer mixture to prepared tube.
6. Incubate the cells for up to 1h at 37°C, shaking. Afterwards plate the reaction onto LB agar plates including corresponding antibiotics.

5.2. Cultivation of *Ustilago maydis*

Ustilago maydis strains were grown under aerobe conditions at 28°C in $YEPS_{light}$ (yeast extract peptone sucrose) broth (modified from Tsukuda *et al.*, 1988) or on PD (potato dextrose) agar plates. To avoid the growth of untransformed cells or foreign bacteria, certain antibiotics were added (Table 5.2).

Table 5.2 Antibiotics used for *Ustilago maydis* cultures and their characteristics.

Antibiotic	Stock solution	Liquid medium	Solid medium	Bottom Reg. Agar	Notes
Carboxin	5 mg/mL in methanol	2 µg/mL	2 µg/mL	4 µg/mL	Store at -20°C
Geneticin G418	50 mg/mL in PBS	400 µg/mL	400 µg/mL	800 µg/mL	Store at 4°C
Hygromycin	50 mg/mL in H_2O	200 µg/mL	200 µg/mL	400 µg/mL	Store at 4°C
Phleomycin	20 mg/mL in H_2O	40 µg/mL	5 µg/mL	80 µg/mL	Store at -20°C

$YEPS_{light}$ medium
0.4% bacto-peptone
0.4% bacto yeast extract
2.0% sucrose
- autoclave

PD agar
2.4 % potato dextrose broth (w/v)
2.0 % bacto agar (w/v)
- autoclave

5.2.1. *Ustilago maydis* glycerol stocks

Aliquots (750 µL) from fresh ON cultures of fungal strains were combined with an equal volume of sterile NSY Glycerol in tubes, incubated for 15 min at RT and stored at -80 °C.

NSY Glycerol
0.8% (w/v) nutrient broth
0.1% (w/v) yeast extract
0.5% (w/v) sucrose
69.6% (v/v) glycerol
- autoclave

5.2.2. Preparation of *Ustilago maydis* protoplasts for transformation

Transformation of *U. maydis* was performed using protoplasts obtained following a protocol modified from Schulz *et al.*, 1990 and Gillissen *et al.*, 1992.

1. Inoculate 4 mL $YEPS_{light}$ with fungal material from a plate and grow the culture ON at 28°C and 200 rpm.
2. In the afternoon of the next day inoculate the main culture by diluting the pre-culture 1:3000 in 100 mL $YEPS_{light}$.
3. The next morning measure the OD_{600} (should be between 0.6-1.0) and pellet the cells in falcon tubes by centrifugation (10 min, 3500 rpm at RT). Discard the supernatant.
4. Re-suspend the cells in 20 mL SCS and spin for 10 min at 3500 rpm (RT). In the meantime prepare the enzyme solution that will degrade the fungal cell wall. To do so, dissolve 10 mg/mL glucanex in 4 mL SCS buffer and filter sterilize the solution.
5. Discard the supernatant and re-suspend the pellet in the SCS-Glucanex solution (2mL per falcon). After 7-10 min observe the cells under the microscope. If 2/3 of the cells are round, add 10 mL SCS buffer and pellet the cells (10 min, 2000 rpm, cool down to 4°C while spinning). From now on store the cells on ice. Also cool down the SCS buffer and the STC buffer.
6. Discard the supernatant and wash the pellet three times with 10 mL SCS. Make sure to always re-suspend the pellet carefully.
7. Discard the supernatant and wash the pellet once with 10 mL STC.
8. Discard the supernatant and carefully re-suspend the pellet in 1 mL cold STC.
9. Aliquot the protoplasts (100 µL) in micro centrifuge tubes. Store on ice until use or put in -80°C freezer for long term storage.

SCS buffer
Solution1: 0.02 M sodium citrate x $2H_2O$
1 M sorbitol

Solution 2: 0.02 M citric acid x H_2O
1 M sorbitol

- add Solution 2 to Solution 1 until pH5.8 is reached
- autoclave

STC buffer
1 M sorbitol

10 mM Tris HCl pH7.5
100 mM $CaCl_2$
- autoclave

5.2.3. Transformation of *Ustilago maydis* protoplasts

Transformation of *Ustilago maydis* is achieved making use of homologous recombination in a PEG (polyethylene glycol) based protocol. Therefore, the used plasmid DNA has to be linearized and purified before starting the procedure described below.

1. Boil Reg. Agar and let it cool to 50-60°C. Add the needed antibiotic agent and pour a 10 mL bottom layer in a petri dish. Store the Regeneration agar (Reg. Agar) bottle in 55 °C incubator. In parallel cool down STC-PEG to 4°C.
2. Thaw protoplasts on ice. After thawing, add linear DNA (5 µg in max. 20 µL) and 1 µL Heparin (15 mg/mL). Incubate on ice for 15 min. While waiting pour the top layer of Reg. Agar (10 mL).
3. Add 500 µL precooled STC-PEG to the DNA/protoplast mix and carefully pipette up and down several times. Incubate the solution on ice for exactly 15 min.
4. Carefully plate the protoplasts on the poured Reg. Agar plate. Incubate the plate a minimum of four days at 28°C to get colonies.

STC PEG
40% (v/v) PEG
in STC buffer
- filter sterilize

Reg. Agar
(Tsukuda *et al.*, 1988)
1.0% (w/v) yeast extract
2.0% (w/v) bacto peptone
2.0 % (w/v) sucrose
18.22% (w/v) sorbitol
1.5 % (w/v) Agar
- autoclave

5.2.4. Stress assay

For colony growth assays, *U. maydis* strains were spotted on plates with media providing different stresses. The plates contained either NM (Nitrogen minimal medium) agar, AM (ammonium minimal medium) agar or CM (complete medium) agar with various stress-inducing compounds including calcofluor (45 µg/mL), H_2O_2 (1.5 mM), congored (70 µg/mL) and NaCl (1M).

The cultures were grown to an OD_{600} of 0.6-1, pelleted (10 min, 3500rpm, RT) and re-suspended in enough water to set the OD_{600} to 1. Serial dilutions of these cultures were spotted on the mentioned plates and then incubated for 48h at 28°C.

CM agar
(Holliday, 1974)
0.6 % NH_4NO_3 (w/v)
1.0 % casamino acids (w/v)
0.1 % herring sperm DNA (w/v)
2.0 % yeast extract (w/v)
2.0 % vitamin solution
2.0 % bacto agar (w/v)
- autoclave
- add glucose (1%)

NM agar (Holliday, 1974)
0.30 %KNO_3 (w/v)
6.25 %Salt solution (v/v)
2.0 %bacto agar (w/v)
- pH7, NaOH
- autoclave
- add glucose (1%)

AM Agar (Holliday, 1974)
0.30 %$(NH_4)_2SO_4$ (w/v)
6.25 %Salt solution (v/v)
2.0 %bacto agar (w/v)
- pH7, NaOH
- autoclave
- add glucose (1%)

5.2.5. Filamentous growth of *Ustilago maydis*

A prerequisite of Ustilagos' pathogenic life style is the ability to form filaments (Kahmann & Kämper, 2004). Therefore, all generated strains need to be tested for this capability. To do so it was made use of the observation that activated charcoal induces exactly this filament formation. The exact procedure is described below.

U. maydis strains were grown in liquid $YEPS_{light}$ medium at 28°C until they reach an OD_{600} of 0.8. After harvesting the cells (3500 rpm, RT, 5 min), the pellet was re-suspended in sterile water and the OD_{600} of the culture was adjusted to 1.0. Of this cell solution 5 µL were spotted on PD-Charcoal plates and incubated at 28°C for 24 hours.

Filamentous growth was characterized by the formation of a white mycelium that is easily identified by its fuzziness.

PD charcoal Agar
2.4 % potato dextrose broth (w/v)
2.0 %bacto agar (w/v)
1.0 %activated charcoal (w/v)
- autoclave

5.3. Cultivation of *Saccharomyces cerevisiae*

Saccharomyces cerevisiae was grown under aerobe conditions at 28°C in YPD (yeast extract peptone dextrose) or SD (synthetic dextrose) broth (tubes) or on YPD/SD agar (plates). To avoid the growth of untransformed or foreign yeast, certain amino acids were not added to the medium, allowing only those yeast strains to grow that express the corresponding auxotrophy marker genes.

YPD medium
1 % yeast extract (w/v)
2 % bacto-peptone (w/v)
[optional for plates: 2% bacto agar]
- autoclave
- add glucose (2%)

SD medium
0.67 % yeast nitrogen base without amino acids (w/v)
0.06 % dropout amino acids (leu –trp –his –ade) (w/v)
[optional for plates: 2% bacto agar]
- autoclave
- add glucose (2%)

- to generate the different dropout combinations certain amino acids were added after autoclaving (e.g. 0.02 g/L adenine, 0.02g tryptophan, 0.02g histidine, 0.04g leucine)

5.3.1. *Saccharomyces cerevisiae* glycerol stocks

Aliquots (750 µL) from fresh ON cultures were combined with an equal volume of sterile glycerol stock medium in tubes, incubated for 15 min at RT and stored at -80 °C.

Glycerol stock medium 65 % Glycerol (v/v)
100 mM $MgSO_4$
25 mM Tris-HCl (pH8.0)

5.3.2. Preparation of competent *S. cerevisiae* cells

Generation of competent yeast cells was done using the protocol described below.

1. Start the pre-culture by inoculating 5 mL YPD with yeast material from a plate and growing the culture ON at 28°C and 200 rpm.
2. Inoculate 50 mL YEPD with 1 mL of your ON culture to start the main culture.
3. Grow at 30°C to an OD_{600} = 0.5-0.7 (ca. 4-6h).
4. Pellet the cells in falcon tubes by centrifuging them for 3 min at 500g. Discard the supernatant.
5. Wash the cells first with 15 mL ddH_2O and then with 10mL SORB.
6. In parallel, boil the carrier DNA (10mg/mL denatured salmon sperm DNA; Invitrogen) for 10 min and then snap cool it on ice.
7. Dissolve the cells in 360 µL SORB and add 40 µL carrier DNA. From this step on, the cells are kept on ice. Dispense cells into 50 µL aliquots in micro centrifuge tubes, freeze them using liquid nitrogen and then store them at -80°C.

5.3.1. Transformation of *S. cerevisiae*

S. cerevisiae was transformed using a PEG based protocol described below.

1. Thaw competent yeast cells on ice.
2. Add 5-10 µL plasmid DNA and mix the components by flicking.
3. Add 300 µL sterile PEG solution and mix again.
4. Incubate the cells for 30 min at 30°C while shaking (800rpm):
5. Perform a heat shock by incubating the cells for 15 min at 42°C.
6. Add 800 µL YPD medium to reaction and mix carefully.
7. Centrifuge the tubes for 3 min at 500g and discard the supernatant.
8. Wash the cells once with 1mL YEPD and then re-suspend the cells in 1 mL YEPD.
9. Incubate the reaction in a shaker for 30 min at 30°C.
10. Centrifuge the cells for 3 min at 500g, discard the supernatant and resolve pellet in 100µL ddH_2O. Spread the cells on selective plates and incubate them at 28°C for 2-3 days.

SORB 100 mM lithium acetate
10 mM Tris HCl, pH8
1 mM EDTA, pH8

1 M sorbitol
- pH8, acetic acid
- Filter sterilize

PEG solution 100 mM lithium acetate
10 mM Tris HCl, pH8
1 mM EDTA, pH8
40% PEG 3350
- Filter sterilize

5.4. Extraction, purification and analysis of nucleic acids

5.4.1. Common procedures

Basic procedures including restriction digestion, ligation, DNA amplification by PCR, purification of DNA from PCR reactions/agarose gels were conducted using the supplied manuals (New England Biolabs, Analytik Jena). Sequencing of DNA was done by the in-house facility Molecular Biology service (IMBA/IMP/GMI core facilities).

5.4.2. Isolation of plasmid DNA from *Escherichia coli*

For several purposes like restriction analyses, ligations or transformations it is necessary to isolate plasmid DNA. Plasmids are circular, double stranded DNA molecules which are replicated in the bacterial cell independent of the chromosomal DNA. The method used is based on the principle of alkaline lysis (Birnboim & Doly, 1979). The principle of alkaline lysis is based on the different characteristics of plasmid and genomic DNA after the denaturation in alkaline solutions and the following renaturation. After alkaline denaturation the pH is rapidly reduced. Plasmid DNA stays in solution during this process, in contrast to genomic DNA. Genomic DNA sticks to the leftovers of the cell-wall and to proteins, which allows the centrifugation of chromosomal DNA.

A combination of commercially available equipment (P2 and N3, Qiagen; columns Centic Biotec), as well as, self-made solutions (P1, PB, PE), was used for the protocol below.

1. Grow bacterial liquid cultures in selective LB medium ON (rolling at 37°C).
2. Transfer 1.5-4.0 mL of the culture to a tube and centrifuge (1 minute, 11.000 rpm) to pellet the bacteria.
3. Discard the supernatant and add 250 µL of buffer P1. Re-suspend the cell pellet by vigorous vortexing. The RNase present in P1 will hydrolyse RNA, whereas the EDTA accomplishes the chelation of divalent cations. The chelation will destabilize the cell walls and remove the co-factors of DNases.
4. Add 250 µL P2 to denature DNA and lyse the cells. Invert the tube 6-8 times and incubate up to 5 min at RT or until the solution is clear. Within this time the included sodium-

hydroxide denatures proteins and chromosomal DNA, whereas SDS, a strong detergent, is lysing the cells.

5. Neutralize the reaction by adding 350 µL N3. Invert the tubes 6-8 times. The potassium acetate precipitates chromosomal DNA and proteins. Pellet the precipitate by spinning the tube for 10 min at full speed. The plasmid molecules remain in the supernatant and will be purified in the following wash steps.
6. Transfer the supernatant to the column. Spin for 1 min at full speed and discard the supernatant.
7. Add 500 µL buffer PB. Spin for 1 min at full speed and discard the supernatant.
8. Add 750 µL buffer PE. Spin for 1 min at full speed, discard the supernatant and spin again for 2 min at full speed to remove residual ethanol.
9. Elute the pellet using 30-50 µL ddH_2O or a suitable buffer. If DNA was to be sent for sequencing, 1µL plasmid DNA was mixed with 10 nM primer and filled with water up to 7.5µL.

P1 50 mM Tris-HCl; pH8
10 mM EDTA
0.1 mg/mL RNase

PB 5 M guanidine hydrochloride
30% isopropanol

PE 10 mM Tris HCl, pH7.5
80% ethanol

5.4.1. Plasmid DNA isolation from *Saccharomyces cerevisiae*

Plasmid DNA isolation from *S. cerevisiae* was performed to elucidate the nature of possible interaction partners obtained from the yeast two-hybrid screen. The used protocol is described below.

1. Inoculate 4 mL YPD/SD with yeast material from a plate and incubate the culture ON at 28°C and 200 rpm.
2. Harvest the cells by centrifuging them at full speed for 1 min and discard the supernatant.
3. Re-suspend cells in 400 µL yeast lysis buffer.
4. Add 400 µL phenol-chloroform and a spoon of glass beads to the tube and shake tubes vigorously for 5 min.
5. Centrifuge reactions at full speed for 30 min and carefully transfer the upper layer into a fresh tube.
6. Add 400 µL chloroform to the reaction and shake vigorously for 3 min.
7. Centrifuge the tubes at full speed for 20 min and transfer the upper layer into a new tube.
8. Add 2.5 V ethanol abs., mix, centrifuge the tubes at full speed for 15 min and carefully remove supernatant.
9. Wash DNA pellet with 1 mL 70% ethanol. Remove supernatant.
10. To ensure removal of residual ethanol place tubes at RT with open lids.
11. Re-suspend the DNA in 30 µL TE-buffer or ddH_2O.

Yeast lysis buffer 2 % Triton X-100
1 % SDS
100 mM NaCl

10 mM Tris HCl, pH8.0
1mM EDTA

5.4.2. Isolation of genomic DNA from *Ustilago maydis*

Genomic DNA from *U. maydis* had to be isolated for various purposes and was done as described below.

1. Inoculate 4 mL $YEPS_{light}$ with fungal material from a plate and grow the culture ON at 28°C and 200 rpm.
2. Transfer 1 mL culture into a prepared micro centrifuge tube (with one spoon of glass beads) and spin for 1 min at full speed. Discard supernatant. Freeze pellets at -20°C for long term storage but at least for a few hours to ease cell disruption.
3. Add 500 µL Phenol-Chloroform and 400 µL Ustilago lysis buffer and shake tubes for 15 min vigorously.
4. Spin the tubes for 30 min at full speed. In the meanwhile, prepare new micro centrifuge tubes with 1 mL of 100% ethanol.
5. After centrifugation add 400 µL of the upper, aqueous layer and transfer it to the prepared tubes. Mix by inverting the tubes several times.
6. Spin the tubes for 5 min at full speed and discard the supernatant.
7. Wash the pellet with 1 mL 80% ethanol to remove residual salts. Spin 2 min at full speed and remove the supernatant carefully.
8. Add 20-30 µL TE-RNase and re-suspend the pellet. Incubate the tubes for 15 min at 55°C on a Thermoblock with open lids to remove residual ethanol. Store DNA at -20°C.

Ustilago lysis buffer
2.0 % Triton X
1.0 % SDS
10 mM Tris HCl, pH8
100mM NaCl
1 mM EDTA

5.4.3. Ethanol precipitation of DNA

DNA precipitation was used to purify or concentrate DNA from a solution (e.g. restriction digest). Therefore, two components were added to a DNA solution (1/10V 3M sodium acetate, pH5.2 and 3V ethanol abs.). After mixing, the reaction was incubated for 30 min at -20°C to allow for DNA precipitation. Next, the reaction was centrifuged for 30 min at full speed and 4°C. The supernatant was carefully removed and the pellet washed with 1 mL 70% ethanol. After removal of the supernatant, the pellet was re-suspended in the desired amount of water or TE buffer. To ensure complete removal of ethanol the reaction tubes were incubated at 55°C with open lids for 15 min.

5.4.4. Agarose gel electrophoresis

Agarose gel electrophoresis is a method to separate DNA molecules by size in order to identify or purify DNA fragments. After applying a potential between 30-120 V the DNA

diffuses to the anode, due to the negative charged phosphate groups. The mobility of the nucleic acids depends of the molecule size and the density of the gel matrix. The buffer used can be either TBE (Tris, Borate, EDTA) or TAE (Tris, Acetate, EDTA). TAE buffer was the commonly used buffer. RNA samples were run in TBE buffer.

The used polymatrix was in TAE- or TBE buffer solubilized agarose (0.8-1.2%). Therefore, the buffer was boiled in the microwave. After cooling down to 60°C, peqGreen (PEQLAB) was added (3µl/100ml) and the still liquid agarose-gel-solution was filled in a horizontal, sealed tray to set. PeqGreen intercalates into the backbone of nucleic acids and fluoresces under UV-light. To visualize the movement of the samples within the gel, loading dye was added.

TAE-Buffer	40 mM Tris 1 mM EDTA 0.1 % acetate
TBE-Buffer	89 mM Tris 89 mM borate 2.5 mM EDTA
6x loading dye	50 % sucrose (v/v) 0.1 % bromophenol blue (v/v) in TE buffer

5.4.5. Golden Gate

Golden Gate cloning is a recently developed cloning technique allowing standardized, quasi-scarless, multi-part DNA assembly (Engler *et al.*, 2008). To do so, it makes use of Type II endonucleases. This kind of restriction enzymes (e.g. BsaI, BsmBI, SapI) cleaves DNA distal from the recognition sites, in contrast to classical restriction enzymes cutting within the recognition site. Thereby, 3-4 bp overhangs are generated that are context specific and can be freely chosen by the researcher. Ligation of two overhangs from DNA strands not having the recognition site will generate a recognition site-free DNA molecule. Cleverly designed, the desired product cannot be re-digested, in contrast to undesired products, leading to an accumulation of wanted DNA molecules over time. To use this cloning strategy, fragments carrying recognitions sites with compatible overhangs will be added to one direction. The reaction will be exposed to a cycle of ideal conditions for the restriction enzyme (e.g. 37°C) and ideal conditions for the ligase (16°C, Table 5.3). Afterwards 3 µL of the reaction are used to transform *E. coli* cells (5.1.3.4 Chemical transformation of *Escherichia coli*).

Golden Gate reaction	x µL Vector (~10ng) y µL Insert (100g) 2 µL T4 Ligase buffer 0.5 µL T4 Ligase 0.5 µL Type II restriction enzyme add to 20 µL ddH_2O

Table 5.3 Cycling conditions for a Golden Gate reaction

Golden Gate cycling conditions	37°C for 10 min 37°C for 5 min 16 °C for 10 min ← 10 x 37°C for 10 min → 50°C for 5 min 80°C for 5 min 12°C for ∞

5.4.6. Southern Blot

1. **Restriction digestion of DNA (2-4 h)**

   The common restriction digestion protocol is used. It is recommended to use about 10 µg DNA per sample. 1 µL of restriction enzyme should be sufficient. The digestion should be performed for up to four hours to ensure complete digestion.

2. **Electrophoresis (1-16 h)**

   Decide on the percentage and the size of the gel required. Follow the normal protocol for gel electrophoresis. For genomic DNA it is best to run the DNA at low voltage (90 V) to achieve an adequate separation of the DNA fragments.

3. **Preparation of transfer (2-3 h)**
   - Transfer the gel carefully to a transilluminator and take a photograph.
   - Depurinate the gel by completely immersing it in 0.25M HCl for 15 min or until the color of the loading dye is changed from blue to yellow. This step is best carried out in a tray with rocking. The removal of purines facilitates the transfer of big DNA molecules.
   - Replace the solution with 0.4M NaOH and leave for further 15 min. This step neutralizes the gel and the color of the loading dye should change back to blue.

4. **Transfer setup (15 min)**
   - For transfer assemble the components in a way that the buffer is soaked through the agarose gel over the nylon membrane into a stack of paper.
   - Immerse the filter paper and transfer membrane by first floating them on the surface of the solution; otherwise air will be trapped in patches, which leads to uneven transfer.
   - Fill the tray with 20× SSC (saline-sodium citrate buffer) and lay a glass plate over it; soak a filter paper in 20× SSC and lay it over the plate, dipping into the tray on both sides.
   - Remove the gel from the neutralizing solution and lay it upside down on the wet filter paper on top of the glass. Seal the sides of the gel using parafilm.
   - Lay the membrane on top of the gel. Take care in aligning the gel before it makes contact with the membrane and lay it down by ‘rolling’ from one edge to avoid trapping air between the gel and the membrane. Once it is placed, do not move the membrane, as transfer of DNA may already have taken place.

- Place three layers of filter paper on top and then additionally a stack of tissue paper. Do not put a heavy weight on top, as this may flatten and distort the gel during the transfer process, making final size comparisons more difficult.

5. **Transfer (3-16 h for transfer)**
    - Let the transfer setup stand to allow transfer to take place. The minimum time required for complete transfer depends on the size of the fragments and the gel concentration (2-20 h). During transfer it may be necessary to occasionally add more 20× SSC to the bottom sheet of filter paper. If the paper dries too much, the gel will shrink against the membrane and liquid contact will be broken. The paper may be flooded but one has to take care that liquid does not fill the air spaces between the gel and the parafilm, bypassing the gel.
    - At the end of the transfer period lift the membrane carefully so that the gel remains attached to its underside.
    - Turn over the membrane and mark the outline of the gel in pencil.
    - Peel the gel off the membrane. Any DNA remaining in the gel can be seen by viewing the gel in ultraviolet light.
6. **Prehybridization (1 h) and Hybridization (4 h - ON)**

    Prehybridization will block unspecific binding sites on the membrane. The process can be performed for 30 min up to several hours. In general, higher temperatures (up to 68°C) will result in faster and more efficient prehybridization.
    - Place membrane into hybridization tube with hybridization buffer for at least 30 min.
    - Heat denature your probe at 100°C for 10 min (Probe was prepared using the DIG labelling mix from Roche).
    - Discard buffer and add denatured probe to 20 mL pre-warmed (68°C) hybridization buffer. Add the mix to the membrane and incubate the membrane rotating at 68°C ON
    - Store hybridization buffer with probe at -20°C to reuse it.
    - Wash the membrane two times with Southern wash buffer rotating at 68°C for 15 min
7. **Detection**

All steps should be done while slightly shaking (still in the hybridization oven, but at RT)

- Incubate membrane in 20 mL DIG wash buffer for 5 min.
- Discard buffer and perform blocking by adding 100 mL DIG2 to the membrane and rotating it for at least 30 min.
- Discard DIG2 and add 20 mL antibody solution for at least 30 min.
- Wash membrane two times with DIG wash buffer for 15 min
- Equilibrate membrane in 20 mL DIG3 for 5 min
- Place membrane into small plastic bag and drop 5 mL CDP-star solution evenly on it. Incubate for 5 min. Remove superfluous CDP star solution and transfer membrane into a new plastic bag. Seal the bag and incubate the membrane at 37°C for 15 min.
- Place membrane on film and develop it.

SSC (20x)	3.0 M NaCl 0.3 M sodium citrate ➢ pH7, NaOH or HCl
Hybridisation buffer	0.5 M $NaPO_4$, pH7 7 % SDS
Southern wash buffer	0.1 M $NaPO_4$, pH7 1 % SDS
DIG wash buffer	DIG buffer 1 0.3 % Tween 20
DIG buffer 1	0.10M maleic acid 0.15M NaCl ➢ pH7.5 (NaOH)
DIG 2	DIG buffer 1 1 % milk powder
DIG 3	0.1M Tris-HCl, pH9.5 0.1M NaCl 0.05M $MgCl_2$
Antibody solution	DIG2 1:10000 Anti DIG
CDP star solution	DIG3 1:100 CDP star ➢ can be reused, store at -20°C, light sensitive

5.4.7. RNA extraction

RNA was extracted from fungal liquid culture or infected plant material. Accordingly the material had to be prepared differently. The protocol itself however is identical.

To isolate RNA from fungal cultures cells grown to an OD_{600} of 0.8, pelleted and immediately frozen in liquid nitrogen. Pellets from 15 mL culture were used for one sample and one scoop of small glass-beads was added before proceeding.

For plant tissue, the tissue was harvested, frozen in liquid nitrogen and ground to a fine powder using mortal and pistil. About 250 mg powder was used in one reaction.

The RNA extraction was conducted as described below:

1. Add 1mL TRIzol® to the frozen sample and vortex immediately, until the material is well suspended. Shake reactions on the vibrax for 15 min.
2. Centrifuge the samples for 5 min at full speed and 4°C. Transfer the supernatant to a new micro-centrifuge tube.
3. Add 200 µL chloroform and vortex each sample thoroughly for 10-15 seconds. Afterwards incubate the samples at RT for 3 min.
4. Centrifuge again at full speed for 15 min at 4°C. In the meantime: prepare fresh tubes by adding 500 µL cold isopropanol to each of them.
5. Carefully transfer the upper, aqueous phase (400-500 µL) into the prepared tubes and mix by inverting the tubes several times.
6. Incubate samples at RT for at least 10 min to allow for precipitation of RNA. Afterwards spin the tubes at full speed for 15 min (4°C) and carefully discard the supernatant.
7. Wash RNA pellet with 1 mL 80% ethanol and carefully remove the supernatant. Spin again to remove residual ethanol.
8. After drying the RNA pellet at RT for no longer than 5 min, re-suspend it in 35 µL RNase free water.
9. Incubate the samples at 50°C for 15 min and store RNA at -80°C afterwards.

10. Before continuing to work with RNA control its integrity by running it on a TBE agarose gel supplied with 0.2% bleach to remove RNases (Aranda *et al.*, 2012).

5.4.8. DNase treatment of RNA and cDNA generation

To remove residual DNA contaminations after isolation from RNA the samples were treated with DNases using the 'Ambion TURBO DNA-*free*™' Kit (Invitrogen).
Per reaction approximately 5µg RNA are used. The protocol is described below:

1. Add 0.1V of 10x Turbo DNase buffer and 1 µL of DNase.
2. Mix gently and incubate the samples at 37°C for 30 min.
3. Add 0.1V of DNase Inactivation reagent, mix well and incubate the reaction for 2 min at RT under occasional mixing.
4. Centrifuge the samples at full speed for 2 min. And transfer the supernatant to a fresh tube.
5. After confirming the RNA integrity on an agarose gel, proceed to cDNA generation.

Typically 1 µg of RNA was used to obtain cDNA by reverse transcription. To do so the instructions provided by the SuperScript® III First-Strand Synthesis Kit (Thermo Fisher Scientific) were followed.

5.4.9. Real time PCR

Real time PCR allows for the quantification of in cDNA transcribed mRNA. The protocol used is based on the Platinum® SYBR® Green qPCR SuperMix-UDG (Invitrogen). As the transcripts aimed to amplify within this thesis were of low abundance, 1 µL cDNA was used per downscaled 25 µL reaction.

5.4.10. Yeast two-hybrid screen

A yeast two-hybrid screen allows for the identification of proteins that interact with the protein of interest. The protein of interest acts as a bait that is exposed to a library of possible interacting proteins. Detection of the interaction is based on the GAL4 system consisting of a GAL4 activation domain (AD) and a GAL4 DNA binding domain (BD). The yeast strain carrying the bait protein is mated with the library that was cloned into a compatible strain. In case of an interaction of the bait (fused to the BD) and another protein from the library (all fused to the AD), AD and BD get in close proximity which allows for the transcription of reporter genes.

For this screen it was made use of a phage-derived library (Stratagene Phagemid library; Farfsing, 2004) obtained from *Zea mays* leaves infected with *Ustilago maydis* fused to the AD to screen for interaction partners of ApB73. ApB73 itself and UbApB73 respectively were fused to the BD and expressed in the haploid *S. cerevisiae* strain

AH109 (Clontech). The library fused to AD was expressed in the compatible haploid *S. cerevisiae* strain Y187. The auxotrophy markers genes *ade2* and *his3* were used as reporter genes.

The transformation of the library as well as the mating was performed as described in the manual "Matchmaker™ GAL4 Two-Hybrid System 3 & Libraries User Manual" (Clontech, 2007). For the library transformation 420µg of library DNA were used and the transformants of strain Y187 were selected on SD –trp plates. After mating of the library with the bait strain, diploid yeast cells were selected for on SD –leu –trp plates. After an incubation time of three days, the diploid cells were washed off and pooled using 1x TE buffer. The pooled diploid cells were then plated on to high stringency medium (SD –leu –trp –his -ade) and incubated for three days. Yeast colonies were inoculated in high stringency liquid medium and pelleted for plasmid DNA isolation. The isolated plasmid DNA was transformed into electro competent *E. coli* cells isolated and sent for sequencing to determine possible interaction partners.

5.5. Biochemical Methods

5.5.1. Processing of *Ustilago maydis* cell pellets for Western blot

For various experiments, denatured proteins of *Ustilago maydis* whole cell extracts (pellets) were needed. As fungi have cell walls the following procedure had to be applied to free proteins. Cell pellets were re-suspended in 50 µL PBS and 25 µL SDS loading dye and one spoon of sand and glass beads were added. The cells were disrupted using a ball mill (Retsch) for six minutes (30 m/s). Than the samples were incubated at 98°C for 5 minutes and centrifuged at for 5 min at full speed. After transferring the supernatant to a new tube, the samples were incubated at 98°C for 2 min and pelleted one last time by spinning them for 2 min at full speed. From the obtained solutions 2-5 µL were loaded on a SDS polyacrylamide gel for further analysis.

6x SDS loading dye	100mM	Tris-HCl, pH 8.0
	4M	urea
	4 %	SDS (v/v)
	40 %	glycerol
	3.5 %	DTT
	0.15 %	bromophenol blue (w/v)

5.5.2. Processing of tobacco leaves for Western blot

For Western blot analysis of *Agrobacterium tumefaciens* infected *Nicotiana benthamiana* plants, leaves were harvested three days post infection using liquid nitrogen.

The plant material was ground to a fine powder using mortal and pistil. Around 250 mg of the plant powder were mixed with 250 µL Tris pH9 + 1% NP40, 25 µL 100mM

DTT and 100 µL Protein Loading dye. After boiling the reaction for 5 min, the mixture was centrifuged for 5 min at full speed. The supernatant was transferred to another tube and subjected to Western blot analysis.

5.5.3. Plasma membrane enrichment

Plasma membrane enrichment was conducted using a published protocol but adapting it in the preparation of the samples (Santoni, 2007). In contrast to the published protocol, the used starting materials were axenic cultures and therefore the mechanical disruption had to be done differently:

The fungal pellets were re-suspended in the published homogenization medium and disrupted using a heavy-duty cell disrupter (Santoni, 2007). The cells were passed through the disrupter at incremental pressures from 10, 15, 20, 25 kpsi at 4°C. The resulting homogenate was centrifuged at 10000g for 10 min to pellet unbroken cells and debris. The supernatant was pelleted at 84000g for 20 min at 4°C to obtain the microsomal pellet. The enrichment of the plasma membrane from the microsomal pellet was done as described (Santoni, 2007).

5.5.4. Secretion Assay

One hallmark of effector proteins is their secretion by *U. maydis* into the biotrophic interface. Secretion is believed to be enhanced in filaments. Filamentation is controlled by the *b*-genes that are only activated when the fungus is switching to pathogenic development. To test for this under laboratory conditions it is made use of AB33, a genetically manipulated *U. maydis* strain (Brachmann *et al.*, 2001). In the AB33 strain the *b*-genes are expressed under the control of a nitrogen-inducible promoter. After induction of filaments the protein of interest is secreted into the surrounding medium. From there it can be precipitated and subjected to Western blot analysis. The exact protocol is described below.

a) Filament induction
    1. Inoculate 2 mL of $YEPS_{light}$ liquid medium with fungal material and grow for 24 hours at 28°C.
    2. Inoculate the main culture by adding 150 µL pre-culture to 400 mL CM medium. Shake at 28°C ON.
    3. Harvest the cells when they reach OD_{600}=0.6 by centrifugation (2500rpm, 10 min, RT). Discard the supernatant and wash the cells once with NM medium.
    4. Re-suspend the cells in 400 mL NM medium and shake at 28°C for six hours to induce filamentation. The filamentation process was monitored microscopically.

5. After six hours the cultures were transferred through a paper filter into a cooled centrifugation tube. The filter ensures that only the medium and no cells are transferred. Make sure to keep some cells from the filter as a control (5.5.1Processing of *Ustilago maydis* cell pellets for Western blot). Spin at 2500 rpm for 10 minutes (4°C). From now on everything needs to be done on ice.
6. After the centrifugation carefully transfer the supernatant into a new tube.

b) Precipitation

1. Add 4 mL (1:100) of 2% sodium deoxycholate (DOC) to the supernatant from the previous step. Mix and incubate on ice for 20min.
2. Add 40 mL (1:10) 100% trichloroacetic acid (TCA), mix again and incubate the reaction on ice ON.
3. Pellet the precipitated proteins (8000 rpm, 40 min, 4°C) and wash the protein pellet twice using 4 mL 100 % acetone (13000 rpm, 2 min, 4°C).
4. Dissolve the pellet in 20 µL 1M Tris-HCl, pH8. Add SDS loading dye and boil the samples to denature the precipitated proteins.
5. Continue with SDS PAGE and Western Blot.

CM liquid medium
(Holliday, 1974)

- 0.6 % NH_4NO_3 (w/v)
- 1.0 % casamino acids (w/v)
- 0.1 % herring sperm DNA (w/v)
- 2.0 % yeast extract (w/v)
- 2.0 % vitamin solution
- ➢ autoclave
- ➢ add glucose (2%)

Vitamin solution
(Holliday, 1974)

- 0.10 ‰ thiamine (w/v)
- 0.05 ‰ riboflavin (w/v)
- 0.05 ‰ pyridoxine (w/v)
- 0.20 ‰ calcium pantothenate (w/v)
- 0.05 ‰ para-aminobenzoic acid (w/v)
- 0.20 ‰ nicotinic acid (w/v)
- 0.20 ‰ choline chloride (w/v)
- 1.00 ‰ myo-Inositol (w/v)
- ➢ filter sterilize
- ➢ store at -20°C

NM liquid medium
(Holliday, 1974)

- 0.30 % KNO_3 (w/v)
- 6.25 % Salt solution (v/v)
- ➢ pH 7, NaOH
- ➢ add glucose (1%)

Salt solution
(Holliday, 1974)

- 1.6 % KH_2PO_4 (w/v)
- 0.4 % Na_2SO_4 (w/v)
- 0.8 % KCl (w/v)
- 0.4 % $MgSO_4 * 7H_2O$ (w/v)
- 0.132 % $CaCl_2 * 2H_2O$ (w/v)
- 0.8 % trace element solution (v/v)

Trace element solution
(Holliday, 1974)

- 6 ‰ H_3BO_3 (w/v)
- 14 ‰ $MnCl_2 \times 4H_2O$ (w/v)
- 40 ‰ $ZnCl_2$ (w/v)
- 4 ‰ $NaMoO_4 \times 2H_2O$ (w/v)
- 10 ‰ $FeCl_3 \times 6H_2O$ (w/v)
- 4 ‰ $CuSO_4 \times 5H_2O$ (w/v)

5.5.5. SDS PAGE

To separate protein extracts according to their molecular weight SDS PAGE (sodium dodecyl sulfate polyacrylamide gel electrophoresis) was conducted (Laemmli, 1970). Here, the separation of proteins takes place in vertical bisacrylamide gels. To prepare the protein samples, they were denatured by adding SDS loading dye and boiling them for 5 min. The ionic detergent SDS unfolds proteins and binds to them with its hydrophobic domains. Thereby the whole protein becomes negatively charged and can be separated in an electric field according to its size. The loading dye contains DTT and β-mercaptoethanol as reducing agents.

Electrophoresis was performed with a constant current of 20-25 mA per gel immersed in SDS running buffer. As a size standard the PageRuler, Prestained Protein Ladder (Fermentas) was used.

Resolving Gel	10.0% (w/v) Acrylamide/Bisacrylamide 300 mM Tris/HCl, pH 8.8 0.08% (w/v) sodium dodecyl sulfate (SDS) 0.03% (v/v) N,N,N',N'-Tetramethylethylenediamine (TEMED) 0.02% (w/v) ammonium persulfate (APS)
Stacking Gel	4.00% (w/v) Acrylamide/Bisacrylamide 125 mM Tris HCl, pH6.8 0.10% (w/v) SDS 0.08% (v/v) TEMED 0.03% (w/v) APS
SDS running buffer	192 mM Glycine 25 mM Tris HCl, pH8.3 4.0 mM SDS

5.5.6. Western Blot Analysis

Protein mixtures can be qualitatively analysed with the help of specific protein ligand interactions. To do so proteins separated by SDS PAGE were transferred onto PVDF membrane by Western blot (Towbin *et al.*, 1979). Afterwards the proteins were analysed using specific antibodies.

5.5.6.1. Western Blot

In the following the blotting procedure is explained. After SDS PAGE, the acrylamide gels were placed on two in buffer equilibrated filter paper. On top of the gel, the PVDF membrane and another set of two filter papers were placed. Afterwards, everything was placed into a holder and transferred into the blotting chamber filled with transfer buffer. The protein transfer was conducted vertically in an electric field with 700 mA for 80 min. Within the blotting chamber the organization was as depicted below.

cathode (-)
Filter paper (2x)
Gel
PVDF membrane
Filter paper (2x)
anode (+)

SDS running buffer 192 mM glycine
25 mM Tris HCl, pH8.3
20% methanol

5.5.6.2. Immunodetection of proteins

To identify specific proteins in complex protein extracts, they can be transferred onto PVDF membranes and detected by specific antibodies. Before detection however, area on the membrane not carrying proteins have to be blocked with an unspecific protein that will not be detected by the antibody. Therefore the membrane is immersed in blocking buffer and put on a rocking tray for at least one hour at room temperature. Superfluous blocking buffer is removed by washing the membrane three times with TBST for five minutes.

Next, the first antibody solution is added to the membrane and left for incubation at 4°C ON. For the detection of proteins two antibodies are needed. The primary antibody specifically binds the protein of interest, whereas the secondary antibody binds to the primary antibody. Here, the used primary antibodies were obtained from mice and act as an antigen for the secondary antibody obtained from goat (IRDye® 800CW Goat anti-Mouse IgG (H + L); Licor). The secondary antibody is coupled to a dye that emits infrared light that can be detected using the Odyssey Infrared Imaging System. Before addition of the secondary antibody the membrane is washed three times for five minutes with TBST to remove unbound primary antibodies. After incubation with the secondary antibody for at least two hours, the membrane was washed three more times using TBST and then developed using the Odyssey system.

TBS, pH 7.5 150 mM sodium chloride
50 mM Tris

TBST, pH 7.5 TBS
0.1% (v/v) Tween 20

Blocking buffer TBST (1x)
5% milk powder

Table 5.4 Used Antibodies, their concentration and supplier.

Antibody	used concentration	Company
α-actin	1:2000	Thermo Pierce
α-HA	1:2000	Sigma Aldrich
IRDye 800CW Goat-α-mouse	1:10000	Licor

5.6. Methods involving plants

5.6.1. Growth conditions

During the course of this study two different plant species were used: *Zea mays* and *Nicotiana benthamiana*.

Z. mays was grown in a glass house using the soil 'Sondermischung Topf+TonL+Fe +MO' (Gramoflor GmbH & Co. KG). The growth conditions were 16 hours light (28°C) and 8 hours dark (20°C), with watering by flooding every 72 h. The provided light intensity ranged between 28000 lux and 90000 lux depending on the weather conditions.

N. benthamiana was grown in controlled short day conditions (16h light/8h dark) at 22°C. The used soil was 'Einheitserde SP ED63 T' (Einheitserdewerke Werkverband e.V.) and the tobacco plants were watered by flooding for 15 min every two days.

5.6.2. Virulence assay using *Ustilago maydis* and *Zea mays*

This method is used to assess virulence of *U. maydis* strains on maize (Kämper *et al.*, 2006). The used strains can either be derivatives of the solopathogenic strain SG200 or derivatives of the wildtype strains FB1 and FB2. When working with FB1 and FB2, two strains with compatible mating types have to be mixed before infection.

As *U. maydis* can induce tumors on all aerial parts of maize two different infection protocols were conducted within the course of this thesis aiming at tumor formation on young seedlings (Seedling infection) or male floral organs (Tassel infection).

5.6.2.1. Seedling infection assay

The protocol described below works for all *U. maydis* strains and is performed on seven day old seedlings independent of the used maize variety.

1. Inoculate 4 mL $YEPS_{light}$ with fungal material from a plate and grow the culture ON at 28°C and 200 rpm.
2. Inoculate the main culture by diluting your pre-culture 1:3000. The final volume needed depends on the number of plants that need to be infected. In most cases 50 mL will be sufficient. Shake at 28°C ON.
3. Harvest the cells when an OD_{600} of 0.6-1 is reached. To do so transfer cells into a falcon and spin them for 10 min at 3500rpm. Discard supernatant.
4. Set the OD_{600} of your cell suspension to 1 by re-suspending your cells in the appropriate amount of water.
5. To infect the seven day old maize seedlings use a needle and a syringe. Inject the culture into the centre of the leaf whorl around 1 cm above the soil.

6. Seven or twelve days later the disease symptoms are scored. Each plant is looked at individually and sorted into one of eight possible categories. Only the most severe symptom on a plant is scored. The possible categories are:
    - No symptoms
    - Chlorosis
    - Ligula swelling
    - Small tumors
    - Normal tumors
    - Heavy tumors
    - Stunted growth
    - Dead

5.6.2.2. Tassel infection assay

This protocol describes the infection of male reproductive inflorescences and was performed on the maize cv. Gaspe Flint. The tassel infections were performed using a syringe based method on 15 day old plants.
The location of immature tassels was identified without cutting the plant. The tassel terminates the shoot, and above it the leaf sheaths overlap without a detectable solid centre indicating the location of the inflorescence.

Cultures were prepared as described earlier (5.6.2.1 Seedling infection assay) and 1 mL of the *U. maydis* solution was injected into the centre of the leave whorl. As the inoculum seeps into the air space around the tassel it reaches the entire floral meristem. Disease symptoms were scored 18 days after infection in cv. Gaspe Flint. For tassel infections the symptoms are differentiated into the following categories (Schilling *et al.*, 2014):

- No symptoms
- Small tumors on <50% of the tassel
- Large tumors on <50% of the tassel
- Small tumors on >50% of the tassel
- Large tumors on >50% of the tassel
- Stunted tassels

5.6.3. Agrobacterium mediated transient expression of tobacco

For localization experiments *Nicotiana benthamiana* plants were transiently transformed using *Agrobacterium tumefaciens* mediated transformation. This was done using the protocol below:

1. Inoculate your Agrobacterium cultures in 8 mL liquid LB (MES AS) containing the appropriate antibiotics.
2. Measure the cultures' optical density and pellet your cells by centrifugation (3000g, 10 min, RT). Discard the supernatant. Re-suspend the cells to an OD_{600} of 0.2 in Agrobacterium resuspension medium (ARM). If you want to co-transform your tobacco plants using several agrobacterium strains, optical density has to be adjusted so that in the final culture each strain has an OD_{600} of 0.2.
3. Incubate the cultures at RT for 3-24h.

4. Mix the cultures and infiltrate the suspension into *Nicotiana benthamiana* plants grown under short day conditions at 22°C. Young plants at the 4-6 leaf stage are ideal.
5. Harvest infiltrated tissue three days post infiltration for microscopy or protein expression.

LB (MES AS)	10 mM MES NaOH, pH5.6 0.02 mM Acetosyringone in LB
ARM	10 mM MES NaOH, pH5.6 10 mM $MgCl_2$ 0.15 mM Acetosyringone

5.6.4. Statistical evaluation of scoring data

For disease scoring evaluation an R-script was used processing the data as described below. Class counts for each genotype of the three biological replicates were summarized. Then, for each pair of genotypes, Fisher's exact test was used to evaluate if the distribution of counts between classes is significantly different between the genotypes. The resulting p-values were multiple testing corrected for g by the Benjamini-Hochberg algorithm (Benjamini & Hochberg, 1995). For figures, the counts for each genotype and replicate were converted to relative counts. Error bars depict the standard deviation of the relative counts in the three replicates. Significance of each genotype in comparison to the defined reference is indicated by stars (*, P<0.05; **, P <0.01; ***, P <0.001; ****, P <0.0001).

5.7. Microscopy

5.7.1. WGA-AF488 staining

Two stains were used when performing microscopy on maize leaves infected with *U. maydis*: Wheat germ agglutinin (WGA) coupled to Alexa Fluor488 (AF488) and propidium iodide (PI). WGA has a high affinity to β-1,4-GlcNAc oligomers, the building blocks of chitin the main constituent of fungal cell walls. As WGA is not fluorescent by itself it is conjugated to AF. PI is used to stain plant cell walls, but cannot penetrate the cells unless they are dead.

Tissue of infected maize leaves was harvested and the middle lamella was removed. Typically the area 1cm beneath the infection site was harvested to ensure the presence of fungal cells. The leaves were de-stained in absolute ethanol for at least 48 hours.

Afterwards, the ethanol was discarded and exchanged with a 10 % KOH solution. The tubes were incubated at 85°C for three hours. The KOH was discarded and the leaves washed with 1x PBS buffer until the pH reached a value of pH7.4. Next, the leaves were covered with staining solution and three times exposed to a vacuum of two

minutes. In-between the leaves were allowed to rest for 10 min. The staining solution was removed and the leaves covered in 1x PBS for imaging.

Staining solution 20 µg/mL PI
10 µg/mL WGA-AF488
0.02% Tween 20
in 1x PBS, pH7.4

5.7.2. Calcofluor White stain

To visualize *on planta* hyphae of *U. maydis*, infected plant material was harvested 18-24 hours post infection. Therefore, a 2 cm long piece was cut from the third leaf of the plant just below the infection site (syringe holes). The leaf was stained by immerging it in Calcofluor White (Fluorescent Brightener 28, 10 ng/ml) for 30 sec. Afterwards the leaf was washed once with water, the middle lamella was removed, and the leaf was placed on a microscope slide with the bottom side up.

6 Appendix

6.1. Index of abbreviations

Within this thesis, the International system of units (SI-units) and those mentioned within the SI were used, including their officially accepted abbreviations (Except temperature: degree Celsius, °C). For amino acids applies the one or three letter code.

35S promoter	Promoter driving the 35S gene of the cauliflower mosaic virus
aa	Amino acids
ApB73/UmApB73	Apathogenic in B73, UMAG_02011
AD	GAL4 activation domain
AF488	AlexaFluor488
Amp	Ampicillin
APS	Ammonium persulfate
ARM	Agrobacteriumresuspension medium
Avr protein	Avirulence protein
BD	GAL4 DNA binding domain
BFP	Blue fluorescent protein
bla	Gene encoding the ß-lactamase
BLAST	Basic local alignment search tool
bp	base pair (s)
Carb	Carbenicillin
cat	chloramphenicol acetyltransferase
CBX	Carboxin
*ccd*B	coupled cell division B gene
cDNA	complementary DNA
CDS	coding sequence
ChlA	Chloramphenicol
Co-IP	Proteincomplex immunoprecipitation
ddH_2O	Double distilled water
DNA	Deoxyribonucleic acid
DOC	Sodium deoxycholate
DMSO	Dimethyl sulfoxide
DTT	Dithiothreitol
DUF	Domain of unknown function
e.g.	exemplī grātiā, for example
EDTA	Ethylenediaminetetraacetic acid
EGB	Early Golden Bantam
ER	Endoplasmatic reticulum
ETI	Effector triggered immunity
ETS	Effector triggered susceptibility
Gent	Gentamycin
GFP	Green fluorescent protein
HA	Tag, Human influenza hemagglutinin (aa 98-106)
HygR	Hygromycin resistance gene
i.e.	id est, that is
Kan	Kanamycin
kb	kilo base pairs
kDa	kilo Dalton
LB	Luria-Bertani
LRR	Leucine rich repeat domain
MES	2-(N-morpholino)ethanesulfonic acid
min	minutes
MOPS	3-(N-morpholino)propanesulfonic acid
MpApB73	*Melanopsichium pennsylvanicum* ortholog of ApBN73 (MP05899)
NB	Nucleotide binding domain
NOS Term	Nopaline synthase terminator of *A. tumefaciens*
nt	nucleotide(s)
OD	optical density
ON	over night
PAMP	Pathogen associated molecular pattern
PEG	polyethylene glycol
PBS	Phosphate buffered saline
PCR	Polymerase chain reaction
Phleo	Phleomycin
PM	Plasma membrane
ppi	peptidyl-prolyl isomerase
PRR	Pattern recognition receptor
PTI	PAMP triggered immunity
R protein	Resistance protein
Rif	Rifampicin
RNA	Ribonucleic acid
ROS	Reactive oxygen species
rpm	rounds per minute
RT	room temperature
ScApB73	*Sporisorium scitamineum* ortholog of ApB73 (SPSC_03285)
SD	synthetic dextrose
SDS	Sodium dodecyl sulfate
SMC	structural maintenance of chromosomes
SOC	Super optimal broth with catabolite repression
SP	signal peptide, secretion signal
Spec	Spectinomycin
SrApB73	*Sporisorium reilianum* ortholog of ApB73 (sr12972)
TAE	Tris, Acetate, EDTA
TBE	Tris, Borate, EDTA
TCA	Trichloroacetic acid
TE	Tris EDTA
TEMED	N,N,N',N'-Tetramethylethylenediamine
Tet	Tetracycline
TM	Transmembrane domain
Tris	2-Amino-2-hydroxymethyl-1,3-propandiol
UbApB73	*Ustilago bromivora* ortholog of ApB73 (UBRO_02986)
UBQ10	*UBIQUITIN10* terminator
UhApB73	*Ustilago hordei* ortholog of ApB73 (UHOR_02986)
V	volt
WGA	Wheat germ agglutinin
YEPS	yeast extract peptone sorbitol
YFP	Yellow fluorescent protein
YPD	Yeast extract peptone dextrose
Δ	Deletion
Ω	Omega leader sequence

6.2. List of Figures

6.3. List of Tables

6.4. Oligonucleotides

Table 6.1 Oligonucleotides used in this study.

#	Name	5´-3´ sequence	Primer# (Djamei Group)	used for plasmid #	Description/application
1	RT_UmApB73_5	GCACCCTTACAGCGACGAAG	#3586	-	Real-time PCR primer (*apB73*)
2	RT_UmApB73_3	CGGGCGGATCGAACAAAACT	#3587	-	Real-time PCR primer (*apB73*)
3	RT-Ppi_5	AAAGAACACCGGACTTGG	#20	-	Real-time PCR primer (*ppi*)
4	RT-Ppi_3	ACATCGTCAAGGCTATCG	#19	-	Real-time PCR primer (*ppi*)
5	5_Um02011_RB	ATATgctcttcACGAACACATCTTGGCTGGCCAAC	PI G9	#1	For UMAG_02011 deletion construct, SapI
6	3_Um02011_RB	ATATgctcttcTCGCGGCGCGCCCCATCTGGCTCGGTGACAGG	PI G9	#1	For UMAG_02011 deletion construct, SapI
7	5_Um02011_LB	ATATgctcttcACAGGGCGCGCCGATGCTGTTGGACTTAGG	PI G9	#1	For UMAG_02011 deletion construct, SapI
8	3_Um02011_LB	ATATgctcttcTGCCTTGATCGAGAAGTTTCGC	PI G9	#1	For UMAG_02011 deletion construct, SapI
9	5_Hyg-1	ATAGGTCTCgctcttcAGGCCTAGATCGCCACAGGATACCACAGGACATCTGGGATATCAGAAGTTCCTATTCTCGAGAAAG	#2222	#1	to amplify HYG cassette for deletion construct, SapI
10	3_Hyg-2	TATGGTCTCgctcttcATCGGCCACTCACGCCACAGGATACCACAGGACATCTGGGATATCCGGGAAGTTCCTATACTTTCTCG	#2225	#1	to amplify HYG cassette for deletion construct, SapI
11	5_poma_Bsa_module	ATATggtctcAcccaCTCGAGCAGGGGGATTCGAG	#3437	#2	to amplify *oma* promoter, BsaI
12	3_poma_Bsa_module	ATATggtctcATGATAGAGTAAGGTAGTTGATTTG	#3438	#2	to amplify *oma* promoter, BsaI
13	5_UmApB73HAStrep_BsaI	ATATggtctcAatcaATGCGATTTCTTCTAGCAGCCC	#3517	#2	to amplify UmApB73HAStrep, BsaI
14	3_UmApB73HAStrep_BsaI	TATggtctcTctccTTATTACTTCTCGAACTGCGGGTG	#3518	#2	to amplify UmApB73HAStrep, BsaI
15	5_Um2011_Pro_p123	AGACTAcatatgCGTGGGTTGGTAGACTGAATG	#3037	#3	to amplify full length promoter and CDS of UMAG_02011, NdeI
16	3_Um2011_Pro_p123	TATgcggccgcTTAAGCGTAATCTGGAACATCGTATGGGTAACTGGTAGAGAAAGTAGAGC	#3038	#3	to amplify full length promoter and CDS of UMAG_02011, NotI
17	5_SacUm02011-HA	ATAgagctcAGTCCCATGCTTCCTCAGC	#3358	#4	to amplify UmApB73$_{649-709}$-mCherry-HA, SacI
18	3_mCherryHA_Not	TATgcggccgcTTATTAAGCGTAATCTGGAACATCGTATGG	#3364	#4	to amplify UmApB73$_{649-709}$-mCherry-HA, NotI
19	5_Um2011_Top	catgCGATTTCTTCTAGCAGCCCT	#3039	#5, 26	to amplify full length UmApB73-HA, NcoI, PCR Product Annealing
20	5_Um2011_Bot	CGATTTCTTCTAGCAGCCCT	#3040	#5, 26	to amplify full length UmApB73-HA, NcoI, PCR Product Annealing
21	3_Um02011HA_NotTop	gcTTAAGCGTAATCTGGAACATCGTATGGGTAACTGGTAGAGAAAGTAGAGC	#3172	#5, 26	to amplify full length UmApB73-HA, NotI, PCR Product Annealing
22	3_Um02011HA_NotBot	ggccgcTTAAGCGTAATCTGGAACATCGTATGGGTAACTGGTAGAGAAAGTAGAGC	#3173	#5, 26	to amplify full length UmApB73-HA, NotI, PCR Product Annealing
23	5_N-Um2011_NcoI	ccatgGAATTCTTACGAGAACATGG	#3043	#25	to amplify UmApB73$_{20-709}$, NcoI
24	3_N-Um2011_pEnt	gcggccgccACTGGTAGAGAAAGTAGAGCG	#3044	#25	to amplify UmApB73$_{20-709}$, NotI
25	5_3xHA-DE	ATATGGTCTCAtcagcaGGCCGCGAGGCCAACGCG	#4005	#6	to amplify 3xHA for GreenGate system, BsaI
26	3_3xHA-DE	ATATGGTCTCTgcagGCCGGCGCGCCCTAATAG	#4006	#6	to amplify 3xHA for GreenGate system, BsaI
27	5_apB73_CD_BsaI	ATATGGTCTCAggctCAATGCGATTTCTTCTAGCAGC	#3893	#29	to amplify *apB73* for GreenGate system, BsaI
28	3_apB73_CD_BsaI	ATATggtctcActgaACTGGTAGAGAAAGTAGAGC	#3894	#7,10,11	to amplify *apB73* for GreenGate system, BsaI
29	5_apB73$_{20-709}$ CD_BsaI	ATATggtctcAggctCAATGGAATTCTTACGAGAAC	#3895	#8,11	to amplify ApB73$_{20-709}$(-mCherry) for GreenGate system, BsaI
30	5_NOST_F	ATATggtctcACTGCGGCCGCCCGGCTGCAGATCG	#3938	#6,7,8,10,11	to amplify NosT for GreenGate system, BsaI
31	3_NOST_R	ATATATggtctcCTAGTCTCATGTTTGACAGCTTATC	#3939	#6,7,8,10,11	to amplify NosT for GreenGate system, BsaI
32	5_linkermCherry	ATATggtctcAtcagcaGCCTCGG	#4097	#7,10	to amplify mCherry-linker-3xHA for

	_DE	CAGGAGCAGGTGCTGGCAGC ATGGTGAGCAAGGGCGAGG			GreenGate system, BsaI
33	3_mCherry3xHA _DE	ATATggtctcTgcagTTACTAATA GTCGGGCACGTCG	#4098	#7,10	to amplify mCherry-linker-3xHA for GreenGate system, BsaI
34	5_ApB73$_{1-19}$ _BC_bsa	ATATggtctcAaacaATGCGATTT CTTCTAGCAGC	#3961	#6,7,11	to amplify ApB73$_{1-19}$ for GreenGate system, BsaI
35	3_ApB73$_{1-19}$ BC_bsa	ATATggtctcAagccTGCCTGACA AGTGGCTGAC	#3962	#6,7,11	to amplify ApB73$_{1-19}$ for GreenGate system, BsaI
36	3_mCherry_CD S	atatGGTCTCACTGACTTGTAC AGCTCGTC	#4801	#8	to amplify ApB73$_{20-709}$-mCherry, BsaI
37	5_otef_AB_BsaI	ATATggtctcAacctTATGGCATG CCCGTACCGAG	#3889	#7,8	to amplify *otef* promoter for GreenGate system, BsaI
38	3_otef_AB_BsaI	ATATggtctcAtgttTCGTGGATGA TGTTGTCTG	#3890	#7,8	to amplify *otef* promoter for GreenGate system, BsaI
39	5_Pit2SP_BC_ BsaI	ATATggtctcAaacaATGCTGTTT CGCTCAGCCTTTG	#3902	#10	to amplify Pit2$_{1-25}$ for GreenGate system, BsaI
40	3_Pit2SP_BC_ BsaI	ATATggtctcAagccAGCTTGAAC ATGTTGCACC	#3903	#10	to amplify Pit2$_{1-25}$ for GreenGate system, BsaI
41	5_ApB73Pro_A B_BsaI	ATATggtctcAacctCGTGGGTTG GTAGACTGAATG	#3885	#10,11	to amplify *apB73* promoter for GreenGate system, BsaI
42	3_ApB73Pro_A B_BsaI	ATATggtctcAtgttTTTGATCGAG AAGTTTCGCTATAGATATACC	#3886	#10,11	to amplify *apB73* promoter for GreenGate system, BsaI
43	5_N-Um2011 pEntry	ccatggAATTCTTACGAGAACAT GG	#3043	#9	to amplify ApB73$_{20-709}$-mCherry-HA, NcoI
44	3_mCherryHA_ Not	TATgcggccgcTTATTAAGCGTA ATCTGGAACATCGTATGG	#3364	#9	to amplify ApB73$_{20-709}$-mCherry-HA, NotI
45	5_UbApB73_SP _Top	catgCGTTTTGCACGTCCAAGC	#3179	#12	to amplify full length UbApB73-HA, NcoI, PCR Product Annealing
46	5_UbApB73_SP _Bot	CGTTTTGCACGTCCAAGCAC GTTTC	#3180	#12	to amplify full length UbApB73-HA, NcoI, PCR Product Annealing
47	3_UbApB73HA_ Top	gcTTAAGCGTAATCTGGAACA TCGTATGGGTACGTTGCATCT TTTAATTCCC	#3181	#12	to amplify full length UbApB73-HA, NotI, PCR Product Annealing
48	3_UbApB73HA_ Bot	ggccgcTTAAGCGTAATCTGGA ACATCGTATGGGTACGTTGCA TCTTTTAATTCCC	#3182	#12	to amplify full length UbApB73-HA, NotI, PCR Product Annealing
49	5_SrApB73_Nco Bot	CGTCTGCGATATGTGACTCTG	#3990	#13	to amplify full length SrApB73-HA, NcoI, PCR Product Annealing
50	5_SrApB73_Nco Top	catgCGTCTGCGATATGTGAC	#3991	#13	to amplify full length SrApB73-HA, NcoI, PCR Product Annealing
51	3_SrApB73-HA_Bot	ggccgcAGCGTAATCTGGAACA TCGTATGGGTAGTGCGCAGA AATCGACG	#3992	#13	to amplify full length SrApB73-HA, NotI, PCR Product Annealing
52	3_SrApB73-HA_Top	gcAGCGTAATCTGGAACATCG TATGGGTAGTGCGCAGAAAT CGACGGTC	#3993	#13	to amplify full length SrApB73-HA, NotI, PCR Product Annealing
53	5_MpApB73_Bo t	CGCATCCTCCTTCTAGCATG	#3994	#14	to amplify full length MpApB73-HA, NcoI, PCR Product Annealing
54	5_MpApB73_To p	catgCGCATCCTCCTTCTAGC	#3995	#14	to amplify full length MpApB73-HA, NcoI, PCR Product Annealing
55	3_MpApB73-HA_Bot	ggccgcAGCGTAATCTGGAACA TCGTATGGGTATGGCTGTGC GGGTAGTG	#3996	#14	to amplify full length MpApB73-HA, NotI, PCR Product Annealing
56	3_MpApB73-HA_Top	cgcAGCGTAATCTGGAACATC GTATGGGTATGGCTGTGCGG GTAGTG	#3997	#14	to amplify full length MpApB73-HA, NotI, PCR Product Annealing
57	5_Stp1Pro_AB_ BsaI	ATATggtctcAacctGACATATTGT CGTTAGAAC	#3881	#15	to amplify *stp1* promoter for GreenGate system, BsaI
58	3_Stp1Pro_AB_ BsaI	ATATggtctcAtgttCGTGTTCTCT GCTTTATTTTC	#3882	#15	to amplify *stp1* promoter for GreenGate system, BsaI
59	5_Pit2Pro_AB_ BsaI	AACAggtctcAacctCATACTTATA GCAAAGCAC	#3876	#16	to amplify *pit2* promoter for GreenGate system, BsaI
60	3_Pit2Pro_AB_ BsaI	AACAggtctcAtgttTGCTGCGTTT GGTCGTTTG	#3879	#16	to amplify *pit2* promoter for GreenGate system, BsaI
61	5_N-UbAp2_Bsa	atatGGTCTCacccaATGCGGCA AGTCATCTCTTGC	#3184	#17,20-22	to amplify *ubapB73*$_{22-753}$ for GreenGate system, BsaI
62	3_UbAp2-HA_Bsa	atatGGTCTCtctccAGCGTAATC TGGAACATCGTATGGGTACG TTGCATCTTTTAATTCCCC	#3185	#17,19, 20,23	to amplify *ubapB73*$_{22-753}$ for GreenGate system, BsaI
63	3_UbAp2Mod1	TATGGTCTCTCGGACTGGCTT GTCCACTTGG	#4624	#20-22	to amplify module of UbApB73 for GreenGate system, BsaI
64	5_UbAp2Mod2	ATAGGTCTCAtccgCTGCGAGA CGGAGTCTCCG	#4625	#18,19, 21	to amplify module of UbApB73 for GreenGate system, BsaI
65	3_UbAp2Mod2	AATGGTCTCTTAGTGCTGGAT CATGATTGTAG	#4626	#18,19, 21	to amplify module of UbApB73 for GreenGate system, BsaI

66	5_UbAp2Mod3	ATAGGTCTCAactaGGGCAAACAGGAAAGGCGCAG	#4627	#19,20,23	to amplify module of UbApB73 for GreenGate system, BsaI
67	3_UmAp2Mod1	AATGGTCTCTcGGACCTGCTTGCTGATGTG	#4628	#18,19,23	to amplify module of UmApB73 for GreenGate system, BsaI
68	5_UmAp2Mod2	ATAGGTCTCAtccgACTCAGAATCCAGAACAGCC	#4629	#20,22,23	to amplify module of UmApB73 for GreenGate system, BsaI
69	3_UmAp2Mod2	AATGGTCTCTtAGtGAAGCATGGTCATAGACGGTG	#4630	#20,22,23	to amplify module of UmApB73 for GreenGate system, BsaI
70	5_UmAp2Mod3	ATAGGTCTCAactaGATGGACGTCGTCAATTTGC	#4631	#18,21,22	to amplify module of UmApB73 for GreenGate system, BsaI
71	5_LOC103626210_Nco	ATAccatggAAAGCAGTGAAAGGG	#4608	#38	to amplify Golgin for yeast interaction test
72	5_noSMC_LOC103626210_Nco	ATAccatggCTTCTCTTACCAATGAG	#4609	#38	to amplify GolginΔSMC for yeast interaction test, NcoI
73	3_LOC103626210_Stp_Not	gcggccgccTACGGCTCTGTTCTTGATTTC	#4610	#37,38,39	to amplify Golgin/GolginΔSMC for yeast interaction test, NotI
74	5_GolginSMC	ataccatgGAACAACTAAGGAATGGATTACAGg	#5663	#37	to amplify Golgin for yeast interaction test, NcoI
75	3_JustSMC	atatGCGGCCGCctaCAATGCAGATGCAATCTC	#5664	#39	to amplify SMC for yeast interaction test, NcoI
76	5_pit1_CD_bsaI	AACAggtctcAggctCAATGGAGCGTCACGATGGTGAAG	#3891	#41	to amplify *pit1* CDS for GreenGate system, BsaI
77	3_pit1_CD_bsaI	AACAggtctcActgaCATGTATGGGGCCGGAAGG	#3892	#41	to amplify *pit1* CDS for GreenGate system, BsaI

7 References

Agrios GN. 1988. *Plant Pathology.* New York.

Aranda PS, LaJoie DM, Jorcyk CL. 2012. Bleach gel: A simple agarose gel for analyzing RNA quality. *Electrophoresis* **33**(2): 366-369.

Asai S, Rallapalli G, Piquerez SJM, Caillaud M-C, Furzer OJ, Ishaque N, Wirthmueller L, Fabro G, Shirasu K, Jones JDG. 2014. Expression profiling during Arabidopsis/downy mildew interaction reveals a highly-expressed effector that attenuates responses to salicylic acid. *PLOS Pathogens* **10**(10): e1004443.

Asai S, Shirasu K. 2015. Plant cells under siege: plant immune system versus pathogen effectors. *Current Opinion in Plant Biology* **28**: 1-8.

Ausubel FM, Brent R, Kingston RE, Moore DD, Seidmann JG, Smith JA, Struhl K. 2003. *Current protocols in molecular biology*: John Wiley & Sons Inc.

Banuett F, Herskowitz I. 1989. Different a-alleles of *Ustilago maydis* are necessary for maintenance of filamentous growth but not for meiosis. *Proceedings of the National Academy of Sciences of the United States of America* **86**(15): 5878-5882.

Banuett F, Herskowitz I. 1996. Discrete developmental stages during teliospore formation in the corn smut fungus, *Ustilago maydis*. *Development* **122**: 2965-2976.

Baumgarten AM, Suresh J, May G, Phillips RL. 2007. Mapping QTLs contributing to *Ustilago maydis* resistance in specific plant tissues of maize. *Theoretical and Applied Genetics* **114**(7): 1229-1238.

Benjamini Y, Hochberg Y. 1995. Controlling the False Discovery Rate: A Practical and Powerful Approach to Multiple Testing. *Journal of the Royal Statistical Society.* **57**(1): 289-300.

Bent AF, Mackey D. 2007. Elicitors, effectors, and R genes: the new paradigm and a lifetime supply of questions. *Annual Review of Phytopathology* **45**(1): 399-436.

Bielska E, Higuchi Y, Schuster M, Steinberg N, Kilaru S, Talbot NJ, Steinberg G. 2014. Long-distance endosome trafficking drives fungal effector production during plant infection. *Nature Communications* **5**: 5097.

Birnboim HC, Doly J. 1979. A rapid alkaline extraction procedure for screening recombinant plasmid DNA. *Nucleic Acids Res* **7**(6): 1513-1523.

Birren B, Fink G, Lander E 2003. Fungal genome initiative: A white paper for fungal comparative genomics. Cambridge, USA.

Bos JIB, Armstrong MR, Gilroy EM, Boevink PC, Hein I, Taylor RM, Zhendong T, Engelhardt S, Vetukuri RR, Harrower B, et al. 2010. Phytophthora infestans effector AVR3a is essential for virulence and manipulates plant immunity by stabilizing host E3 ligase CMPG1. *Proceedings of the National Academy of Sciences* **107**(21): 9909-9914.

Bozkurt TO, Schornack S, Win J, Shindo T, Ilyas M, Oliva R, Cano LM, Jones AME, Huitema E, van der Hoorn RAL, et al. 2011. Phytophthora infestans effector AVRblb2 prevents secretion of a plant immune protease at the haustorial interface. *Proceedings of the National Academy of Sciences of the United States of America* **108**(51): 20832-20837.

Brachmann A, Weinzierl G, Kamper J, Kahmann R. 2001. Identification of genes in the bW/bE regulatory cascade in *Ustilago maydis*. *Molecular Microbiology* **42**(4): 1047-1063.

Brefort T, Doehlemann G, Mendoza-Mendoza A, Reissmann S, Djamei A, Kahmann R. 2009. *Ustilago maydis* as a pathogen. *Annual Review of Phytopathology* **47**(1): 423-445.

Buxdorf K, Rahat I, Gafni A, Levy M. 2013. The epiphytic fungus *Pseudozyma aphidis* induces jasmonic acid- and salicylic acid/nonexpressor of PR1-independent local and systemic resistance. *Plant Physiology* **161**(4): 2014-2022.

Callow JA. 1975. Endopolyploidy in maize smut neoplasms induced by the maize smut fungus, *Ustilago maydis*. *New Phytologist* **75**: 253-257.

Catanzariti AM, Dodds PN, Lawrence GJ, Ayliffe MA, Ellisa JG. 2006. Haustorially expressed secreted proteins from flax rust are highly enriched for avirulence elicitors. *The Plant Cell Online* **18**(1): 243-256.

Christensen JJ. 1963. Corn smut caused by *Ustilago maydis*. *American Phytopathological Society Monograph* **2**: 35-41.

Clontech. 2007. *Matchmaker™ GAL4 Two-Hybrid System 3 & Libraries User Manual*.

de Jonge R, van Esse HP, Kombrink A, Shinya T, Desaki Y, Bours R, van der Krol S, Shibuya N, Joosten MHAJ, Thomma BPHJ. 2010. Conserved fungal LysM effector Ecp6 prevents chitin-triggered immunity in plants. *SCIENCE* **329**(5994): 953-955.

Djamei A, Kahmann R. 2012. *Ustilago maydis*: Dissecting the molecular interface between pathogen and plant. *PLOS Pathogens* **8**(11).

Djamei A, Schipper K, Rabe F, Ghosh A, Vincon V, Kahnt J, Osorio S, Tohge T, Fernie AR, Feussner I, et al. 2011. Metabolic priming by a secreted fungal effector. *Nature* **478**(7369): 395-398.

Doehlemann G, Reissmann S, Aßmann D, Fleckenstein M, Kahmann R. 2011. Two linked genes encoding a secreted effector and a membrane protein are essential for *Ustilago maydis*-induced tumour formation. *Molecular Microbiology* **81**(3): 751-766.

Doehlemann G, van der Linde K, Aßmann D, Schwammbach D, Hof A, Mohanty A, Jackson D, Kahmann R. 2009. Pep1, a Secreted Effector Protein of *Ustilago maydis*, Is Required for Successful Invasion of Plant Cells. *PLOS Pathogens* **5**(2): e1000290.

Doehlemann G, Wahl R, Horst RJ, Voll LM, Usadel B, Poree F, Stitt M, Pons-Kühnemann J, Sonnewald U, Kahmann R, et al. 2008. Reprogramming a maize plant: transcriptional and metabolic changes induced by the fungal biotroph *Ustilago maydis*. *The Plant Journal* **56**(2): 181-195.

Ellis JG, Rafiqi M, Gan P, Chakrabarti A, Dodds PN. 2009. Recent progress in discovery and functional analysis of effector proteins of fungal and oomycete plant pathogens. *Current Opinion in Plant Biology* **12**(4): 399-405.

Engler C, Kandzia R, Marillonnet S. 2008. A one pot, one step, precision cloning method with high throughput capability. *PLoS One* **3**(11): e3647.

Farfsing JW. 2004. *Regulation des Mais-induzierten mig2-Genclusters in U. maydis.* PhD, Philipps-Universität Marburg Marburg.

Felle HH, Herrmann A, Hanstein S, Huckelhoven R, Kogel KH. 2004. Apoplastic pH signaling in barley leaves attacked by the powdery mildew fungus Blumeria graminis f. sp hordei. *Molecular Plant-Microbe Interactions* **17**(1): 118-123.

Feng F, Yang F, Rong W, Wu X, Zhang J, Chen S, He C, Zhou J-M. 2012. A Xanthomonas uridine 5′-monophosphate transferase inhibits plant immune kinases. *Nature* **485**(7396): 114-118.

Fernández-Álvarez A, Marín-Menguiano M, Lanver D, Jiménez-Martín A, Elías-Villalobos A, Pérez-Pulido AJ, Kahmann R, Ibeas JI. 2012. Identification of O-mannosylated Virulence Factors in Ustilago maydis. *PLOS Pathogens* **8**(3): e1002563.

Flor-Parra I. 2006. Biz1, a zinc finger protein required for plant invasion by *Ustilago maydis*, regulates the levels of a mitotic cyclin. *The Plant Cell* **18**(9): 2369-2387.

Gillissen B, Bergemann J, Sandmann C, Schroeer B, Bolker M, Kahmann R. 1992. A two-component regulatory system for self/non-self recognition in Ustilago maydis. *Cell* **68**(4): 647-657.

Hampel M, Jakobi M, Schmitz L, Meyer U, Finkernagel F, Doehlemann G, Heimel K. 2016. Unfolded Protein Response (UPR) Regulator Cib1 Controls Expression of Genes Encoding Secreted Virulence Factors in Ustilago maydis. *PLoS One* **11**(4): e0153861.

Hellens RP, Edwards EA, Leyland NR, Bean S, Mullineaux PM. 2000. pGreen: a versatile and flexible binary Ti vector for Agrobacterium-mediated plant transformation. *Plant Molecular Biology* **42**(6): 819-832.

Hemetsberger C, Mueller AN, Matei A, Herrberger C, Hensel G, Kumlehn J, Mishra B, Sharma R, Thines M, Hückelhoven R, et al. 2015. The fungal core effector Pep1 is conserved across smuts of dicots and monocots. *New Phytologist* **206**(3): 1116-1126.

Holliday R 1974. Ustilago maydis. In: King RC ed. *Bacteria, Bacteriophages, and Fungi: Volume 1*. Boston, MA: Springer US, 575-595.

Immunomedicine Group UCdM 2015. SIAS - Software to calculate Sequence Identity And Similarity URL http://imed.med.ucm.es/Tools/sias.html [accessed 21. February 2016].

Jia Y, McAdams SA, Bryan GT, Hershey HP, Valent B. 2000. Direct interaction of resistance gene and avirulence gene products confers rice blast resistance. *The EMBO Journal* **19**(15): 4004-4014.

Jones JDG, Dangl JL. 2006. The plant immune system. *Nature* **444**(7117): 323-329.

Kahmann R, Kämper J. 2004. *Ustilago maydis*: how its biology relates to pathogenic development. *New Phytologist* **164**(1): 31-42.

Kamoun S. 2006. A catalogue of the effector secretome of plant pathogenic oomycetes. *Annual Review of Phytopathology* **44**: 41-60.

Kämper J, Kahmann R, Bölker M, Ma L-J, Brefort T, Saville BJ, Banuett F, Kronstad JW, Gold SE, Müller O, et al. 2006. Insights from the genome of the biotrophic fungal plant pathogen *Ustilago maydis*. *Nature* **444**(7115): 97-101.

Keon JPR, White GA, Hargreaves JA. 1991. Isolation, characterization and sequence of a gene conferring resistance to the systemic fungicide carboxin from the maize smut pathogen, *Ustilago maydis*. *Current Genetics* **19**(6): 475-481.

Koeck M, Hardham AR, Dodds PN. 2011. The role of effectors of biotrophic and hemibiotrophic fungi in infection. *Cellular Microbiology* **13**(12): 1849-1857.

Koncz C, Schell J. 1986. The promoter of T_L-DNA gene 5 controls the tissue-specific expression of chimaeric genes carried by a novel type of *Agrobacterium* binary vector. *Molecular and General Genetics MGG* **204**(3): 383-396.

Laemmli UK. 1970. Cleavage of structural proteins during the assembly of the head of bacteriophage T4. *Nature* **227**(5259): 680-685.

Lampropoulos A, Sutikovic Z, Wenzl C, Maegele I, Lohmann JU, Forner J. 2013. GreenGate - A novel, versatile, and efficient cloning system for plant transgenesis. *PLoS One* **8**(12): e83043.

Le Roux C, Huet G, Jauneau A, Camborde L, Trémousaygue D, Kraut A, Zhou B, Levaillant M, Adachi H, Yoshioka H, et al. 2015. A receptor pair with an integrated decoy converts pathogen disabling of transcription factors to immunity. *Cell* **161**(5): 1074-1088.

Lindeberg M, Cunnac S, Collmer A. 2012. *Pseudomonas syringae* type III effector repertoires: last words in endless arguments. *Trends in Microbiology* **20**(4): 199-208.

Liu T, Song T, Zhang X, Yuan H, Su L, Li W, Xu J, Liu S, Chen L, Chen T, et al. 2014. Unconventionally secreted effectors of two filamentous pathogens target plant salicylate biosynthesis. *Nat Commun* **5**: 4686.

Llopis J, McCaffery JM, Miyawaki A, Farquhar MG, Tsien RY. 1998. Measurement of cytosolic, mitochondrial, and Golgi pH in single living cells with green fluorescent proteins. *Proc Natl Acad Sci U S A* **95**(12): 6803-6808.

Loubradou G, Brachmann A, Feldbrugge M, Kahmann R. 2001. A homologue of the transcriptional repressor Ssn6p antagonizes cAMP signalling in *Ustilago maydis*. *Molecular Microbiology* **40**(3): 719-730.

Marchler-Bauer A, Derbyshire MK, Gonzales NR, Lu S, Chitsaz F, Geer LY, Geer RC, He J, Gwadz M, Hurwitz DI, et al. 2014. CDD: NCBI's conserved domain database. *Nucleic Acids Research* **43**(D1): D222-D226.

Marshall R, Kombrink A, Motteram J, Loza-Reyes E, Lucas J, Hammond-Kosack KE, Thomma BPHJ, Rudd JJ. 2011. Analysis of two in planta expressed LysM effector homologs from the fungus *Mycosphaerella graminicola* reveals novel functional properties and varying contributions to virulence on wheat. *Plant Physiology* **156**(2): 756-769.

Mattanovich D, Ruker F, Machado AC, Laimer M, Regner F, Steinkellner H, Himmler G, Katinger H. 1989. Efficient transformation of Agrobacterium spp. by electroporation. *Nucleic Acids Res* **17**(16): 6747.

McHale L, Tan X, Koehl P, Michelmore RW. 2006. Plant NBS-LRR proteins: adaptable guards. *Genome Biology* **7**(4): 212.

Mendoza-Mendoza A, Berndt P, Djamei A, Weise C, Linne U, Marahiel M, Vraneš M, Kämper J, Kahmann R. 2009. Physical-chemical plant-derived signals induce differentiation in *Ustilago maydis*. *Molecular Microbiology* **71**(4): 895-911.

Mentlak TA, Kombrink A, Shinya T, Ryder LS, Otomo I, Saitoh H, Terauchi R, Nishizawa Y, Shibuya N, Thomma BPHJ, et al. 2012. Effector-mediated suppression of chitin-triggered immunity by *Magnaporthe oryzae* is necessary for rice blast disease. *The Plant Cell* **24**(1): 322-335.

Milutinovich M, Koshland DE. 2003. Molecular biology. SMC complexes--wrapped up in controversy. *SCIENCE* **300**(5622): 1101-1102.

Mueller AN, Ziemann S, Treitschke S, Aßmann D, Doehlemann G. 2013. Compatibility in the *Ustilago maydis*–Maize interaction requires inhibition of host cysteine proteases by the fungal effector Pit2. *PLOS Pathogens* **9**(2): e1003177.

Mueller O, Kahmann R, Aguilar G, Trejo-Aguilar B, Wu A, de Vries RP. 2008. The secretome of the maize pathogen *Ustilago maydis*. *Fungal Genetics and Biology* **45**: S63-S70.

Mukhtar MS, Carvunis AR, Dreze M, Epple P, Steinbrenner J, Moore J, Tasan M, Galli M, Hao T, Nishimura MT, et al. 2011. Independently evolved virulence effectors converge onto hubs in a plant immune system network. *SCIENCE* **333**(6042): 596-601.

Nikić I, Plass T, Schraidt O, Szymański J, Briggs JAG, Schultz C, Lemke EA. 2014. Minimal Tags for Rapid Dual-Color Live-Cell Labeling and Super-Resolution Microscopy. *Angewandte Chemie International Edition* **53**(8): 2245-2249.

Nurnberger T, Brunner F, Kemmerling B, Piater L. 2004. Innate immunity in plants and animals: striking similarities and obvious differences. *Immunological Reviews* **198**: 249-266.

Park CH, Chen S, Shirsekar G, Zhou B, Khang CH, Songkumarn P, Afzal AJ, Ning Y, Wang R, Bellizzi M, et al. 2012. The *Magnaporthe oryzae* effector AvrPiz-t targets the RING E3 ubiquitin ligase APIP6 to suppress pathogen-associated molecular pattern-triggered immunity in rice. *The Plant Cell* **24**(11): 4748-4762.

Pelham HR. 1990. The retention signal for soluble proteins of the endoplasmic reticulum. *Trends Biochem Sci* **15**(12): 483-486.

Petersen TN, Brunak S, von Heijne G, Nielsen H. 2011. SignalP 4.0: discriminating signal peptides from transmembrane regions. *Nature Methods* **8**(10): 785-786.

Redkar A. 2014. *Functional characterization of an organ specific effector See1 of Ustilago maydis.* PhD, Philipps-Universität Marburg Marburg.

Redkar A, Hoser R, Schilling L, Zechmann B, Krzymowska M, Walbot V, Doehlemann G. 2015a. A secreted effector protein of *Ustilago maydis* guides maize leaf cells to form tumors. *The Plant Cell* **27**(4): 1332-1351.

Redkar A, Villajuana- Bonequi M, Doehlemann G. 2015b. Conservation of the *Ustilago maydis* effector See1 in related smuts. *Plant Signaling & Behavior* **10**(12): e1086855.

Saitoh H, Fujisawa S, Mitsuoka C, Ito A, Hirabuchi A, Ikeda K, Irieda H, Yoshino K, Yoshida K, Matsumura H, et al. 2012. Large-scale gene disruption in *Magnaporthe oryzae* identifies MC69, a secreted protein required for infection by monocot and dicot fungal pathogens. *PLOS Pathogens* **8**(5): e1002711.

Sambrook J, Fritsch EF, Maniatis T. 1989. *Molecular cloning: A laboratory manual.* . New York: Cold Spring Harbor Laboratory Press.

Sankaranarayanan S, De Angelis D, Rothman JE, Ryan TA. 2000. The use of pHluorins for optical measurements of presynaptic activity. *Biophysical Journal* **79**(4): 2199-2208.

Santoni V. 2007. Plant plasma membrane protein extraction and solubilization for proteomic analysis. *Methods Mol Biol* **355**: 93-109.

Schilling L, Matei A, Redkar A, Walbot V, Doehlemann G. 2014. Virulence of the maize smut *Ustilago maydis* is shaped by organ-specific effectors. *Molecular Plant Pathology* **15**(8): 780-789.

Schipper K. 2009. *Charakterisierung eines Ustilago maydis Genclusters, das für drei neuartige sekretierte Effektoren kodiert.* Philipps-Universität Marburg.

Schirawski J, Mannhaupt G, Munch K, Brefort T, Schipper K, Doehlemann G, Di Stasio M, Rossel N, Mendoza-Mendoza A, Pester D, et al. 2010. Pathogenicity determinants in smut fungi revealed by genome comparison. *SCIENCE* **330**(6010): 1546-1548.

Schnable PS, Ware D, Fulton RS, Stein JC, Wei FS, Pasternak S, Liang CZ, Zhang JW, Fulton L, Graves TA, et al. 2009. The B73 maize genome: complexity, diversity, and dynamics. *SCIENCE* **326**(5956): 1112-1115.

Schulz B, Banuett F, Dahl M, Schlesinger R, Schafer W, Martin T, Herskowitz I, Kahmann R. 1990. The b alleles of *U. maydis*, whose combinations program pathogenic development, code for polypeptides containing a homeodomain-related motif. *Cell* **60**(2): 295-306.

Shabab M, Shindo T, Gu C, Kaschani F, Pansuriya T, Chintha R, Harzen A, Colby T, Kamoun S, van der Hoorn RAL. 2008. Fungal effector protein AVR2 targets diversifying defense-related cys proteases of tomato. *The Plant Cell Online* **20**(4): 1169-1183.

Sharma R, De Vleesschauwer D, Sharma MK, Ronald PC. 2013. Recent advances in dissecting stress-regulatory crosstalk in rice. *Molecular Plant* **6**(2): 250-260.

Sharma R, Mishra B, Runge F, Thines M. 2014. Gene loss rather than gene gain is associated with a host jump from monocots to dicots in the smut fungus *Melanopsichium pennsylvanicum*. *Genome Biology and Evolution* **6**(8): 2034-2049.

Skibbe DS, Doehlemann G, Fernandes J, Walbot V. 2010. Maize tumors caused by *Ustilago maydis* require organ-specific genes in host and pathogen. *SCIENCE* **328**.

Snetselaar K, Mims CW. 1992. Sporidial Fusion and Infection of Maize Seedlings by the Smut Fungus Ustilago maydis. *Mycologia* **84**(2): 193-203.

Snetselaar KM, Mims CW. 1993. Infection of maize stigmas by *Ustilago maydis*: light and electron microscopy. *Phytopathology*(83): 843-850.

Spellig T, Bottin A, Kahmann R. 1996. Green fluorescent protein (GFP) as a new vital marker in the phytopathogenic fungus *Ustilago maydis*. *MGG Molecular & General Genetics* **252**(5): 503-509.

Sperschneider J, Dodds PN, Gardiner DM, Manners JM, Singh KB, Taylor JM. 2015a. Advances and challenges in computational prediction of effectors from plant pathogenic fungi. *PLOS Pathogens* **11**(5): e1004806.

Sperschneider J, Gardiner DM, Dodds PN, Tini F, Covarelli L, Singh KB, Manners JM, Taylor JM. 2015b. EffectorP: predicting fungal effector proteins from secretomes using machine learning. *New Phytologist*: n/a-n/a.

Stergiopoulos I, de Wit PJGM. 2009. Fungal Effector Proteins. *Annual Review of Phytopathology* **47**(1): 233-263.

Stukenbrock EH, McDonald BA. 2008. The origins of plant pathogens in agro-ecosystems. *Annual Review of Phytopathology* **46**(1): 75-100.

Tanaka S, Brefort T, Neidig N, Djamei A, Kahnt J, Vermerris W, Koenig S, Feussner K, Feussner I, Kahmann R. 2014. A secreted Ustilago maydis effector promotes virulence by targeting anthocyanin biosynthesis in maize. *eLife* **3**.

Tanaka S, Djamei A, Presti LL, Schipper K, Winterberg S, Amati S, Becker D, Büchner H, Kumlehn J, Reissmann S, et al. 2015. Experimental approaches to investigate effector translocation into host cells in the *Ustilago maydis*/maize pathosystem. *European Journal of Cell Biology* **94**(7-9): 349-358.

Tian M, Win J, Song J, van der Hoorn R, van der Knaap E, Kamoun S. 2007. A *Phytophthora infestans* cystatin-like protein targets a novel tomato papain-like apoplastic protease. *Plant Physiology* **143**(1): 364-377.

Towbin H, Staehelin T, Gordon J. 1979. Electrophoretic transfer of proteins from polyacrylamide gels to nitrocellulose sheets: procedure and some applications. *Proc Natl Acad Sci U S A* **76**(9): 4350-4354.

Tsukuda T, Carleton S, Fotheringham S, Holloman WK. 1988. Isolation and characterization of an autonomously replicating sequence from Ustilago maydis. *Mol Cell Biol* **8**(9): 3703-3709.

van den Burg HA, Harrison SJ, Joosten MH, Vervoort J, de Wit PJ. 2006. *Cladosporium fulvum* Avr4 protects fungal cell walls against hydrolysis by plant chitinases accumulating during infection. *Mol Plant Microbe Interact* **19**(12): 1420-1430.

van Esse HP, Bolton MD, Stergiopoulos I, de Wit PJGM, Thomma BPHJ. 2007. The chitin-binding *Cladosporium fulvum* effector protein Avr4 is a virulence factor. *Molecular Plant-Microbe Interactions* **20**(9): 1092-1101.

Wedlich-Soldner R. 2002. Dynein supports motility of Endoplasmic Reticulum in the fungus *Ustilago maydis*. *Molecular Biology of the Cell* **13**(3): 965-977.

White DG. 1999. *Compendium of Corn Diseases.* . St. Paul: APS Press.

Wisser RJ, Balint-Kurti PJ, Nelson RJ. 2006. The genetic architecture of disease resistance in maize: a synthesis of published studies. *Phytopathology* **96**(2): 120-129.

Young KH. 1998. Yeast two-hybrid: so many interactions, (in) so little time. *Biol Reprod* **58**(2): 302-311.

Zipfel C. 2014. Plant pattern-recognition receptors. *Trends in Immunology* **35**(7): 345-351.